Table of contents

Chapter 1 Problem statements and literature survey

1.1	Introduction	14
1.2	Towards the improvement of order tracking analysis	18
1.2.1	Computed order tracking	19
1.2.2	Vold-Kalman filter order tracking	21
1.2.3	Intrinsic mode functions through empirical mode decomposition	22
1.2.4	Improved order tracking	24
1.3	A review of three basic order tracking methods	27
1.3.1	Computed order tracking	27
1.3.2	Vold-Kalman filter order tracking	34
1.3.3	Intrinsic mode functions through empirical mode decomposition	37
1.4	Scope of work	41

Chapter 2 Logic developments of three novel improved order tracking approaches

2.1	Vold-Kalman filter and computed order tracking	46
2.1.1	Discussions on Vold-Kalman filter order tracking	46
2.1.2	Discussions on computed order tracking	48
2.1.3	Development of Vold-Kalman filter and computed order tracking	49
2.2	Intrinsic mode function and Vold-Kalman filter order tracking	51
2.2.1	Discussions on the relationship between an intrinsic mode function and an order wave in time domain	52
2.2.2	Discussions on the relationship between an intrinsic mode function and an order wave in order domain	55
2.2.3	Discussions on the resolution of an IMF	56
2.2.4	Combined use of empirical mode decomposition and Vold-Kalman filter order tracking	59
2.3	Intrinsic cycle re-sampling	62
2.3.1	Development of intrinsic cycle re-sampling	62
2.3.2	Interpretation on the reconstructed intrinsic mode function result	67
2.3.3	Discussions on intrinsic cycle re-sampling in terms of rotating machine vibration signals	70
2.4	Summary	71

Chapter 3 Simulation studies

3.1	Single-degree-of-freedom rotor model simulation analysis	73
3.1.1	Single-degree-of-freedom rotor modelling	73
3.1.2	Equations of motion for the single-degree-of-freedom system	76
3.1.3	Single-degree-of-freedom system analysis	77
3.1.3.1	Application of Vold-Kalman filter and computed order tracking	78
3.1.3.2	Application of intrinsic mode function and Vold-Kalman filter order tracking	84
3.2	Simplified gear mesh model simulation analysis	95
3.2.1	Simplified gear mesh modelling	95
3.2.2	Application of intrinsic cycle re-sampling method	98
3.3	Summary	110

Chapter 4 Experimental studies

4.1	Automotive alternator set-up data analysis	112
4.1.1	Experimental automotive alternator set-up	112
4.1.2	Experimental fault description	114
4.1.3	Application of VKC-OT and IVK-OT techniques on alternator experimental set-up	115
4.1.3.1	Application of Vold-Kalman filter and computed order tracking	115
4.1.3.2	Application of intrinsic mode function and Vold-Kalman filter order tracking	118
4.2	Transmission gear box set-up data analysis	126
4.2.1	Experimental gear box set-up	126
4.2.2	Experimental fault description	127
4.2.3	Application of intrinsic cycle re-sampling	128
4.3	Summary	135

Chapter 5 Conclusions

5.1	Contributions of the research	136
5.1.1	A review of the development of three improved order tracking approaches	136
5.1.2	Contributions of each improved order tracking approach	138
5.1.3	Contributions of the three improved order tracking approaches as a whole in order related vibration signals	142
5.2	Future work	143
	Appendix	144
	Reference	147

Chapter 1 Problem statement and literature survey

1.1 Introduction

The order tracking technique is one of the important and effective vibration analysis techniques for rotating machinery. The advantages of order tracking over other vibration techniques mainly lie in analysing non-stationary noise and vibration signals which vary in frequency with the rotation of a reference shaft or shafts. The analysis of non-stationary conditions requires additional information, as compared to steady state conditions, for accurate results to be obtained. Normally the additional information is provided in the form of a tachometer signal measured on a reference shaft or shafts of the machine.

Order domain analysis relates the vibration signal to the rotational speed of the shaft, instead of an absolute frequency base. In this way, vibration components that are proportional to multiples of the running speed can easily be identified. In the early stages, order tracking was performed by sampling the analog vibration signal at constant shaft increments, directly with the help of an analog instrument. However due to the high cost and complexity of the equipment, this kind of method is being used less and less. The mainstay of modern order tracking is post-process order tracking. It entails measuring the vibration signal and additional rotational speed information (usually a tachometer signal) simultaneously and processing the data after the measurement, which makes the whole process more economical and flexible. In the literature, many different order tracking techniques which rely on post-processing order tracking, are described. Some of these are frequently discussed and researched in the context of condition monitoring of machinery. Each technique has its own advantages

and disadvantages. However nearly all of them have unique advantages in their own right and therefore it is worthwhile to study these techniques intensively.

Firstly, the simplest and most commonly used method is Fourier Transform based Order Tracking (FT-OT). This is a widely used method however it suffers from the limitations of Fourier analysis (Blough, 2003). Secondly, another frequently used and extensively researched technique is angle domain sampling based order tracking (AD-OT) or computed order tracking (COT). It re-samples uniform time domain data into the angle domain and therefore overcomes the limitation of non-stationarity due to the variation in rotational speed. But the process of re-sampling brings unavoidable assumptions and constraints (Fyfe and Munck, 1997) which compromise the ability of this kind of order tracking technique. Thirdly, a recent waveform reconstruction based method is Vold-Kalman filter order tracking (VKF-OT). (The term 'waveform reconstruction' used in the context of order tracking analysis was first introduced by Pan, Liao and Chiu, 2007). It is a technique that extracts time domain order information from the raw data and features unique advantages in overcoming many of the limitations of other order tracking techniques, such as allowing high-performance tracking of harmonic responses or orders and allowing beat free extraction of close and crossing orders, etc. (Brüel and Kjær, 2007). Similarly, another well known waveform reconstruction order tracking technique is Gabor order tracking proposed by Albright and Qian (2001). This is a technique that claims to be more intuitive, more powerful and can be used when rotational speed is not available. Although these two techniques have excellent abilities of extracting order signals in the time domain, neither of them however can get rid of the non-stationary effects in the extracted or filtered time domain signals due to the variation of rotational speed, and therefore pose difficulties for further analysis of the time domain signals by conventional signal processing techniques such as Fourier analysis. Lastly, a useful technique that deals with non-stationary and nonlinear signals and which was not specifically developed for order tracking may also be

treated as a special waveform reconstruction order tracking technique. This is the intrinsic mode function (IMF) from empirical mode decomposition (EMD). In recent years, many researchers have done a great deal of research by using this technique to monitor rotating machinery conditions and have proven it to be effective. This will be extensively investigated in the following. However, the relationship between an order and an IMF from the EMD method for rotating machinery vibrations and the fact that it can indeed capture order information from rotating machinery vibration data has not been analysed in the literature.

Besides, there are still some other order tracking techniques, such as time variant discrete Fourier transform order tracking (TVDFT), the maximum likelihood process and the Prony residue estimation process, as well as methods based on conventional digital filtering (Blough, 2003). Yet these techniques have not attracted much interest in condition monitoring, compared to the order tracking methods mentioned above. In fact, they usually suffer from various constraints which discourage their application. For example, Blough (2003) mentions that the Prony residue estimation process has several disadvantages in its computational complexity and the requirement that a model order of the data must be known. Determination of the model order, or number of orders and resonances in the data, is not trivial, because it is typically a function of rotational speed and the resonances which are excited at certain instant in time. He further mentions that order tracking methods that are based on conventional digital filtering all appear inferior to the Vold/Vold–Kalman filtering methods because of their pass band shapes. These filtering methods also tend to be computationally demanding.

In general, each order tracking technique has its own advantages and disadvantages. It is not easy to conclude that one method is absolutely superior to the others, since they all have benefits for different applications. However, in terms of real application of signal processing in vibration monitoring of rotating

machines, those more widely available and proven effective order tracking methods deserve intensive emphasis for investigating order and related vibration signals.

From a vibration monitoring point of view, order signals as well as an understanding of these orders and its related vibration signals are of great importance for monitoring rotating machine conditions. Fortunately, with the development of computer capabilities in recent years, researchers can now more easily work on the application of different order tracking techniques in monitoring of rotating machines. General speaking, most of the research described in the literature focus on the interpretation of the theory of each order tracking technique and the application of techniques in simulation models or real machinery environments. Examples of this are Potter (1990), Fyfe and Munck (1997), Huang et al. (1998), Gade et al., (1999), Blough (2003), Brandt et al. (2005), Pan and Lin (2006) and Feldman (2008, 2009), etc.. In practical applications, various companies have commercialized order tracking methods in their signal analyzers, such as, PULSE which is supplied by Brüel and Kjær, the Rotate software supplied by ATA Engineering, Vibratools from Matlab, The Dewetron, LMS international, Benstone Instruments (Fieldpaq2+1 channel dynamic signal analyzer), Lambda photometics (SR785 dynamic signal analyzer), Xi'an space star technology (SS-DY dynamic signal analyzer), OROS, etc.. One can easily find all kinds of signal analyzers which include either COT, VKF-OT or both. However the ideal of using these techniques together has not been reported. The improvement of order tracking analysis capability through the use of different order tracking techniques for diagnosing machine faults, has not yet attracted intensive research in the field. Thus, it is clear that order tracking techniques have been intensively studied in their theories and widely implemented in real practice on their own, however combining different order tracking methods and exploiting abilities in machine fault diagnostics are few reported and deserve further researches. It is, therefore proposed in this research that significant added value may be obtained in

order tracking research by exploiting the distinct characteristics of different order tracking techniques and combining them into enhanced diagnostic tools for rotating machinery diagnosis.

Thus, in this research, three widely researched order tracking techniques are studied and developed into improved techniques that combine the abilities of different order tracking methods to achieve augmented order tracking for rotating machine diagnostics.

In the following, firstly, the strengths and weaknesses of different traditional order tracking methods in condition monitoring are discussed. Based upon these discussions, directions into which order tracking techniques for condition monitoring may be improved, are proposed. The research will then use three widely available order tracking techniques to exploit these avenues to develop improved techniques.

1.2 Towards the improvement of order tracking analysis

It is not surprising to find that in the literature each order tracking technique has been studied and developed extensively in its own right. However, it may be hypothesised that through combining different order tracking techniques together, instead of focusing on each individual method alone, one may also bring about several useful advantages in the order tracking field of study. This would however require a systematic understanding of which would be the most appropriate order tracking techniques and how to combine them in order to extract maximal benefit.

In the literature order tracking techniques are classified into two categories, namely, waveform reconstruction and non-reconstruction schemes (Pan, Liao and Chiu, 2007). Vold-Kalman filter order tracking is a typical example of a

waveform reconstruction scheme. The distinct characteristic of this scheme is that it finally yields time domain order waveforms without intentionally transforming signals. The waveform non-reconstruction scheme, however, will not lead to time domain data, such as computed order tracking where the time domain signals are re-sampled in the angle domain, using various kinds of interpolation methods. Different kinds of order tracking methods may be developed, but they are basically being classified in one of the schemes mentioned above.

To improve order tracking analysis, one should therefore investigate both schemes of methods. For implementation in this research, it is therefore essential to consider typical and widely used order tracking methods from both schemes. Thus, computed order tracking (a waveform non-reconstruction scheme), Vold-Kalman filter order tracking (a waveform reconstruction scheme) and intrinsic mode function from empirical mode decomposition (another waveform reconstruction scheme) are emphasized and studied. In this context the intrinsic mode function from empirical mode decomposition is also treated as a special kind of order tracking method. Its unique characteristics in terms of order signals will be explored in chapter 2. In the following, some aspects regarding the strengths and weaknesses of the selected techniques are discussed so that directions for possible improvements in the order tracking may be clarified. The inter-relationship between the three independent order tracking techniques is also explained in the following scope of work, so that the reader may understand how this work integrates these three order tracking methods.

1.2.1 Computed order tracking

To begin with, the strengths and weaknesses of computed order tracking (COT) are first investigated. Important background to COT is given by authors such as Potter (1990) and Fyfe and Munck (1997). Except for the detailed studies of the

COT technique itself in these papers, such as different interpolation methods, influence factors of accuracy, etc., some advantages of the method in terms of condition monitoring are discussed in the following.

Firstly, the idea of the technique is essentially to simplify the application of Fourier analysis, since the kernels of Fourier analysis are constant frequency (Blough, 2003). Whatever procedures are used for re-sampling of the data by COT, the final Fourier analysis is intended to yield clear figures through the transformation of signals where frequency variations in speed has been excluded. Fourier analysis is a very common signal processing method and this makes the COT technique easier to access and understand. Secondly, COT has been proved very useful in real practice (such as Eggers, Heyns and Stander, 2007) and also been commercialized into software in several vibration monitoring tool packages (such as Matlab). Thirdly, COT analysis may provide a clear picture of the raw signal in terms of rotational speed. This is a very useful perspective for an analyst to understand rotating machine vibrations. Nowadays, COT is one of the important mainstream order tracking methods and a well established technique.

Apart from these key advantages of the technique, some limitations should also be pointed out. Firstly, the COT method is normally set to deal with signals where several rotational speed harmonic vibrations may coexist, therefore usually the final spectrum map will yield several order components. This may lead to some non-dominant order signals easily being neglected and analysts have to accept this inconvenience throughout the analysis process. The shortcoming of the inability to focus on each individual order signal, sometimes limits the application of COT. Secondly, since the whole re-sampling process is strictly based upon rotational speed signals, those signals that are not strictly related to rotational speed information will be naturally de-emphasized, such as response at the natural frequencies of the system. This may lead to a loss of some important system information in the order domain. Thirdly, its unavoidable assumptions and

different interpolation errors will, of course, influence the accuracy of the results. Besides, for COT, rotational speed information is crucial for its calculation. In the absence of rotational speed information, the COT method is no longer applicable.

From the above it may be surmised that while the COT technique is a very practical and useful order tracking method, if breakthroughs could be made with respect to these limitations, it could definitely enhance the technique.

1.2.2 Vold-Kalman filter order tracking

For Vold-Kalman filter order tracking (VKF-OT), the following papers are key to understanding the technique: Herlufsen et al. (1999), Blough (2003), Tůma (2005), as well as Pan and Lin (2006). The above-mentioned papers give detailed accounts of its theory and applications. Here we point out some of the advantages and limitations associated with VKF-OT. Firstly, VKF-OT does not involve the assumptions and interpolations as are done in COT and may therefore achieve more accurate results. This is because of the use of a concise mathematical adaptive filter instead of re-sampling signals. This leads to VKF-OT having several advantages over other order tracking methods. This will be further discussed in the following VKF-OT literature survey. Secondly, the use of an adaptive filter also leads to the order signals remaining in the familiar time domain and allows focusing on the order of interest, excluding the influences from other signals. Figurative speaking, the technique provides a pair of spectacles to specifically see certain information of interest. These characteristics make VKF-OT unique and very useful in the field of order tracking.

On the other hand, the limitations of the technique are also obvious. First of all, again due to the use of the adaptive filter, the signal variation, such as frequency

variation caused by rotational speed, still remains in the filtered order signal. This, of course, influences Fourier analysis of the filtered time domain signal. Secondly, the technique is not easy to grasp for an inexperienced analyst, and it usually takes time to become familiar with the technique. This is also pointed out in some papers (such as Blough, 2003). Thirdly, the advantage of filtering specific orders from raw signals may also become a disadvantage in terms of condition monitoring, since it may easily lose vibration signals that modulate orders of interest, which usually contain useful machine condition information.

In short, VKF-OT may offer more advantages compared to other order tracking methods in order extraction. Through its strict mathematical adaptive filter, orders of interest can be specifically focused on for examination. However, its adaptive nature also brings disadvantages with respect to Fourier analysis and its difficulty in grasping sometimes becomes a barrier for its advancement in practical applications.

1.2.3 Intrinsic mode functions through empirical mode decomposition

Decomposition of intrinsic mode functions (IMF) through the empirical mode decomposition (EMD) method is also discussed in this research, as a special kind of order tracking method. The main reason why it may be considered as a special kind of order tracking analysis, can be ascribed to its empirical adaptive nature to decompose signals. Researchers such as Flandrin, Rilling and Gonçalvés (2004) conclude that the EMD process act more like a group of narrow band filters, and the method can be treated as a self-adaptive dyadic filter bank. Once one understands VKF-OT and IMFs from EMD in theory, it becomes easy to find connections between IMFs and VKF-OT results. Both of the two methods use adaptive filters to extract time domain signals. The difference is that one is a strictly mathematically defined filter (VKF-OT) while the other is empirical (EMD). Consequently, we may treat an IMF from EMD as a special kind of

order tracking for rotating machine vibration signals. For details of the relationship between an order and an IMF, the reader may refer to chapter 2.

However, the question remains as to the advantages and limitations for this special kind of order tracking analysis for the analysis of vibrations in the context of condition monitoring. As indicated by the word 'empirical' in the name, the IMF is based upon the signal itself and in the process of empirical mode decomposition to obtain IMFs, no additional information is needed, such as machine speed information, therefore it is not limited to the case where rotational speed must be available. This is totally different form COT and VKF-OT. Most importantly, the advantage of this empirical nature is very useful for fault diagnosis of rotating machines. Machine fault related vibrations are synchronous or non-synchronous with rotational speed. These vibration signals modulate regular order signals. They are usually unpredictable, and the empirical nature of the EMD method helps the analyst to capture all kinds of these possible vibrations together with the orders of interest. It should also be borne in mind that, for rotating machines, order signals will usually dominate the vibration response. And IMFs are very well suited to include both order signals and other vibrations that could possibly modulate them. The EMD process therefore decomposes the rotating machine vibration signals in the form of different IMFs, through which orders and vibrations that modulate them are packaged together and distributed into different IMFs. This effect is not possible to achieve by using any other traditional order tracking methods. Thus, it is worthwhile investigating the abilities of IMF in terms of orders for condition monitoring. Furthermore, though the process of decomposing IMFs through EMD is not guided through a strict mathematical filter, the procedures of EMD however also enforce the distinct nature of the signal structure.

Huang et al. (1998) state that an abstract intrinsic mode function (IMF) as a signal satisfies two conditions:

- In the whole signal segment, the number of extrema and the number of zero crossings must be either equal or differ at most by one.
- At any point, the mean value of the envelope defined by the local maxima and the envelope defined by the local minima is zero.

From this original definition of IMF it is easy to infer that each IMF is a symmetric and zero mean natured oscillation wave. This excludes two or more peaks within two successive zero crossings. (Huang et al., 1998) The simple structure of an IMF may also bring advantages for the analysis process. This characteristic is used in the current research and discussed in detail in Chapter 2. Lastly, another important advantage of IMFs is the absence of the need for rotational speed information during the EMD process. This makes this technique more accessible and practical in real application.

However from another perspective, the above mentioned advantages of IMFs may also become its limitations. The empirical nature and the absence of rotational speed information imply that more than one mode of oscillating signals can be included in one IMF. Therefore in practice it is usually not easy to extract single order signals alone through an IMF. Though ideally, an IMF is to extract one oscillation mode and therefore a single order signal is supposed to be extracted, the resolution of IMF however limits its ability to focus on a single order signal alone, especially when different vibrations are entwined together. The resolution obtainable through IMF is further studied in Chapter 2, paragraph 2.2.3.

This is an obvious disadvantage compared with VKF-OT. However, this technique actually enriches the content of order signals for condition monitoring purposes and deserves more in-depth research in the context of order analysis.

1.2.4 Improved order tracking

The discussions in the previous paragraph have pointed out some of the important pros and cons of different order tracking techniques. This points towards a number of possible improvements of order tracking techniques which should be researched. Advantages could be further developed and limitations may be avoided where applicable. Naturally not all the advantages and limitations of these techniques will be addressed. Intelligent use of different characteristics of these techniques should be introduced to exploit the advantages and avoid the limitations for condition monitoring purposes. Through studies of the above order tracking techniques, three aspects are identified and highlighted for the integration of three independent order tracking methods, namely:

1. Whether rotational speed information is required or not,
2. Whether order signals can be extracted for study, and
3. Whether the effect of speed variation can be handled.

As a result, improved approaches are therefore developed. This is summarised in Table 1.1.

Table 1.1 Approaches to improving order tracking methods

	Order tracking method	Need for rotational speed info (√/×)	An order can be extracted for study (√/×)	Speed variation effects can be handled (√/×)	
IMF/COT	COT	√	×	√	VKF/COT
	VKF-OT	√	√	×	
	IMF	×	√*	×	IMF/VKF

* For an IMF, an order signal can be extracted, but the whole signal comprises the order signal plus other possible vibrations that modulate the order.

Based upon the previous discussions and Table 1.1, three approaches to the improvement of order tracking are proposed here:

VKF/COT:

Combining the advantage of VKF-OT in its ability to focus on individual orders and the advantage of COT to get rid of speed variation effects, a sequentially combined application of Vold-Kalman filtering and computed order tracking (VKC–OT) may be developed. The shortcoming of possible non-stationarity, due to the rotational speed in VKF-OT is overcome by COT. And the shortcoming of COT with its inability to focus on each individual order, is compensated for by VKF-OT. The combination of these two techniques enhances the ability of condition monitoring by complementary use of two traditional order tracking methods. The usefulness of this improved order tracking technique mainly lies in the ability to obtain a clear and focused order component which can be tracked.

IMF/VKF:

Here we take advantage of the fact that an IMF may include order signals plus other possible vibrations that modulate the orders, as well as the VKF-OT advantage to strictly focus on order signals. Subtracting order focused VKF-OT results from an IMF, order signals and other possible vibrations that modulate orders can be separated and therefore an IMF can be further decomposed in terms of rotational speed. In this way one may extract useful machine condition information which is intractable by application of EMD or VKF-OT in isolation

alone. Therefore, an intrinsic mode function and Vold-Kalman filter order tracking method (IVK-OT) is developed to further decompose an IMF. This may render useful machine fault information for condition monitoring.

IMF/COT:

Taking advantage of the simple data structure of an IMF and the lack of required rotational speed information, while at the same time borrowing re-sampling ideas from COT to get rid of speed varying effects, an intrinsic cycle re-sampling (ICR) method is developed, so that an approximation of computed order tracking effects is possible, without the need for rotational speed. In this approach, COT is not directly used together with the intrinsic mode function, but the re-sampling idea is borrowed from COT and applied onto an IMF. This leads to a practical alternative method for condition monitoring.

Three new approaches to improved order tracking are therefore proposed. They are the main contributions of this work. They will be further explained and discussed in detail in chapter 2 to clarify how these techniques are being combined. Their usefulness as well as effectiveness in condition monitoring is subsequently demonstrated in Chapters 3 and 4 through simulation and experimental studies. But before that, a comprehensive literature survey of the three basic order tracking techniques is conducted. After that, the inter-relationship between COT, VKF-OT and IMF from EMD will be discussed in the scope of work, so as to elucidate of how this work integrates these ideas.

1.3 A review of three basic order tracking methods

1.3.1 Computed order tracking

Computed order tracking (COT) can also be called angle domain sampling based order tracking (AD-OT). This technique was originally published by Potter and his colleagues from Hewlett Packard in 1989 (Potter, 1990). However Hewlett Packard considers the exact implementation of the technique to be proprietary, and as such has not published many of the details. It has been more than 20 years since this method was first introduced, and some papers discussing the theory and implementation of this specific technique have become widely available. In discussing COT, the most important part is to understand the re-sampling process. In the context of this work this is particularly important since the intrinsic cycle re-sampling (ICR) technique which will be introduced later will use some of the ideas from the re-sampling process. Therefore, in the following, the re-sampling process will be discussed in detail and the current research in COT will be surveyed thereafter.

a. The re-sampling process

Basically, COT requires sampling of the vibration signal at constant angular increments of the shaft and hence at a rate proportional to the shaft speed. Therefore, the core of the re-sampling process is to capture the relationship between the time and rotational angle based upon shaft speed. However, if the variation of shaft speed is involved in the relationship, then consideration of the acceleration of the shaft is unavoidable. The assumption is usually made that the shaft angular acceleration is constant. With regard to this point, a study of the paper by Fyfe and Munck (1997) gives a simple and precise mathematical explanation which is crucial for understanding the re-sampling process. In their research, a constant angular acceleration is assumed and the shaft angle θ is described by a quadratic equation of the following form:

$$\theta(t) = b_0 + b_1 t + b_2 t^2 \tag{1.1}$$

The unknown coefficients b_0, b_1 and b_2 are found by fitting three successive keyphasor arrival times t_1, t_2 and t_3 which occur at known shaft angle increments. Once these values are known, equation (1.1) may be solved for t, yielding

$$t = \left(\frac{1}{2b_2} \left[\sqrt{4b_2(\theta - b_0) + b_1^{\,2}} - b_1 \right] \right) \tag{1.2}$$

From this equation, any value of θ may be entered and the corresponding time t will be returned. This forms the basis of the re-sampling algorithm.

Based upon the above explanation of re-sampling, one should discuss some of the key assumptions. Obviously, since the assumption of constant angular acceleration, $\ddot{\theta}(t) = 2b_2$ the above calculation is not an ideal solution for the re-sampling problem. For the real machine start-up or coast down, the angular acceleration may generally not be constant. Therefore the angular velocity may not be linear. Figure 1.1 illustrates an exaggerated case: the continuous line is a possible real angular speed time history, while the dashed straight line may be used in COT analysis under the assumption of constant angular acceleration.

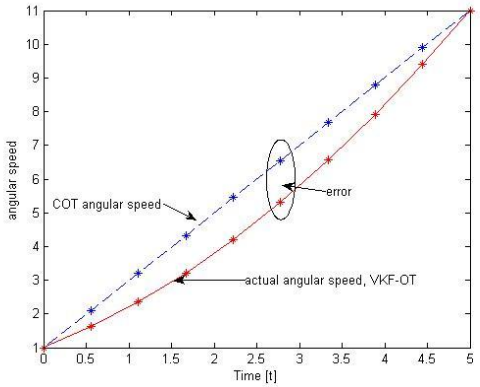

Figure 1.1 Possible real angular speed time history and the COT assumption

From Figure 1.1, the angular speed error introduced by the assumption is clear. In some software (such as: Vibratools in Matlab, 2005), this is even further simplified by assuming zero angular acceleration for one revolution, with a

corresponding constant angular velocity. This is of course not an ideal choice, especially when rotational speed is slow and ever changing as is the case shown in Figure 1.1. However it becomes a comparatively better choice when one considers high speed rotating machines with small angular acceleration. For normal machinery, a sharp acceleration start-up or coast down is not desirable for the sake of machine life, and hence the shaft acceleration is usually small. Thus, the assumption of zero angular acceleration within one revolution becomes a reasonable choice. In the following chapters, this assumption will be used as a basis of COT analysis. However the limitations of this assumption should always be borne in mind.

For example: once the zero acceleration assumption is applied, how does the sampling within each revolution influence the final result? Consider for instance the case of 100 samples per revolution, which means that over the period of one sample the angular displacement is $\theta = 360^{\circ}/100 = 3.6^{\circ}$. However, if 10 samples per revolution are taken, the angular displacement between each sample becomes $\theta = 360^{\circ}/10 = 36^{\circ}$. Clearly, the incremental difference here is very large between the different choices of sampling increments. If 100 and 10 samples are used to sample a basic sinusoidal wave over 5 seconds, the results are shown in Figure 1.2.

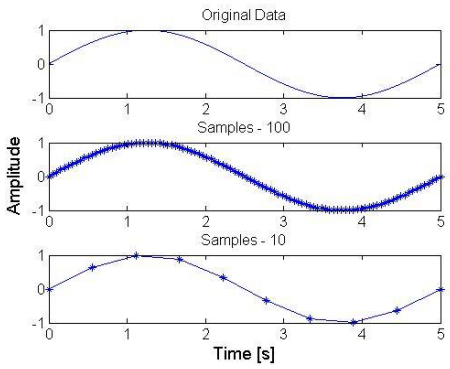

Figure 1.2 Resampling with different numbers of samples per revolution

From Figure 1.2, it can be seen that with the decrease of the number of samples per revolution, the accuracy of the re-sampling result decreases. This is obviously not good for the accuracy of the final results. Since the re-sampled data will be further subjected to Fourier analysis, the more the deviation from a sinusoidal wave, the more order peaks will appear in the final order spectrum map. But all these are due to the low number of sampling points instead of real physical phenomena. Thus, as can be expected, more re-sampling points are desirable for accuracy. Some other influence factors, such as keyphasor timing accuracy, multiple keyphasor pulses, interpolation methods, etc. also definitely influence the final result and have been extensively discussed in literature (see for example Fyfe & Munck, 1997).

Based upon the above analysis, despite the constant speed assumption, COT is nevertheless a very useful order tracking technique. From the non-stationary rotational speed point of view, computed order tracking can effectively transform time domain data to angle domain data. Blough (2003) uses a graphic representation to explain this transforming process on a simple sine wave, as is shown in Figure 1.3

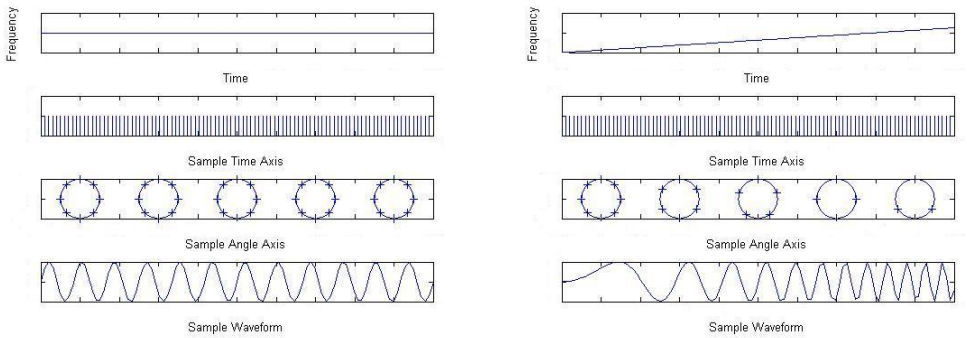

(a) Note: Constant $\Delta t = \text{Constant}\ \Delta\theta$ (b) Note: Constant $\Delta t \neq \text{Constant}\ \Delta\theta$

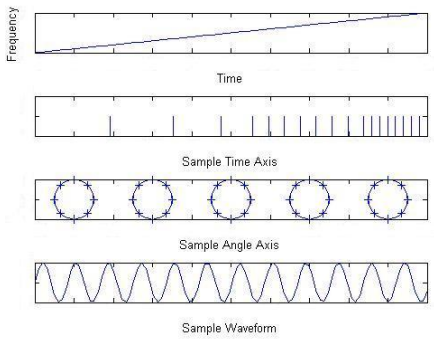

(c) Note: Variable $\Delta t \rightarrow$ Constant $\Delta\theta$

Figure 1.3 Sampling illustration in the time and angle domain with stationary and varying frequencies

Figure 1.3(a) represents the case for a stationary frequency sine wave sampled with a constant Δt. Figure 1.3(b) is the case for a varying frequency sine wave sampled with a constant Δt. Figure 1.3(c) is the case for the same varying frequency data re-sampled with a constant $\Delta\theta$. Clearly, the re-sampled data have properties similar to a stationary sine wave sampled with uniform time intervals. Both Figures 1.3(a) and 1.3(c) finally represent a periodic sine wave. It is interesting to see that the non-stationary sine wave in the time domain (Figure 1.3(b)), has been transformed to the stationary angle domain (Figure 1.3(c)). This uniformly spaced angle domain data is suitable to be processed by using the Fourier Transform to obtain amplitude and phase estimates of the orders of interest. This implies a clearer analysis of the signal using the Fourier Transform and also indicates that the re-sampling can be applied to harmonic waves and is not confined to the data that re-sampled through rotational speed. This characteristic is used in the ICR technique presented in this research. However, it is not difficult to see that COT does not address the quality of the raw data. Imperfections, such as distorted harmonic waves and noise, continue to exist after re-sampling process.

b. Current research on COT

In the literature, there are several papers regarding with the choice of parameters of COT. For instance, Fyfe and Munck (1997) studied the method in detail to examine which factors or assumptions have the greatest effect on the accuracy of COT. They find that this method is extremely sensitive to the timing accuracy of the key phasor pulses and also point out that high order interpolation in the process of re-sampling will greatly improve the spectral accuracy. Similarly, Saavedra and Rodriguez (2006) use data from various simulations to assess the effect of the assumptions inherent in the COT on accuracy and determine the effects of different user-defined factors: the signal and tachometer pulse sampling frequency, the method of amplitude interpolation and the number of tachometer pulses per revolution. Liu and Jiang (2007) also do something similar in discussing the principles of how to select the parameters in COT.

Some researchers compared different order tracking methods with COT. Bossley et al. (1999) comprehensively study three different synchronous sampling schemes: the traditional hardware solution, computed order tracking and a hybrid of the two. The three methods are assessed on data produced from a simulation of the coast down of a gas turbine shaft and therefore allow for studies of various interpolation algorithms. This ensures that the most appropriate algorithms are identified and COT is found to be superior.

Some researchers also focus on the implementation of this technique in real applications. Li (2007) develops a new method of combining COT and bi-spectrum analysis to detect gear crack faults in a gearbox under non-stationary run-up conditions. The experimental results show that order tracking with the bi-spectrum technique can effectively diagnose the gear faults. He, Zhang and Wen (2007) study fault issues of gear wear phenomena by using the COT technique. Their experimental studies prove that COT has the ability to detect the

fault issue of gear wear and compared with the traditional spectral analysis, COT presents several advantages. Eggers, Heyns and Stander (2007) study COT to detect gear condition in a bi-directional rotating mine dragline. Various speed interpolation methods are used to realize COT. Their studies show that COT can be successfully employed in real environments. Guo, Chi and Zheng (2008) use independent component analysis (a statistical method), to reduce the non-order noise for COT analysis and analysis results show the present approach is useful for fault diagnostic applications of rotating machinery.

1.3.2 Vold-Kalman filter order tracking

VKF-OT is a comparatively new technique. It was first adapted to order tracking by Vold and Leuridan (1993). It is a fundamentally different method from Fourier Transform based order tracking and computed order tracking. During the past seventeen years, many researchers like Vold, Mains and Blough (1997), Vold, Herlufson, Mains and Corwin-Renner (1997), Feldbauer and Holdrich (2000), Tůma (2005), Pan and Lin (2006), etc. have reported on the theory of VKF-OT. The characteristics of Vold-Kalman filter order tracking have been presented by Herlufsen et al. (1999). Recently, the main principles and limitations of current order tracking methods have been summarized by Brandt et al. (2005) where the VKF-OT is also discussed as a main theme. Its fundamental theory has therefore become much clearer to the engineering community. Some companies have commercialized this technique into their software, e.g. Brüel & Kjær and MTS Testing Solutions. Brüel & Kjær develops the Vold-Kalman order tracking filter into a commercial product and states that VKF-OT allows high-performance tracking of harmonic responses, or orders, of periodic loads in mechanical and acoustical systems. This method allows beat free extraction of close and crossing orders in systems with multiple shafts, and features a finer frequency and order resolution than conventional techniques. The product material of Brüel & Kjær also documents the advantages of this kind of order tracking method compared

with the computed order tracking method, as that of much shorter transients, no phase bias, no slew rate limitations and order information which can be extracted in the time domain. Blough (2003) points out that one of the key advantages of the second generation Vold-Kalman filter is the lack of constraints on frequency and slew rate. However, Wang and Heyns (2008) point out that during the filtering process, the filtered time domain order waveforms will retain the non-stationary frequency effect as in the raw data. It is therefore not suitable for further Fourier analysis, which is inferior to the COT in this regard. It should also be borne in mind that since the original VKF-OT requires longer computational time due to its mathematics, it is therefore not usually used in online monitoring. Quite recently however, Pan and Wu (2007) proposed an adaptive Vold-Kalman filtering order tracking approach to overcome the drawbacks of the original VKF-OT scheme for condition monitoring on this issue. Their work solves the problem and gives a good accuracy with reasonable computational time for VKF-OT. This makes the technique a more practical and powerful tool and renders online condition monitoring by using VKF-OT possible and feasible.

Tůma (undated study notes) shows that the Vold-Kalman filter is based upon so-called data and structural equations, with both of these equations that are excited by unknown functions on the right hand side. In his study notes, both the first and second generation Vold-Kalman filters as well as their differences are explained clearly in terms of the mathematics. The main difference between the two generations lies in the formula of the data and structural equations. In the first generation Vold-Kalman filter the amplitude and phase modulated order signal is described in a general term, such as $x(n)$. However amplitude envelope and phase for an order signal are considered separately in the second generation of Vold-Kalman filter order tracking, such as $x(n)e^{j\Theta}$ where $x(n)$ does not represent the whole order vibration any more but order envelope. Although $x(n)$ in first generation and $x(n)e^{j\Theta}$ in the second generation look different in their

form, however they are essentially the same and both represent an order vibration. Further, Tůma (2005) presents a paper to deal with the often-neglected issue of setting the filter pass band, which is fundamental to the theory of his MATLAB scripts.

In essence, Herlufsen et al. (1999) argue that the Vold-Kalman filter defines local constraints, which require that the unknown phase assigned orders are smooth and that the sum of the orders should approximate the total measured signal. The smoothness condition is called the structural equation and the relationship with the measured data is called the data equation. In this paper, they discussed characteristics of one, two and three pole Vold-Kalman filters which is a guideline for the choice of suitable pole number for Vold-Kalman filter.

Wang (2008) summarizes in his master's dissertation, what VKF-OT is and how to implement it. He essentially develops a whole package of Vold-Kalman filter application procedures which demonstrate the mathematical fundamentals as well as the choice of filter bandwidth. This forms the basis of the working algorithm and MATLAB scripts that are used in the Vold-Kalman filtering applications in this work. While Wang also mentions that this package is not the only route to the application of VKF-OT, it provides a good introduction to this technique.

Relating to VKF-OT applications, Guo, Tan, Huang and Zhang (2008) use the independent component analysis method to remove crossing noise in VKF-OT so that it overcomes traditional problems for cross-noise decoupling.

The application of VKF-OT on real machinery however is still in the initial period. Not many papers deal with the application of this technique. Pan and Lin (2006) published a comprehensive paper about VKF-OT. They explain the detail of the theory of VKF-OT in two different settings, namely, angular-velocity VKF-OT and angular-displacement VKF-OT. Further they examine the effectiveness of

applying the theory in their experimental work. In 2008, Pan, Li and Cheng (2008) established a whole package for a remote online machine condition monitoring system. In their package, VKF-OT is also used as a key signal processing method to diagnose machine conditions. Recently, Wang and Heyns (2009) studied the choice of Vold-Kalman filter bandwidth in a simple rotor simulation model and further apply the VKF-OT technique in condition monitoring of an automotive alternator stator with faults. The result shows that the VKF-OT is an effective method in condition monitoring.

Based upon the preceding literature survey, it is not difficult to conclude that VKF-OT is an effective and promising tool for condition monitoring rotating machinery, and is clearly one of the best available techniques for performing order tracking. But it needs more research on full practical utilisation of the technique, as well as simplification for new users.

1.3.3 Intrinsic mode functions through empirical mode decomposition

In 1998, Huang and his colleagues (Huang et al., 1998) proposed a novel approach called the Hilbert-Huang transform (HHT) for analysing nonlinear and non-stationary signals. The key part of the method is the empirical mode decomposition (EMD) with which any complicated data set can be decomposed into a finite and often small number of intrinsic mode functions (IMFs) that permits well-behaved Hilbert Transforms.

With EMD, any complicated signal will be broken down into a finite number of IMFs based on the local characteristic time scale of the signal. The IMFs represent a collection of natural oscillatory modes embedded in the signal, from high frequency to low frequency. Originally, IMFs were viewed as mono-components representing some intrinsic physical meaning and making sense of instantaneous frequency for further Hilbert Transformation. The idea of

mono-components however is arguable. Cohen (1995) first introduces the term but does not give a clear definition. For lack of precise definition, the narrow band component defined in the book of Schwartz, Bennett and Stein (1966) is therefore adopted as an alternative way to describe IMF. This makes the EMD process more like a group of narrow band filters, and the method can therefore be treated as a self-adaptive dyadic filter bank (Flandrin, Rilling and Gonçalvés, 2004) which allows each IMF to be determined by the signal itself rather than pre-determined parameters. During the past few years, the HHT and the EMD method have been studied extensively in theory and applications. Unfortunately, there is still no single universally recognized precise mathematical definition for the HHT and EMD.

However some serious mathematical works on its fundamental theory are now available. These include work by Rilling, Flandrin and Gonçalvés (2003, 2004), Daetig and Schlurmann (2004), Sharpley and Vatchev (2006), and Feldman (2008). Very recently, Feldman (2009) further studied the characteristics of the EMD method. He analyzes the very special and useful case of decomposition of two harmonics which sheds some light on the nature of the resolution of each IMF. He describes in his paper the analytical basics of the EMD method and presents a theoretical limiting frequency resolution for EMD to decompose two harmonic tones. This undoubtedly helps a great deal to understand the resolution of EMD as a filter bank. He mentions that frequency and amplitude ratios of two harmonics can be separated into three different groups, to evaluate the resolution of the EMD method for two harmonics and plot these on 2-D and 3-D graphs which enrich the understanding of the fundamentals of resolution for EMD and is a useful contribution in the theoretical study of EMD.

Another important contribution was made by Huang, Wu and Long (2006) who developed an iterative normalized scheme, enabling any IMF to be separated empirically and uniquely into envelope (Amplitude Modulation (AM)) and carrier

(Frequency Modulation (FM)) parts, which resolve many traditional difficulties associated with instantaneous frequency. The technique is therefore called empirical AM/FM demodulation. However, the empirical FM part may contain riding waves and is no longer an intrinsic mode function, which renders the instantaneous frequency nonsensical. (A riding wave is defined as follows: In a signal, if there exists a local minimum greater than zero between two successive local maxima, or if there exists a local maximum less than zero between two successive local minima, the segment between these two successive local maxima (or local minima) is called a riding wave (Yang, Yang, Qing and Huang, 2008). In the paper, there are several examples of riding waves and the existence of riding waves violates the definition of an IMF.) To overcome this drawback, Yang, Yang, Qing and Huang (2008) improve the empirical AM/FM demodulation method into a riding wave turnover-empirical AM/FM demodulation and their experiments show positive results.

Rato, Ortigueira and Batista (2008) review some important questions related to the effective performance of the EMD method. Some drawbacks of EMD are put forward and solutions for these drawbacks are proposed. Numerical simulations are also carried out to empirically evaluate the proposed modified EMD method. This work provides comprehensive guidelines to understand the pros and cons of the EMD method.

In recent years, there have been many papers discussing the application of HHT or EMD in real machinery problems, simulation studies and practical signal processing. For instance in some real machinery problems, Liu, Riemenschneider and Xu (2006) apply HHT to vibration signal analysis for localised gearbox incipient tooth crack fault. The results show that the EMD algorithms and the Hilbert spectrum perform excellently and find that this technique is more effective than the commonly used continuous wavelet transform in the detection of vibration signatures.

Rai and Mohanty (2007) use the Fast Fourier Transform (FFT) of intrinsic mode functions in EMD, to enhance the ability of detecting incipient bearing faults. Their analysis results indicate the effectiveness of using a frequency domain approach in EMD and its efficiency as one of the best-suited techniques for bearing fault diagnosis.

Gao, Duan, Fan and Meng (2008) also investigate the EMD approach for rotating machine fault diagnosis. In their research, they show that IMFs sometimes fail to reveal the signal characteristics due to the effect of noise and hence they develop the combined mode function (CMF) method, which combines the neighbouring IMFs to obtain a more precise oscillation mode. Finally, they apply EMD and CMF methods to a practical fault signal of a power generator. The results show that both of the techniques are effective.

Chen, Yu, Tang and Yang (2009) use EMD to diagnose local rub-impact in a rotor system. Local rub-impact faults in a rotor usually lead to amplitude-modulated vibration signals, which are however submerged in the background of noise. Their studies show that the EMD successfully extracts the modulated vibration signal from local rub-impact, while there are no distinct amplitude-modulated characteristics of the vibration signals under conditions without local rub-impact. It is therefore concluded that the EMD method can be effectively applied for local rub-impact fault diagnosis.

Wu and Qu (2009) mention in their paper that in practice most sub-harmonic signals are closely related to time variables and can manifest in large amplitude fluctuation, transient vibration or modulation signals in the time domain. Therefore, they use the EMD method to extract intrinsic mode functions from some actual vibration signals to diagnose malfunction in large rotating machinery due to rotating stall and pipe excitation related problems in the system. They

conclude that the EMD method provides an attractive alternative to the traditional diagnostic methods.

For some simulation and signal studies, Chen, Yan and Jiang (2007) propose a dynamic-based damage detection method for large structural systems using HHT. Their method is verified numerically by implementing the scheme on a model of a wing box and the results show that the proposed damage detection method is very robust.

Guo and Peng (2007) establish a finite element rotor model with a propagating transverse crack. By analysing the start-up transient response of a rotor, they demonstrate that the HHT is an effective tool for the analysis of non-linear, unsteady transient vibration response.

Li and Meng (2005) study the capability of the EMD method to extract a harmonic signal from a chaotic background. Since numerous observable chaotic signals can be detected in real-world data, such as electrocardiograph signals, extracting a harmonic signal from a chaotic signal becomes very important. They generate a harmonic signal contaminated with a chaotic interference introduced by a Duffing oscillator, and then use the EMD method to extract the harmonic signal from the chaotic interference. Their simulation results show that the harmonic signals can be effectively recovered from the contaminated signals by the EMD approach.

Li, Deng and Dai (2006) develop a technique that combine EMD and wavelet transform to detect the changes of structure response data. By using different test models, they demonstrate that combining EMD and continuous wavelet transform can be used to identify the time at which structural damage occurs more sharply and effectively, than by using the wavelet transform method alone.

1.4 Scope of work

Based upon the problem statements and the literature surveys presented above, it is now necessary to explain the inter-relationship of the three different order tracking techniques and their usefulness in condition monitoring of rotating machines, to further understanding of the significance of this work. In fact, the three improved order tracking approaches have not been chosen arbitrarily, but are based upon the inter-relationship between the order tracking techniques under consideration. The advantages and limitations of each of these techniques are explored above in paragraph 1.2. Figure 1.4 below depicts the relationship of three approaches developed in Table 1.1 in terms of different kinds of arrows that indicate the different relationships between techniques, so that one may have a better idea of how this work integrates these techniques. The following explanation of each approach further highlights the possible benefits in condition monitoring and renders novel methods that will be thoroughly discussed in the thesis.

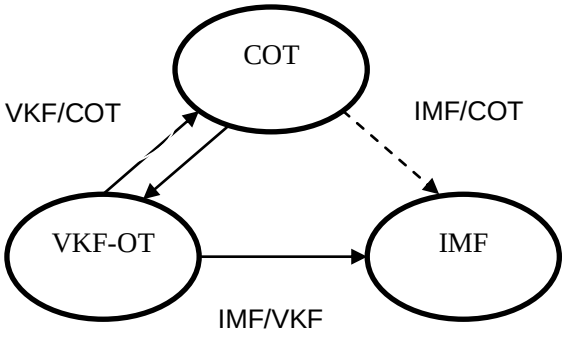

Figure 1.4 Integrating three independent order tracking techniques

VKF/COT → VKC-OT

The two way solid arrows linking VKF-OT and COT emphasize that VKF-OT and COT are indeed complementary to each other, each with distinct advantages and disadvantages which make up for each other. The VKF-OT advantage of

focusing on individual orders and the COT advantage of excluding frequency variation may be combined. The VKF-OT disadvantage of frequency variation which remains in the filtered time domain signals and the COT inability to focus on one individual order may therefore also be overcome. This is why the idea of combined use of these two order tracking techniques is developed in this work. This approach is of significant importance in real applications. In condition monitoring, focusing on an order signal while simultaneously excluding the effect of speed variation from the order spectrum, definitely enhances the ability of specific orders in condition monitoring for rotating machinery. Vold-Kalman filter and computed order tracking, VKC-OT, is therefore presented to fulfill this requirement.

IMF/VKF → IVK-OT

The one way solid arrow linking VKF-OT to IMF explains that the VKF-OT results may belong to the set of IMFs from EMD, in other words, VKF-OT results can be a subset of the IMFs. Each IMF may include one or more orders by the filtering of Vold-Kalman filter. Thus, through subtracting VKF-OT results from an IMF, the separation or differentiation on an IMF becomes possible. Therefore, in this work, VKF-OT will be used to assist further decomposition of IMFs in terms of rotational speed. Then, the sequential use of IMF and VKF-OT (IVK-OT) is developed. Again for condition monitoring purposes, this further decomposition process is of great practical importance. The VKC-OT discussed above, emphasize examining specific orders of interest. As a result, it may lose the ability to examine vibration signals that modulate orders. However, machine faults may result in unpredictably complex vibrations. They may be synchronous or non-synchronous with the rotational speed and modulate dominant order signals, By means of an example a rub-impact of a rotating machine may lead to a complex nonlinear vibration response. Evidently vibration signals that modulate orders are critical information for condition monitoring and not necessarily synchronous with

rotational speed. Therefore, to separate and study these vibrations provide additional useful information for machine fault diagnostics. The IVK-OT may therefore serve as a means for analyst to discover this useful information in IMFs.

IMF/COT → ICR

The one way dashed line arrow between COT and IMF indicates that the two methods are not directly related. However, due to the simple special data structure of an IMF (this will be further explained in chapter 2, paragraph 2.3), the core re-sampling idea of COT that transforms signals from non-stationary to stationary, may be borrowed into an IMF. And therefore speed variation effects in an IMF can be largely excluded, so that an empirical approximation of computed order tracking effects without the aid of rotational speed can be achieved. Thus in this work, a novel reconstruction procedure of an IMF will therefore be developed, namely intrinsic cycle re-sampling method (ICR). Two aspects are considered advantageous in this technique. Firstly, for order tracking analysis a technique which does not require measured rotational speed is of great practical use. Secondly, it is known that IMFs may include abundant machine fault information. If made more readily available in practice through simplified analysis, approximate order analysis may most likely enhance machine fault diagnostic ability and therefore offers an alternative condition monitoring method worthwhile to explore. Indeed, this technique provides a good alternative approach to condition monitoring. This is demonstrated in simulation and experimental studies in chapter 3 and 4 where the ICR method is used to monitor gear mesh faults.

In short, three independent order tracking techniques are integrated to capitalize on their distinct respective advantages and offset their disadvantages. These integrations are all based upon their potential practical significance for condition monitoring. In the following chapter the focus will be on the developments of

three order tracking improved approaches. Then, simulation and experimental studies will prove the effectiveness and usefulness of these improvements.

Chapter 2 Logic developments of three novel improved order tracking approaches

In this chapter, three novel improved order tracking approaches are developed based upon available order tracking methods, namely Vold-Kalman filter order tracking and computed order tracking, Intrinsic mode function and Vold-Kalman filter order tracking and intrinsic cycle re-sampling. The logic of the discussions on three improved approaches is outlined below to simplify understanding of the thesis:

1. The discussions on the Vold-Kalman filter and computed order tracking (VKC-OT) method emphasize the benefits that each order tracking method (VKF-OT and COT) brings to the subsequent Fourier analysis so that the method can provide clearer order spectra.

2. The discussions on the intrinsic mode function and Vold-Kalman filter order tracking (IVK-OT) method emphasize the relationship between an intrinsic mode function and an order wave so that the sequential use of the two methods is developed to distinguish useful information in an IMF in terms of rotational speed.

3. The discussions on intrinsic cycle re-sampling (ICR) method emphasize the logic of exclusion frequency variation effects in an IMF and the interpretation of the resultant reconstructed IMF through empirical re-sampling. So that the rationale of the method to approximate order tracking effects as well as how to use ICR spectra results can be clarified.

2.1 Vold-Kalman filter and computed order tracking

The first technique is a novel technique that combines the use of Vold-Kalman filter order tracking and computed order tracking to improve the subsequent Fourier analysis and therefore to achieve a clear and focused order spectrum. It is called Vold-Kalman filter and computed order tracking (VKC-OT). Combining the use of the two order tracking methods to improve the subsequent Fourier analysis requires an understanding of the nature of these techniques and how their characteristics affect the Fourier analysis. Therefore, in the following each order tracking method will be discussed in terms of its characteristics for the subsequent Fourier analysis.

2.1.1 Discussions on Vold-Kalman filter order tracking

Herlufsen et al. (1999) describe order tracking as the art and science of extracting the sinusoidal content of measurements, with the sinusoidal content or orders/harmonics at frequencies that are multiples of the fundamental rotational frequency. To this end, VKF-OT relies on two equations to complete the filtering, namely the data equation and the structural equation. These equations define local constraints, which ensure that the unknown phase assigned orders are smooth and that the sum of the orders should approximate the total measured signal. This implies that the order components extracted from the Vold-Kalman filter should be harmonic and smooth waves. To explore the reason that these arguments are valid, the analytical form of data and structural equations described by Tůma (2005) are considered here for discussion.

Data equation

Assuming a second-generation Vold-Kalman filter for single order filtering, the data equation is defined as

$$y(n) = x(n)e^{j\Theta(n)} + \eta(n) \tag{2.1}$$

where $y(n)$ is the measured data, $x(n)$ is a complex envelope of filtered signal, $e^{j\Theta(n)}$ is a complex carrier wave, and

$$\Theta(n) = \sum_{i=1}^{n} \omega(i)\Delta t \tag{2.2}$$

where $\omega(i)$ is the discrete angular frequency, and $\eta(n)$ is the random noise and other order components, or error term.

From equation (2.1), it clearly shows that the order component $x(n)e^{j\Theta(n)}$ is a harmonic natured waveform. The frequency modulation of the signal is determined by $e^{j\Theta(n)}$. Further, equation (2.2) indicates that $\Theta(n)$ is the sum of $\omega(i)\Delta t$ from $i = 1,...,n$, and $\omega(i)$ may vary from time to time, or be non-stationary, consequently $x(n)e^{j\Theta(n)}$ may also be non-stationary. It follows from the above analysis that the order component from a Vold-Kalman filter is a harmonic natured wave which may be non-stationary.

Structural equation

The structural equation provides the smoothness of successive digital points of filtered data, by fitting a low-order polynomial to the sequence $x(n)$. This condition is enforced through the structural equation with the unknown non-homogeneity term $\varepsilon(n)$ on the right-hand side of the equation. The polynomial order designates the number of the filter poles. By way of example, the structural equation for a two-pole filter is given by,

$$x(n) - 2x(n+1) + x(n+2) = \varepsilon(n) \tag{2.3}$$

Rearranging

$$x(n) = 2x(n+1) - x(n+2) + \varepsilon(n) \tag{2.4}$$

It can be seen that with the two-pole filter, for any three immediately adjacent points of the sequence $x(n)$ are constrained through the structural equation. This smoothes the filtered order data from the raw data. To demonstrate this idea, the smoothness condition for such a two-pole filter is illustrated in Appendix by rearranging equations (2.3) to (2.4).

Considering the data and structural equations presented above, one may conclude that the order components extracted from the Vold-Kalman filter are smooth and harmonic waves, but they may be non-stationary.

2.1.2 Discussions on computed order tracking

Computed order tracking is a very commonly performed and effective order tracking technique. Although inevitably errors will be introduced during the re-sampling process and its artificial assumptions (Fyfe and Munck, 1997), the technique still renders very useful results, and effectively transforms non-stationary time domain data to stationary angular domain data for rotating machinery. Blough (2003) uses a graphic representation to explain this transformation process on a simple sine wave. This is illustrated in chapter 1 Figure 1.3. It clearly demonstrates that the re-sampled data has the same properties as a stationary frequency sine wave sampled at uniform time intervals. This uniformly spaced re-sampled data or stationary re-sampled data can be effectively processed by using traditional Fourier transform to obtain clear estimates of the orders of interest. This implies a clearer analysis of the signal using the Fourier transform. However, COT does not address the quality of the raw data. Imperfections, such as distorted harmonic waves and noise, continue to exist. Besides, COT can only deal with the raw data as a whole and therefore loses the ability to separate each different order signal from the raw signal.

2.1.3 Development of Vold-Kalman filter and computed order tracking

The main ideas from above discussions about two techniques may be summarized as follows:

- Equation (2.1) indicates that the order components from the Vold-Kalman filter are clearly harmonic in nature.

- Equations (2.1) and (2.2) show that these order components may be harmonic waves of varying frequency due to the possibility of the varying fundamental frequency $\omega(i)$

- Equation (2.3) can be further demonstrated that the filtered order components from the Vold-Kalman filter are smooth waves.

- It can be seen from discussion of computed order tracking that the re-sampling process can transform varying frequency harmonic waves to stationary frequency harmonic waves. A Fourier analysis is then used to transform the re-sampled time domain data to the order domain.

Based upon the discussion of Vold-Kalman filter order tracking above, it is argued that the Vold-Kalman filter enforces the smoothness as well as the harmonic nature of the filtered data. The harmonic nature does not, however, ensure a stationary harmonic wave, although the re-sampling process can transform data from a non-stationary harmonic wave to a stationary harmonic wave in frequency. This suggests the possibility of using a Vold-Kalman filter to obtain smooth but possibly varying frequency harmonic waves and then transforming them to

become stationary in frequency by using the re-sampling process of computed order tracking.

Therefore, if data are obtained from a non-stationary and noisy real machinery system and the data are then processed through a Vold-Kalman filter followed by the re-sampling process of COT, one may obtain order waves that are smooth, stationary frequency harmonic waves. Under these conditions the stringent requirements of Fourier analysis are largely satisfied. One may therefore expect clear and focused order spectra by means of this process. Based upon the above reasoning it follows that if the two order tracking methods are applied in sequence (VKF-OT and then COT), the restrictions of Fourier analysis can be largely satisfied to render clean order spectra. This combined use of order tracking techniques may be referred to as Vold-Kalman filter and computed order tracking (VKC-OT). Figure 2.1 describes graphically the logic of the combined use of the two order tracking techniques in sequence.

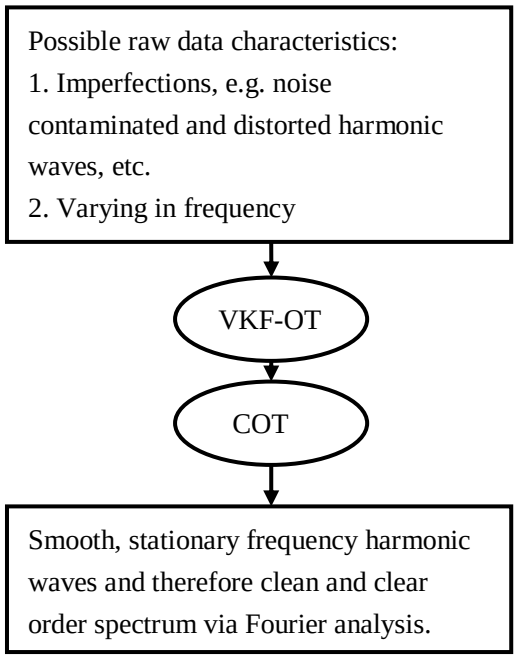

Figure 2.1 Logic of VKC-OT

2.2 Intrinsic mode function and Vold-Kalman filter order tracking

The literature indicates that both IMFs and order tracking techniques are effective in diagnosing faults in rotating machinery, e.g. Eggers et al. (2007); Gao et al. (2008); Wu et al. (2009). This suggests investigating the relationship between IMFs and order waves. However, this has not been explored further in the literature. To this end, the following will firstly exploit the relationship between an intrinsic mode function (IMF) and an order wave in rotating machinery and then develop the Intrinsic mode function and Vold-Kalman filter order tracking (IVK-OT) technique of combining abilities of two kinds of methods.

2.2.1 Discussions on the relationship between an intrinsic mode function and an order waveform in time domain

a. An order waveform

As has been discussed in the literature survey, there are several types of order tracking techniques. Some cannot extract time domain data (e.g. COT) whereas some are capable of extracting time waveforms by using additional information, usually rotational frequency (e.g. VKF-OT). In spite of these distinctions, in essence an order can generally be described as 'a time varying phasor that rotates with an instantaneous frequency related to the rotational frequency of the reference shaft', as shown in equation (2.5) (Blough, 2003).

$$x(t) = A(k,t)\sin\left(2\pi i\left(\frac{k}{p}\right)t + \phi_k\right) \tag{2.5}$$

where $x(t)$ is the order time series, t is time, $A(k.t)$ is the amplitude of the order k which is being tracked as a function of t, p is the period of the primary order in seconds, and ϕ_k is the phase angle of order k. Equation (2.5) defines an order as a time series combining amplitude modulation (AM) and frequency modulation (FM). Both amplitude and frequency modulations are functions of the order of interest k and time t. It should also be noted that equation (2.5) actually enforces an order wave of a sinusoidal nature.

b. An intrinsic mode function from empirical mode decomposition

A discussion about an IMF should start with EMD. For a given signal $x_g(t)$, EMD ends up with a representation of the form (Flandrin et al., 2004):

$$x_g(t) = \sum_{k=1}^{K} d_k(t) + m_K(t) \tag{2.6}$$

where $\{ d_k(t), k = 1,....K \}$ are the modes that are constrained to be zero-mean amplitude modulation frequency modulation waveforms and $m_K(t)$ represents a residue signal. These modes are called intrinsic mode functions (IMFs).

This methodology obviously does not give precise mathematical definitions of each $d_k(t)$ and $m_K(t)$. Flandrin et al. further point out that this makes it difficult to evaluate the performance of EMD. However, researchers (Huang et al., 2006 and Yang et al., 2008) have developed an empirical AM/FM demodulation technique for the purpose of resolving many of the traditional difficulties associated with instantaneous frequency calculations, giving a simple description of an IMF in terms of a normalized frequency modulation part and an amplitude modulation part. Accordingly, any IMF from $\{ d_k(t), k = 1,....K \}$ can be written as:

$$d(t) = A(t)\cos\phi_e(t). \tag{2.7}$$

The suffix k omitted means $d(t)$ can be any one of IMFs where $A(t)$ is the amplitude modulation part, $\cos\phi_e(t)$ is the normalized empirical frequency modulation part and t is time.

In the equation, $A(t)$ is determined by the empirical envelope obtained through the spline fitting of the maxima points of the IMF signal. Both $A(t)$ and $\cos\phi_e(t)$ are dependent on the data itself and are functions of time t. However, it should be noted that the term $\cos\phi_e(t)$ actually enforces the oscillatory nature, though at each time instant, the phase angle and frequency of the carrier wave will not both be defined.

From the basic discussions above regarding an order and an IMF, as well as equations (2.5), (2.6) and (2.7), it can now be observed that:

- An order can be extracted from the original signal as a modulated signal in both amplitude and frequency, as shown in equation (2.5). Similarly, EMD can also decompose the original signal into IMFs, which are amplitude and frequency modulation waveforms plus a residue signal.

- Both an order waveform and an IMF can be treated as two parts, namely amplitude parts $A(k,t)$ and $A(t)$ as well as phase parts $\sin\left(2\pi i\left(\frac{k}{p}\right)t+\phi_k\right)$ and $\cos\phi_e(t)$.

- The amplitude part $A(k,t)$ of the order waveform is a function of time t and order of interest k. The amplitude part $A(t)$ of an IMF is only a function of time t and is determined by the data itself. This implies that the order waveform amplitude can be part of an IMF amplitude or $A(k,t)\in A(t)$.

- Similarly, the phase part $\sin\left(2\pi i\left(\frac{k}{p}\right)t+\phi_k\right)$ of the order waveform and $\cos\phi_e(t)$ of an IMF can also have the relationship $\sin\left(2\pi i\left(\frac{k}{p}\right)t+\phi_k\right)\in\cos\phi_e(t)$.

It can therefore be inferred from these observations that an IMF may include order waveforms plus other relevant information. The combination of order waveforms

and other relevant information must satisfy the definition of an IMF. The definition of an IMF was originally stated by Huang et al. (1998) and has been referred to in Chapter 1 paragraph 1.2.3. This definition guarantees that amplitude and frequency modulation signals can both be extracted as IMFs.

2.2.2 Discussions on the relationship between an intrinsic mode function and an order waveform in order domain

The preceding discussions are based upon equations in the time domain. However, the order domain should also be considered so as to explore the characteristics of an order and an IMF. Firstly, equation (2.5) for an order may be written as an analytical signal:

$$x(\theta) = A_o(k,\theta)e^{jk\theta} \tag{2.8}$$

where $A_o(k,\theta)$ is the amplitude component of order k, $e^{jk\theta}$ is the unit sinusoidal wave of order k, k is the order of interest and θ is the angle.

Similarly, equation (2.7) for an IMF can also be written in the order domain as shown in equation (2.9). In this case, the amplitude and frequency modulations are both functions of angle θ instead of time t. Therefore, they may be considered as amplitude and order modulations in the order domain. Order domain analysis transforms non-stationary time-domain signals into stationary signals in angles for rotating machinery vibrations. Order signals are therefore periodic per revolution and Fourier expansion is suitable for the analysis. According to the Fourier expansion theory, a periodic signal can be approximated by Fourier expansions. Therefore any IMF $d(\theta)$ may also be expanded by Fourier expansion as in equation (2.9) in the order domain.

$$d(\theta) = A_o(\theta)\cos\phi_o(\theta) = \sum_{n=-\infty}^{\infty} C_n(\theta)e^{jn\theta} + R(\theta) \tag{2.9}$$

where $A_o(\theta)$ and $\cos\phi_o(\theta)$ are the amplitude and order modulations in the order domain, $C_n(\theta)$ are Fourier coefficients and $R(\theta)$ is a non-periodic signals in the order domain.

Comparing equations (2.8) and (2.9), one should note the following:

- The amplitude component $A_o(k,\theta)$ in equation (2.8) can be one of the amplitude components $C_n(\theta),\ n \in (1,\infty)$, in equation (2.9), and

- A unit sinusoidal component $e^{jk\theta}$ in equation (2.8) can be one of the components in $e^{jn\theta},\ n \in (1,\infty)$, in equation (2.9).

Clearly, an order wave can be a particular waveform contained in the IMF. However equation (2.9) indicates that an IMF can include signals other than orders. This discovery is in line with the previous time domain discussions.

2.2.3 Discussions on the resolution of an IMF

But considering the converse of equation (2.9), it however may not necessarily hold, i.e. a signal of the form of equation (2.9) may not necessarily constitute an IMF. This is because only signals that satisfy the definition of Huang et al. 1998, qualify as IMFs. If the composition of signals violates the definition, it will be further decomposed into different IMFs. This actually suggests that EMD as a filter bank is selective for each IMF. It is difficult to develop a general rule for this selective characteristic or resolution of each IMF, since in literature there is no universal mathematical equation reported for the EMD so far.

However, Feldman (2009) analyzed the special and useful case of the decomposition of two harmonics, demonstrating some of the important features of EMD, such as the nature of the resolution for each IMF. He describes an analytical basis for the EMD, and presents a theoretical limiting frequency resolution for EMD to decompose two harmonic tones. This helps to understand the resolution of EMD as filters.

Feldman shows that the frequency and amplitude ratios of two harmonics can be separated into three different groups, to evaluate the resolution of EMD for these harmonics:

- Harmonics with very close frequencies and a small amplitude, where $A_2 / A_1 \leq (\omega_1 / \omega_2)^2$ is unsuitable for EMD decomposition.
- Close frequency harmonics where $(\omega_1 / \omega_2)^2 \leq A_2 / A_1 \leq 2.4(\omega_1 / \omega_2)^{1.75}$ requires several sifting iterations for two harmonics to decompose.
- Distant frequencies and large amplitude harmonics where $A_2 / A_1 \geq 2.4(\omega_1 / \omega_2)^{1.75}$ can be well separated for a single iteration.

Based upon these criteria, one knows that if two harmonics have frequency and amplitude ratios of $A_2 / A_1 \leq (\omega_1 / \omega_2)^2$, EMD is incapable of separating them. This requirement is visually represented in Figure 2.2.

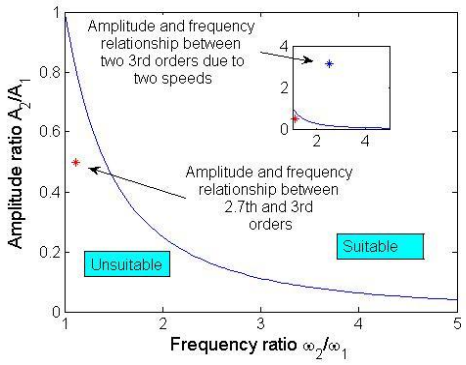

Figure 2.2 Theoretical boundary for the separation of two harmonics $A_2 / A_1 \le (\omega_1 / \omega_2)^2$

It is clear from Figure 2.2 that two harmonic signals can be decomposed by EMD, depending upon the amplitude and frequency ratio. The limiting boundary determines the region to the right where EMD is able to separate harmonics, and the region to the left where EMD cannot separate two harmonics (Feldman, 2009). This criterion is very useful for determining the decomposition of harmonic vibration signals like orders in rotating machines. (This criterion will be used in the simulation studies in Chapter 3 therefore some extra arrows and descriptions are indicated in the figure for future use).

However, the general case of equation (2.9) is not as simple as two harmonic tones, as it is a combination of an order with several other harmonic tones, as well as some other signals, and this is a case where Feldman's theory cannot be applied directly. For rotating machinery, vibrations which are non-synchronous with rotational speed are often small. Therefore if one considers $R(\theta)$ as being negligible over a short period, an order signal and the combination of other harmonic tones may be treated as two quasi-stationary harmonics over that period. Feldman's theory may therefore approximate the resolution of an IMF at each

instant. Though this is mathematically not rigorous, it does help to understand the behaviour of IMF.

In short, from all above discussion of the relationship between an IMF and an order in time and order domain as well as resolution of an IMF, it is clear that IMFs from EMD may include both orders and relevant vibrations. And relevant vibrations will modulate order signals so that, in rotating machine vibrations IMFs are usually order related oscillating waves.

2.2.4 Combined use of empirical mode decomposition and Vold-Kalman filter order tracking

From above studies, although EMD is limited in its ability to separate an order signal from other signals, it does have an edge over the traditional order tracking method, as it can capture signals that modulate the order waves. For a rotating machine, an order as defined in equation (2.5), only one specific AM and FM oscillatory waveform can be extracted. So, to a large extent, order tracking itself loses the capability of capturing signals that modulate the orders. But these signals are also critical for the vibration monitoring of rotating machinery. Vibration signals due to faults such as rotor cracks, looseness, worn-out parts, broken teeth or bearing problems are all closely related to the rotating speed or orders. These machine fault vibrations will usually modulate dominant order waves into modulated oscillating waves, which contain a rich source of machine fault information. As a matter of fact, detecting and separating this information from the dominant orders is of great importance. They are the key signatures of machine deterioration and closely related to the orders.

Besides, from the discussion of the relationship between an IMF and an order, it is clear that order tracking can solely focus on vibration signals that are strictly synchronous with the rotational speed and therefore lacks the ability to deal with

speed non-synchronous vibrations. The information contained in the speed non-synchronous signals however may also be valuable in terms of machine conditions and deserve to be further utilised. Vibrations that modulate dominant orders, however, may be synchronous or non-synchronous with rotational speed and are therefore usually difficult to extract by traditional order tracking methods alone. In this sense, empirical mode decomposition may include these vibrations with the orders into different intrinsic mode functions. Considering the intrinsic nature of both traditional order tracking methods and EMD, the IMFs from EMD may be further decomposed in terms of rotational speed through order tracking methods so that order signals and vibrations that modulate orders in an IMF may be distinguished. Consequently, the sequential use of EMD and Vold-Kalman filter order tracking method to further decompose order related IMFs is introduced in this research as intrinsic mode function and Vold-Kalman filter order tracking (IVK-OT). Figure 2.3 graphically illustrates the process and as for comparison, traditional VKF-OT is also illustrated. And the logic of IVK-OT is graphically summarized in Figure 2.4.

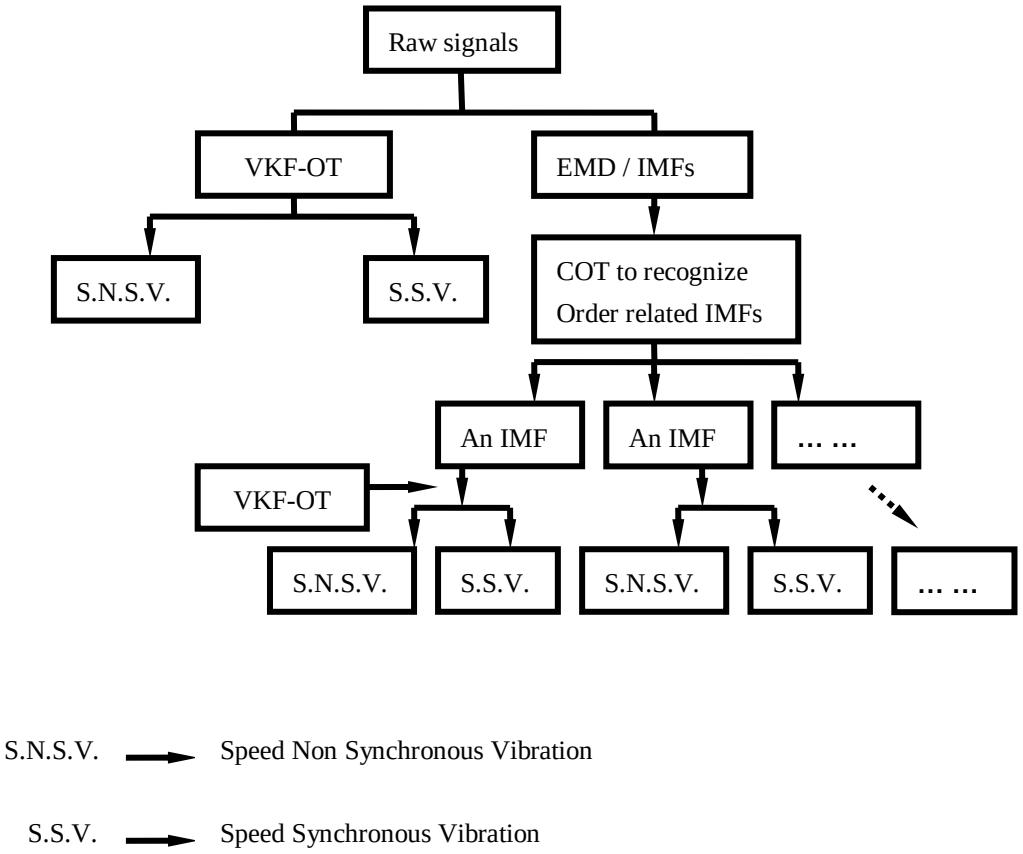

Figure 2.3 Symbolic explanation of IVK-OT the process compared with VKF-OT

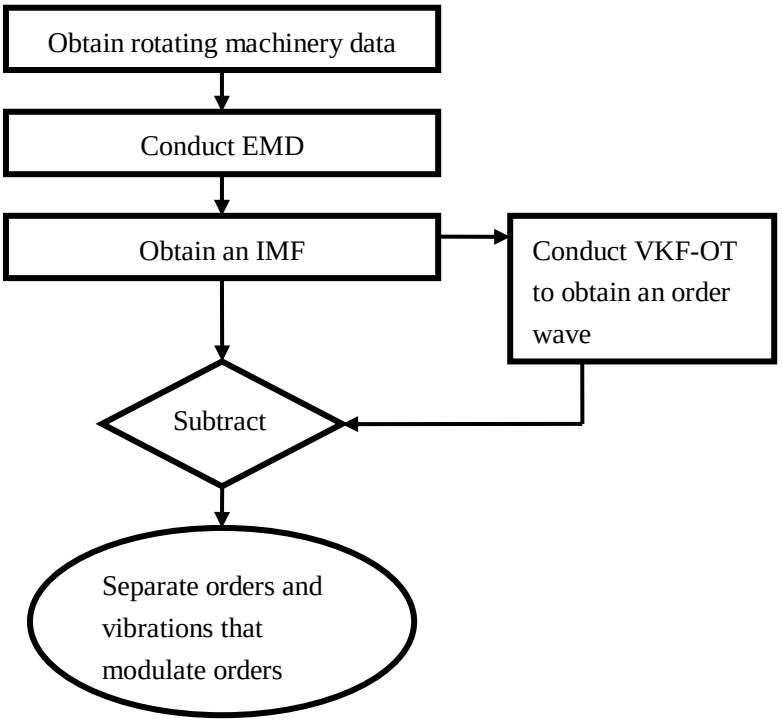

Figure 2.4 Logic of the combined use of EMD and VKT-OT

2.3 Intrinsic cycle re-sampling

The intrinsic cycle re-sampling (ICR) method is a novel way of reconstructing intrinsic mode function (IMF) from empirical mode decomposition (EMD) to approximate the effect of computed order tracking for rotating machine vibration signals. In stead of using traditional speed information to achieve the order tracking effects, an empirical re-sampling method is used on the IMF which approximates the order tracking effects that exclude frequency variations in an IMF. In the following, the logic of the technique to exclude frequency variation effects in an IMF is discussed so that the method can be developed.

2.3.1 Development of intrinsic cycle re-sampling

To begin with the ICR technique, it should repeatedly review the definition of an IMF from EMD. Huang et al. (1998) define an intrinsic mode function as a signal that satisfies two conditions:

- In the whole signal segment, the number of extrema and the number of zero crossings must be either equal or differ at most by one.
- At any point, the mean value of the envelope defined by the local maxima and the envelope defined by the local minima is zero.

From this original definition of an IMF, it can be concluded that each IMF is a symmetric and zero mean oscillation wave. This excludes two or more peaks within two successive zero crossings. However, the definition does not ensure that the frequency content of this symmetric oscillation wave is constant. Since the important purpose of computed order tracking is to exclude frequency variation from the rotational speed, it is, therefore, worthwhile to further investigate IMF signals with regards to the effects of frequency variation.

a. Intrinsic cycle

The intrinsic cycle (IC) is now introduced. Based upon the idea of an IMF, one may consider a symmetric oscillation wave about a zero mean and define the IC as follows:

Start from the first zero crossing of an IMF and consider two successive zero crossings. The entire signal within these three zero crossings constitute one intrinsic cycle. In the same way, the signal from the last zero crossing of a previous intrinsic cycle and including the following two successive zero crossings, constitute another intrinsic cycle, and so on.

The above definition of an IC from an IMF implies that there are one maximum, one minimum and three zero crossings within each IC. Each IC roughly resembles one period of a sine wave. Considering frequency variations in terms of the newly introduced ICs in an IMF, frequency variations in these approximately sinusoidal natured ICs are not constrained. Variations may exist within and between ICs. If the frequency variation of a signal is solely due to the varying rotational speed, order tracking effects can be achieved by eliminating the frequency variations of the ICs. This is therefore discussed below by considering frequency variations within and between ICs in an IMF.

b. Frequency variation within ICs

In computed order tracking (Fyfe and Munck, 1997) the assumption is usually made that the rotating shaft angular acceleration is constant or zero over one revolution, since large angular accelerations or decelerations are usually undesirable in practical machines. This is typically done in commercial software (Vibratools in Matlab, 2005). When there are several ICs within one revolution,

one could also assume angular acceleration within an IC is zero so that frequency variations within the ICs may be considered negligible. If this assumption is made and a constant rotational frequency within an IC is therefore implied, the focus in dealing with frequency variation effects may then shift to the frequency variations between ICs.

c. Frequency variation between ICs

One can now get rid of the frequency variations between ICs by re-sampling with an equal number of intervals within every IC. The frequency variations between ICs may therefore be discarded and render re-sampled intrinsic cycle data. This process is illustrated in Figure 2.5 for an arbitrary intrinsic mode function - a non-stationary sine wave.

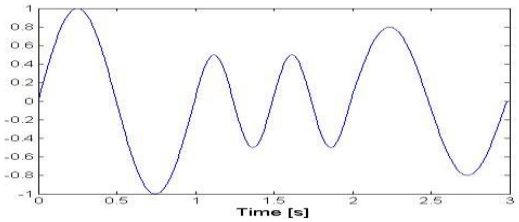

a. An Intrinsic Mode Function

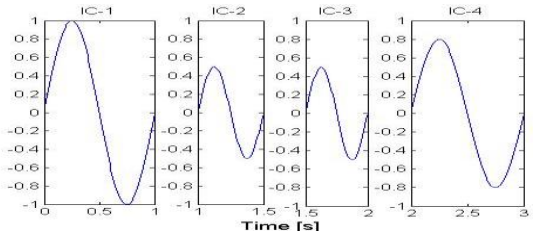

b. Intrinsic Cycles

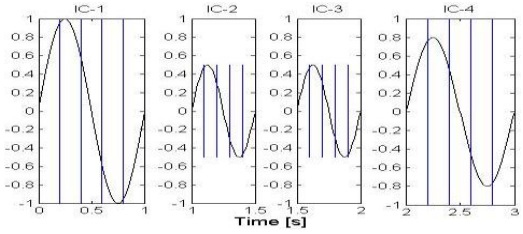

c. Re-sampling

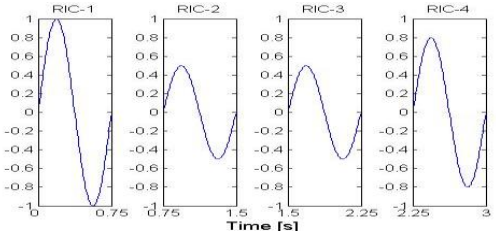

d. Re-sampled Intrinsic Cycles

Figure 2.5 Illustration of re-sampled IC

For this illustration, an arbitrary IMF sine wave is separated into four individual ICs based upon the definition presented above. It can be seen that the periods of these ICs are different. The 1st (IC-1) and 4th (IC-4) ICs have the same period of 1s but different amplitudes and 2nd (IC-2) and 3rd (IC-3) ICs have the same period of 0.5s and the same amplitudes. This causes the non-stationarity of the signal. These signals are re-sampled into 100 equal intervals within each IC. (In order to

clearly illustrate the process visually, only 6 lines are drawn in the figure (c) for each IC and within each line drawn there are 20 equal intervals.) Once the re-sampling is finished, the final wave is reconstructed and features the re-sampled ICs as are shown in (d) which have the same number of equal intervals in each re-sampled IC and each re-sampled IC has the same new period of 0.75s.

The re-sampled ICs have the same periods because each IC has been re-sampled with same number of intervals and a new sampling frequency can be obtained as,

$$f_{new} = \frac{t_{period}}{S_{resample}} \tag{2.10}$$

where f_{new} is the new sampling frequency, $S_{resample}$ is the number of samples of the re-sampled IMF and t_{period} is the time period of the original data.

Clearly, through this re-sampling process, the frequency variations between the ICs are eliminated. Subsequent to obtaining the re-sampled ICs, it can be seen that if frequency variations within ICs are negligible, which follows on the above zero angular acceleration assumption, then frequency variations of the overall signal are excluded in a way similar to eliminating frequency variations during computed order tracking re-sampling. For computed order tracking, the non-stationary time domain data is transformed into stationary angle domain data. In this method, a frequency varying IMF is transformed into a frequency stationary IMF. In this way, rotational speed variation effects in an IMF are eliminated. Fourier analysis can then be used to transform the re-sampled IMF into the frequency domain. Thus, similar computed order tracking effects are achieved through re-sampling the IMF. More importantly, though the present approach may achieve similar effects as to computed order tracking, it however neither requires a tacho signal, nor does it rely on interpolation of signals as is done in normal order tracking analysis.

2.3.2 Interpretation on the reconstructed intrinsic mode function result

From the above it is clear that ICR is a development of an IMF. To understand the ICR results it is therefore necessary to trace its analytical form from the basic definition of the IMF. An IMF $d(t)$ can be written in terms of a normalized amplitude modulation part $A(t)$ and an empirical frequency variation part $\phi_e(t)$, in the time domain as in equation (2.7), here repeat it again,

$$d(t) = A(t)\cos\phi_e(t) \tag{2.7}$$

The ICR method proposed here transforms the possible frequency varied IMF into a frequency stationary IMF (re-sampled IMF). The empirical frequency modulation carrier wave $\cos\phi_e(t)$ in equation (2.7) is therefore transformed into a stationary carrier wave as in equation (2.11)

$$d_{ICR}(t) = A_{ICR}(t)\cos(2\pi f_{ICR}t) \tag{2.11}$$

where $d_{ICR}(t)$ is the re-sampled IMF through ICR, $A_{ICR}(t)$ is the amplitude modulation part of the re-sampled IMF and f_{ICR} is the main frequency of the re-sampled IMF.

Specifically f_{ICR}, the main frequency of re-sampled IMF can be calculated through the ICs as,

$$f_{ICR} = \frac{N_{ICR}}{T_{ICR}} \tag{2.12}$$

where N_{ICR} is the number of intrinsic cycles of the calculated IMF and T_{ICR} is the time period of the calculated IMF.

Through the development of equation (2.11) from (2.7), the original empirical IMF becomes more specific than its original form. In equation (2.11) the parameters

of the re-sampled IMF now become the fixed frequency carrier wave at f_{ICR} with amplitude modulation $A_{ICR}(t)$. As a result, the Fourier spectrum for this kind of signal is affected by only the two variables f_{ICR} and $A_{ICR}(t)$. This simplifies the interpretation of the ICR result. Once the calculated time period in equation (2.12) is selected, the number of intrinsic cycles will determine the main frequency component f_{ICR}. However $A_{ICR}(t)$ can still vary according to the nature of the signals but its variations will be reflected in the sidebands of the main frequency component at f_{ICR}. Thus, equations (2.11) and (2.12) lead to the following guidelines in examining the ICR results:

a) Considering a re-sampled IMF time waveform, when signal amplitude variations occur in the re-sampled ICs but the number of ICs remains the same, equation (2.11) implies that $A_{ICR}(t)$ changed due to the amplitude variations and f_{ICR} is invariant due to the unchanged number of ICs. Thus the final spectrum of ICR will exhibit sideband variations and a stationary main frequency peak.

b) When the number of ICs varies and the amplitude of re-sampled ICs in the time waveform remains constant, i.e. $A_{ICR}(t)$ is invariant and f_{ICR} changes in equation (2.11), the final spectrum will exhibit a shift of main frequency peak and stable sideband shapes.

c) When the signal variations influence both the number of ICs and amplitude of re-sampled ICs in the time waveform, according to equation (2.11) both $A_{ICR}(t)$ and f_{ICR} are varied. One may then expect a shift of the main frequency component as well as a variation in the sidebands.

d) Further, the more the variations of the amplitude modulation $A_{ICR}(t)$ in the re-sampled IMF, the more variations of sidebands will appear in the ICR spectrum. And the larger the number of ICs, the higher the value of the main frequency component f_{ICR} will be.

Firstly, considering rotating machinery faults, incipient machine faults will usually not severely influence the vibration signals, therefore in a re-sampled IMF, one may typically expect variations in the amplitude of the re-sampled ICs without changing the number of ICs. Introduction of a new IC requires at least one extra zero crossing in the signal. A small signal variation in a dominant vibration environment, especially for rotating machine vibrations where rotational speed harmonics are predominant, will not easy to introduce extra IC due to small variations of the signal. Thus, it may only change $A_{ICR}(t)$ and the main frequency component, f_{ICR}, will remain the same. In such a case, the sidebands of the ICR spectrum relative to the main frequency component amplitude can be used for condition monitoring purposes. This corresponds to case (a).

Secondly, if the measured response on the machine does not contain clear machine fault vibrations but only influences from the changes in rotational speed which leads to variations of ICs, f_{ICR} will however shift in the ICR spectrum but the sidebands will retain its original shape. This can be used to detect the influence of rotational speed on the measured signals. This corresponds to case (b).

Lastly, when severe changes in the sidebands and a clear shift of f_{ICR} occur, it usually indicates a machine fault occurred and is developing. This corresponds to case (c). In each condition mentioned in (a), (b) and (c), the severity of signal variations will influence the spectrum of ICR results differently in sidebands, main frequency component or both. This is relevant to case (d).

2.3.3 Discussions on intrinsic cycle re-sampling in terms of rotating machine vibration signals

For rotating machinery the order components will usually dominate the response. EMD can empirically decompose these orders into different IMFs. These characteristic orders in different IMFs usually have different physical meanings relating to machine conditions. Thus, each IMF is of great use in condition monitoring, and therefore ICR on IMF will also have advantages in this regard. Ideally, one IMF should capture one order signal and represent one single order component in the order spectrum, as implied by the word 'intrinsic'. However, the IMF may also include other components due to its empirical nature and it has been discussed in the previous IVK-OT technique in paragraph 2.2.2. And the more other components appear in the IMF, the more pronounced the deviations from the order signal will become. As such the final Fourier spectrum of this IMF may contain more variations. This is in fact extremely useful for fault diagnosis of rotating machines, since most of the machine fault vibrations would modulate the order signals. And the IMF has the ability to include this information together with the order of interest. However it should also be noticed that the IMF from EMD cannot get rid of frequency modulation effects due to the rotational speed variation, despite the fact that the rich information related to the machine faults has been decomposed into different IMFs, if Fourier analysis is applied to the signal. However the smearing effects in the frequency spectrum may also occur which could be an impediment for diagnostic decisions. For this reason, the empirical re-sampling intrinsic cycles through which frequency variation is excluded between intrinsic cycles, are useful for presenting better frequency spectrum and therefore beneficial for machine fault diagnostics.

As mentioned in previous IVK-OT technique, researchers such as Feldman, have discussed the resolution of the EMD method. They proved that one IMF may

include more than one harmonic signals and signals with small amplitudes compared with the dominant harmonics, may easily be included in an IMF. While this is actually a disadvantage of IMF in extracting solely order signals, compared to conventional order tracking techniques, it does however provide a unique ability for capturing signals that modulate dominant order signals. Thus, ICR developed from IMFs can be used as a tool to reflect changes of vibration signals that modulate order signals. And it could be very useful for condition monitoring of rotating machinery. In the following chapter a simplified gear mesh model is used to demonstrate ICR. The logic of performing ICR is first schematically summarized in Figure 2.6.

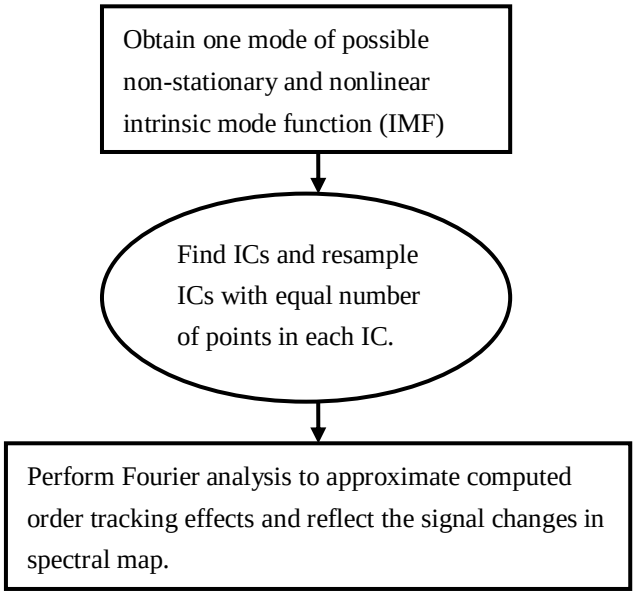

Figure 2.6 Logic of the ICR technique

2.4 Summary

In this chapter, three improved order tracking techniques are theoretically developed. Firstly, Vold-Kalman filter and computed order tracking (VKC-OT) is developed. The discussions are emphasised on their distinct characteristics for subsequent Fourier analysis. Secondly, intrinsic mode function and Vold-Kalman filter order tracking (IVK-OT) is developed. Time and order domain discussions that reveal the relationship between an IMF and an order are presented which fills

the vacant of literature in this regard. Lastly, intrinsic cycle re-sampling method is formed through newly introduced term intrinsic cycle. Its unique interpretation method in terms of reconstructed IMF is also put forward which will bring benefits to condition monitoring rotating machines. In short, theoretical developments for three improved order tracking techniques have been made. In the following, these techniques will be further verified and validated in simulation studies.

Chapter 3 Simulation studies

In chapter 2 three improved order tracking techniques have been developed theoretically. In this chapter, two simulation models will be used to investigate the effectiveness of the improved order tracking techniques. The first simulation model is a simple single-degree-of-freedom rotor model. The Vold-Kalman filter and computed order tracking (VKC-OT) and intrinsic mode function and Vold-Kalman filter order tracking (IVK-OT) will be validated in this model. The intrinsic cycle re-sampling (ICR) technique will be applied to a simplified gear mesh model to investigate its ability. In the following, three simulation studies are present in sequence. The focus in each of these simulation studies is described below:

1. The focus of the simulation studies using VKC-OT will be put on how the method features clear and focused order spectra compared with using each technique alone, so that the advantages of combing two traditional order tracking methods can be clarified.

2. The focus of the simulation studies using IVK-OT will be put on separation of vibrations that modulate orders in an IMF, especially for those speed non-synchronous vibrations so that IVK-OT demonstrates its ability which is intractable through other order tracking methods in isolation alone.

3. The focus of the simulation studies using ICR will be put on how the method interprets the ICR results and comparisons with traditional signal processing methods so as to demonstrate ICR as an alternative condition monitoring tool.

3.1 Single-degree-of-freedom rotor model simulation analysis

3.1.1 Single-degree-of-freedom rotor modelling

The first model treats the lateral response of a symmetric rotor as two uncoupled single-degree-of-freedom systems depicted in Figure 3.1. It is assumed that the rotor of mass M is mounted on bearings of total stiffness K and damping coefficient C, in both x- and y- directions. The rotor is assumed to rotate at an increasing speed. The time dependent external excitation forces $F(t)$ are sinusoidal force combinations. In the first simulation, order terms 3 and 6 are included in the excitation forces. This means that force frequencies $3\times$RPM and $6\times$RPM are included in the model. The arbitrary system characteristics that are used for this investigation are listed in Table 3.1.

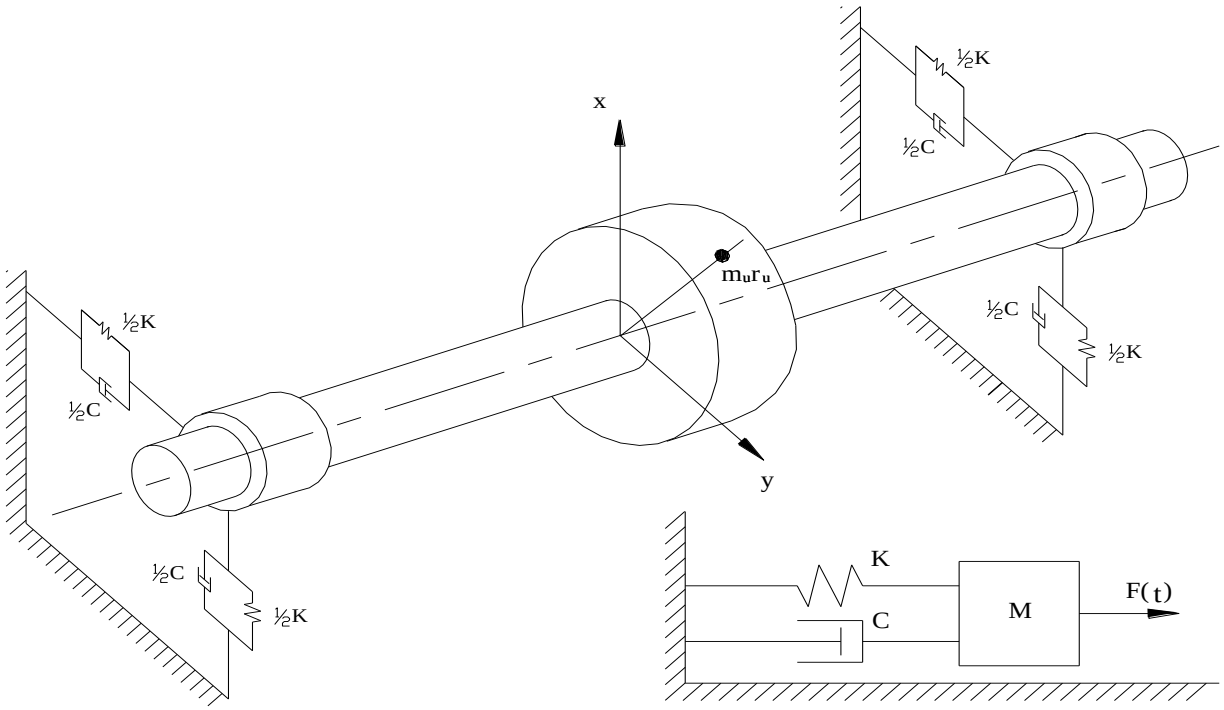

Figure 3.1 Simple symmetric rotor single-degree-of-freedom system

Table 3.1 System characteristics

Parameter	**Value**
Rotor mass M	20 kg
Damping coefficient C	100 Ns/m
Stiffness K	500 000 N/m
Eccentricity r_u	0.1 m
Unbalance mass m_u	0.05 kg
Initial time t_0	0 s
Final time t_f	5 s
Time steps	4096
Number of revolutions	100
Number of re-sampling intervals	100
Angular speed ω	$15.0796t^2$
Scenario 1	Excitation: $F = m_u\omega^2 r_u \sin(3\omega t) + m_u\omega^2 r_u \sin(6\omega t)$
Scenario 2	Excitation: $F = m_u\omega^2 r_u \sin(3\omega t) + m_u\omega^2 r_u \sin(6\omega t)$ Final System response = system response to F +Noise Noise: $100 \times randn(4096,1)$ (Normally distributed random noise with mean zero and standard deviation one).

It is simple to tune the different parameters of the system in the MATLAB environment. However some of the critical parameters must be commented on here. Mass and stiffness are two important parameters that determine the resonance frequency of the system and is proportional to the square root of K/M. Further, the excitation forces can be arbitrarily be generated in MATLAB. This is the one of the advantages of this simulation model, and makes it possible to include as many orders as desired, as well as simulate forces that might exist in real cases, for instance the fluctuation of load or beating external forces which will lead to the system response to be modulated. The familiar Runge-Kutta-Gill method was used to integrate the equations of motion for the simulated model to obtain system response.

3.1.2 Equations of motion for the single-degree-of-freedom system

In this rotor model simulation, the viscously damped case is considered and discussed in the following.

Assuming viscous damping the equation of motion is given by

$$M\ddot{X}(t)+C\dot{X}(t)+KX(t)=F(t) \tag{3.1}$$

where $X(t)$ is the system response in x- direction, and $F(t)$ is the simulated external excitation force function. The mathematical expression for the simulated force used in the VKC-OT method simulation study can be written as:

$$F(t)=m_u\omega^2 r_u \sin(3\omega t)+m_u\omega^2 r_u \sin(6\omega t) \tag{3.2}$$

This external force model is listed as scenario 1 in Table 3.1. For modelling of the external force exerted on the rotor, the force amplitude will be simulated as a normal force. This is not to say that all the force components will in reality be normal. But for simplicity, the mathematical expression for normal force is assumed to be:

$$F_{normal} = m_u \times \omega^2 \times r_u \tag{3.3}$$

where m_u is the mass unit, r_u is the distance from the centre to the mass unit and $\omega = \frac{d\theta}{dt}$ is the angular velocity of the rotor.

3.1.3 Single-degree-of-freedom system analysis

The system lateral acceleration response under the given external excitation force function in the time domain can be depicted as in Figure 3.2.

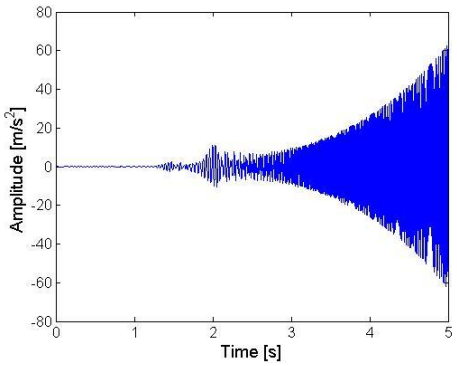

Figure 3.2 System response in the x direction

Based upon the choice of the system parameters and the external excitation force function (scenario 1), results of the system response can be anticipated. Due to the resonance, there must be a peak at 25.16 Hz in the corresponding spectrum. This can be determined from equation (3.4):

$$f = \frac{1}{2\pi}\sqrt{\frac{K}{M}} \tag{3.4}$$

At the same time, the 3rd and 6th orders due to the external forces should also appear in the response spectrum. However, due to the quadratic non-stationarity of the rotational speed, as is shown in Figure 3.3(a), this will definitely influence the appearance of the final spectral. In order to do the following computed order

tracking, the vertical lines in Figure 3.3(a) indicate the start time of each revolution. The RPM spectrum map is plotted to show frequency and amplitude variation of signals for this quadratic speed up case, as is shown in Figure 3.3(b).

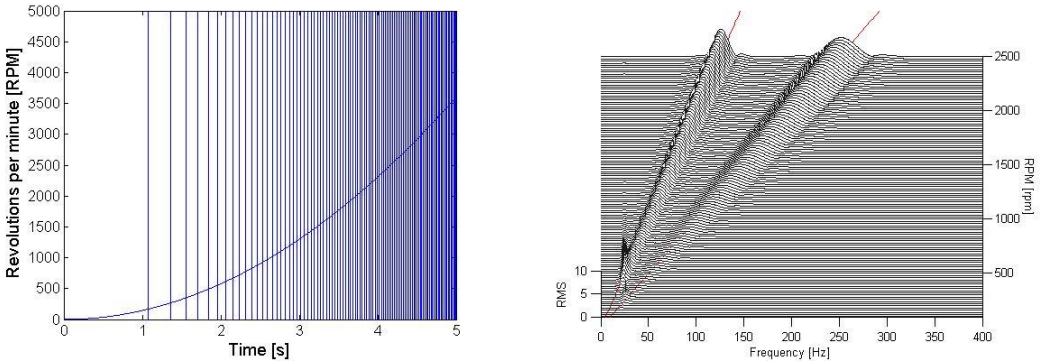

a) RPM b) RPM spectrum map

Figure 3.3 RPM and RPM spectrum map

Figure 3.3(b), shows a resonance at 25.16 Hz, which does not change with speed. Two dominant order related peaks, the 3rd and 6th orders, are marked with two lines. It can be seen that in between order peaks and resonance peak, there are some ripples which are caused by the quadratic rotational speed, although these are quite small. Based upon Figure 3.3(b) a clear picture of the system response with the progression of speed is presented.

3.1.3.1 Application of Vold-Kalman filter and computed order tracking

Once we obtain a clear picture of system response, the VKC-OT can be applied to the signals. And the purpose of this technique is to extract clear individual order components. Thus, let us examine the Power Spectral Density (PSD) results of the raw data, to confirm the observations of the above resonance and orders, and then focus on the 3rd order via VKF-OT, COT as well as VKC-OT. The PSD results of different techniques are then presented in Figure 3.4.

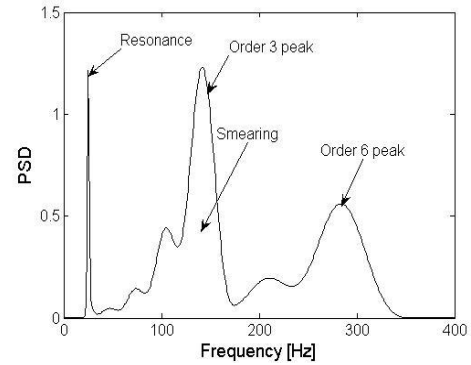

a. PSD on raw data

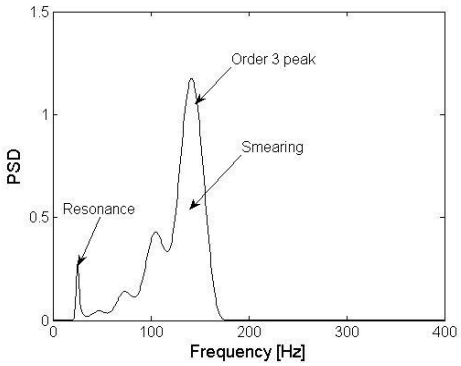

b. PSD on VKF-OT for 3rd order

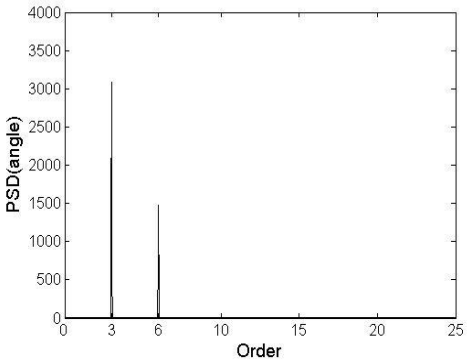

c. PSD on COT data

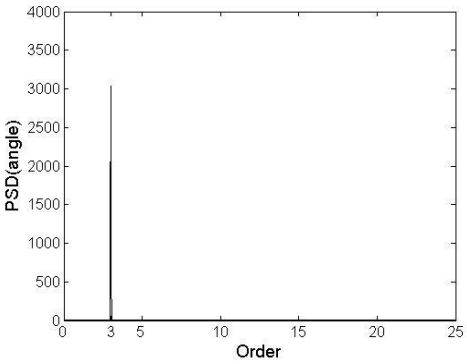

d. PSD on VKC-OT for 3rd order

Figure 3.4 PSD results raw data, VKF-OT for 3rd order, COT, VKC-OT for 3rd order

In Figure 3.4(a), which shows the PSD of the system response, there is one sharp resonance peak (fixed time-based frequency) and two rounded order peaks (smearing due to the non-stationarity of the time-based data caused by the increasing excitation frequencies). Figure 3.4(b) is the result of performing a PSD on VKF-OT which highlights the 3rd order information and removes the 6th order. The non-stationary smearing effect is still visible in the spectrum. The system resonance is also largely removed. Remnants of the resonance remain because of the 50% relative filter bandwidth which was used. (The 50% relative filter bandwidth means that the ratio of the instantaneous absolute filter bandwidth

to the instantaneous rotational speed frequency is 0.5. Here it is necessary to elaborate on the choice of pass band filter for Vold-Kalman filter tracking. One must be very cautious that for the narrower filter bandwidth, better tracking abilities do not necessarily hold. The Vold-Kalman filter obeys a time frequency relationship, $B_{3dB} \times \tau = 0.2$, where B_{3dB} is the $3dB$ bandwidth of the Vold-Kalman filter and τ is the time it takes for the time response to decay by $8.96\,dB$ (Herlufsen, 1999). It should be noticed that the relationship between B_{3dB} and τ is inversely proportional. Therefore, a narrower filter pass band will result in a longer time response to track the changes of signals. As a result, the narrow pass band reduces the permissible rate of change in rotational speed. The choice of filter bandwidth needs to be done very carefully. For an example analysis, the reader may refer to Wang and Heyns (2009) and for details on the choice of the filter bandwidth the reader may refer to Herlufsen (1999).

Figure 3.4(c) displays the result of COT that there are two clear peaks in the order spectrum at the 3rd and 6th orders respectively. This is because of the data being generated for an ideal linear system with sinusoidal external excitation, and the re-sampling process of COT which rearranges the data to become stationary. The data therefore represent stationary harmonic waves which are ideal for Fourier analysis.

It should be noted that the numerical values of the PSDs in Figures 3.4(a and b) and 3.4 (c) differ significantly. It should also be emphasized that the number of samples calculated by COT is different from traditional Fourier analysis. Since the given rotor rotates 100 revolutions within 5s and each revolution is evenly sampled with 100 angular intervals, therefore the resultant samples for COT analysis become 10000 instead of 4096. Besides, in Figures 3.4(a and b) the PSD describes how the energy associated with the time domain series is distributed with

frequency. The unit is $(m/s^2)^2/Hz$. Figure 3.4(c) however describes how the energy of an angular domain series is distributed with order. Fundamentally the energy associated a particular order is distributed over a wide range of frequencies on the time domain based PSD, due to the non-stationary nature of the rotational speed. However on an angle domain based PSD the energy associated with a specific order is reflected at only one order value. The unit is $(m/s^2)^2/order$. It is actually a sum of distributed energies in the frequency domain for a specific order. Thus, in order not to confuse readers, the units of the PSDs are not indicated in the above figures at this time. However, the acronym 'PSD' is used on figures representing time domain based Power Spectra Density, while angle domain based PSD figures are indicated by 'PSD (angle)'.

It can be seen that Figure 3.4(c) present clear peaks. However it should still be borne in mind that the re-sampling process of the angle domain based method changes the number of samples of the raw data. In this case, it is performed under the assumption of zero rotational acceleration within each revolution and thus it re-samples signals in each revolution with equal intervals. Notice that the number of samples per revolution is a parameter that may be chosen arbitrarily by the analyst. These choices may render different numbers of re-sampled samples as well as variation of the value of re-sampled amplitude and as such also influence the final result in numerical values. This has been discussed in Chapter 1 paragraph 1.3.1. Therefore, once the number of samples has been chosen it should be kept consistent in all applications of the technique. Most importantly however, angle domain based PSD (angle) cleans up the smearing spectrum from frequency domain into the order domain and features distinct clear amplitude orders.

Besides, it should also be observed that the system resonance can hardly be recognized in Figure 3.4(c). This is because the re-sampling occurs in the angle

domain, which means the sampling interval changes to constant angle rather than constant time interval, and the Fourier analysis actually only captures periodic signals with respect to angle instead of time (as is the case for resonance). Thus COT deemphasizes the system resonance after the re-sampling.

If the VKC-OT procedure suggested in chapter 2 is however applied, Figure 3.4(d) is obtained. It is the application of COT on the filtered 3rd order by VKF-OT. This figure shows a single clear 3rd order peak in the spectrum, and illustrates the advantage of the combined use VKF-OT and COT to obtain diagnostic information about a system. Although both Figures 3.4(c) and (d) clearly indicate the system information, Figure 3.4(d) separates the individual 3rd order from the raw data, which makes it possible to further investigate the 3rd order information itself and therefore has an advantage compared to Figure 3.4(c).

In the above simulation, the response data are generated from an ideal linear system with ideal sinusoidal external excitation, which simplifies the interpretation of the spectra. But, if external noise is added to the system response, the resultant observed response data = response to the external force + noise. To illustrate this, the simulation model uses scenario 2 (in Table 3.1) and the corresponding PSD results for different techniques are now shown in Figure 3.5.

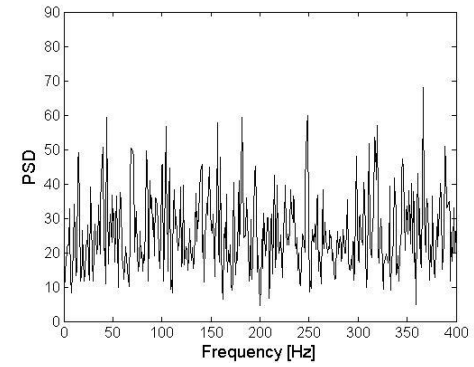

a. PSD on raw data

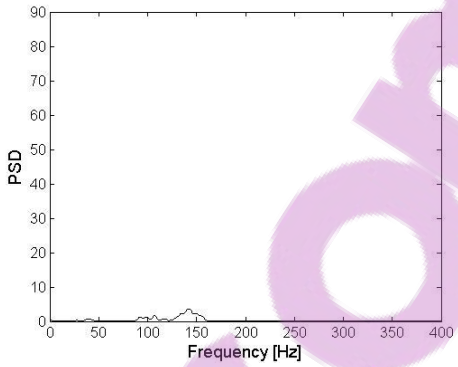

b. PSD on VKF-OT for 3rd order

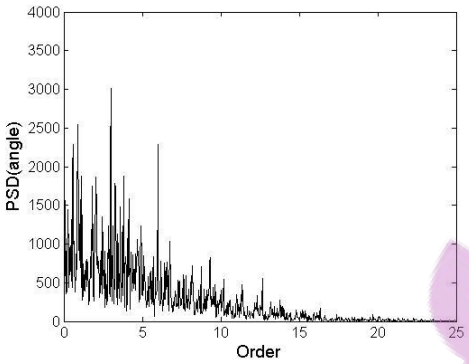

c. PSD on COT data

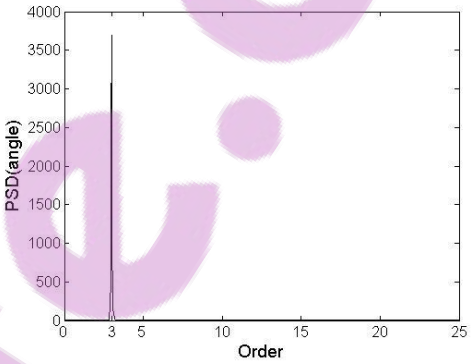

d. PSD on VKC-OT for 3rd order

Figure 3.5 PSD results for scenario 2 (with noise)

Little can be learnt from the spectrum in Figure 3.5(a) because the noise overwhelms the signal. Figures 3.5(b) and (c) are the PSD and PSD (angle) after VKF-OT and COT respectively, and do provide some insight into the system, albeit limited compared to Figure 3.4. It should also be noticed that the energy in Figure 3.5(b) is much lower than Figure 3.5(a). This indicates that the VKF-OT technique largely excludes the influence of noise and focus on the order of interest. Finally however Figure 3.5(d) provides another clear 3rd order peak largely excluding the influence of noise and non-stationarity. This result further demonstrates that combined use of VKF-OT and COT can significantly enhance

the result from Fourier analysis. And the VKC-OT technique does provide an excellent ability to extract clear individual order component.

3.1.3.2 Application of intrinsic mode function and Vold-Kalman filter order tracking

To investigate the ability of the IVK-OT technique, the above simulation model will be used again, however a more complex signal composition is now simulated. Since the main advantage of this technique lies in further decomposition of the IMFs and through the process, order signals and vibrations that modulate orders in IMFs can be separated. Vibrations that modulate orders are often key signatures of machine faults. However they might be quite unpredictable and may be speed synchronous or non-synchronous. Thus a more comprehensive signal should be generated to validate the distinct abilities of the IVK-OT method. Therefore, the characteristics of the model are changed and shown Table 3.2.

Table 3.2 Simulation model characteristics of the SDOF rotor

Parameter	**Value**
Rotor mass M	20 kg
Damping coefficient C	100 Ns/m
Stiffness K	500 000 N/m
Eccentricity r_u	0.1 m
Unbalance mass m_u	0.05 kg
Initial time t_0	0 s
Final time t_f	5 s
Time steps	4096
Number of revolutions	100
Number of re-sampling intervals	100

Angular speed ω_1	$\omega_1 = 15.0796\, t^2$ rad/s
Angular speed ω_2	$\omega_2 = \frac{\omega_1}{2.5} = 6.0318\, t^2$ rad/s
External excitation	$F = A_{m1}\sin(3\omega_1 t) + 0.5A_{m1}\sin((3\times 0.9)\omega_1 t) + A_{m2}\sin(3\omega_2 t)$ N 1) Speed synchronous amplitude $A_{m1} = m_u\omega_1^2 r_u \quad A_{m2} = 2m_u\omega_2^2 r_u$ 2) Speed non-synchronous amplitude $A_{m1} = m_u\omega_1(1-\sin(2\pi f_m t)^2 r_u$ $A_{m2} = 2m_u\omega_2(1-\sin(2\pi f_m t)^2 r_u$ $f_m = 5Hz$
Observed signals	$y = y_F + A\sin(2\pi ft) + noise$ 1) y_F is the response due to the external excitation 2) $A\sin(2\pi ft)$ is a constant sinusoidal component at $f = 100Hz,\ A = 7.5\%rms(y_F)$ 3) Random noise is set to be $noise = 5\%rms(y_F)$ in amplitude.

To clarify the composition of observed signals, the signal composition is categorized as speed synchronous and non-synchronous vibrations which are depicted in Figure 3.6.

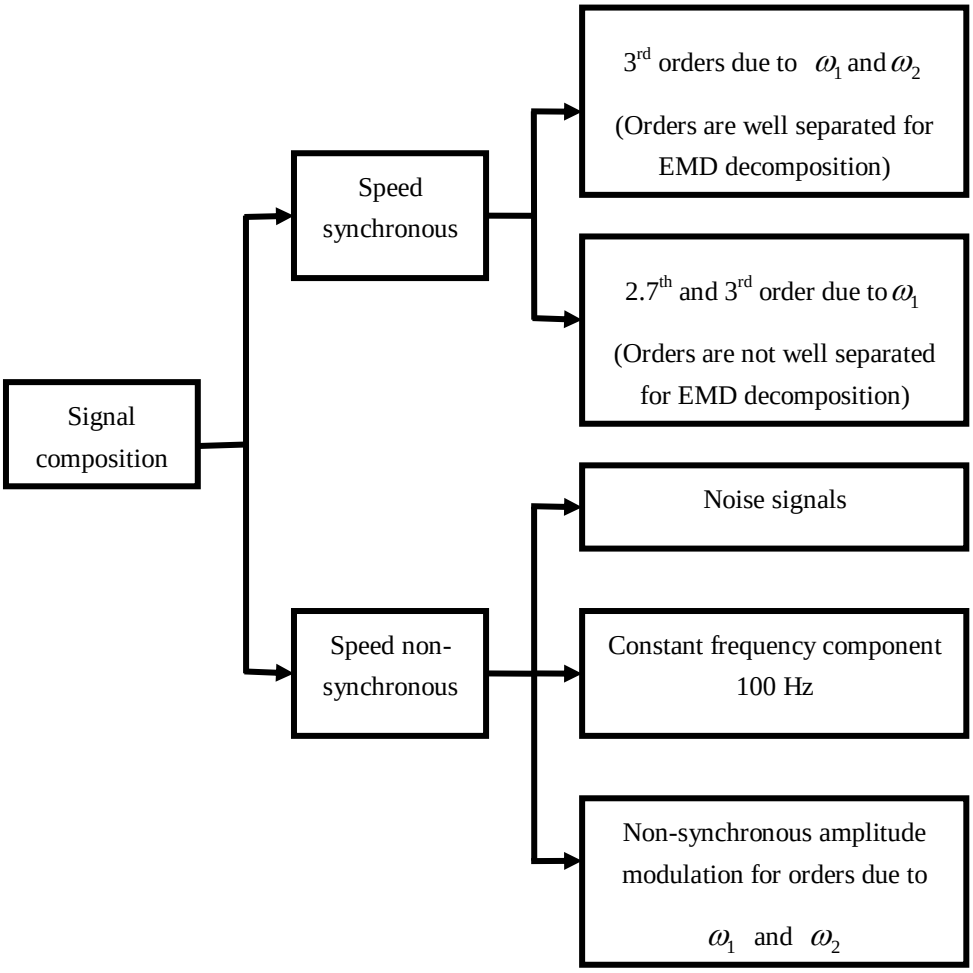

Figure 3.6 Signal composition of simulation study

Firstly, based upon Feldman's separation criterion shown in Figure 2.2 in chapter 2, two cases are considered with the speed synchronous or order signals. The 3rd orders due to rotational speed components ω_1 and ω_2 are well separated for EMD decomposition. The 2.7th and 3rd orders of ω_1 are not suitable for decomposition by EMD. The amplitude and frequency relationships for these cases are also indicated in Figure 2.2.

Among the speed non-synchronous signals, random noise is included since it is inevitable in reality, and a constant signal at 100 Hz is also added to simulate a

typical multiple of electrical line frequency. For comparative purposes, speed synchronous amplitude and speed non-synchronous amplitude modulation for external excitation force are both simulated for comparison. The details are listed in Table 3.2. The Runge-Kutta-Gill method was again used to obtain the system response in a MATLAB environment.

a. Overall signal analysis

Considering the response in the vertical x- direction, the calculated acceleration time response, the corresponding frequency spectrum and the RPM spectrum map are plotted in Figure 3.7 for displaying the nature of the signals by traditional signal processing methods. Where not specifically mentioned, all the figures are obtained for the speed non-synchronous amplitude modulation case.

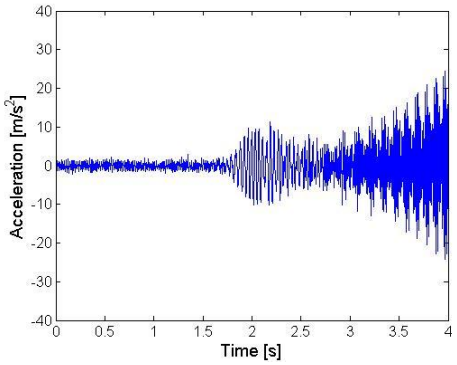

a. Time response

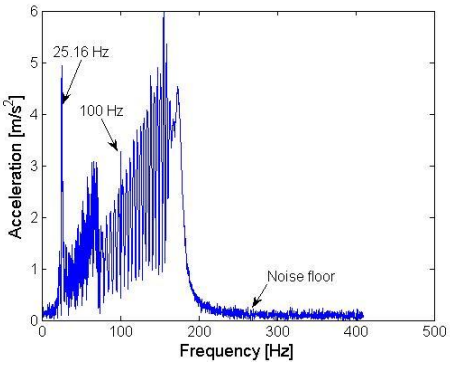

b. Frequency spectrum

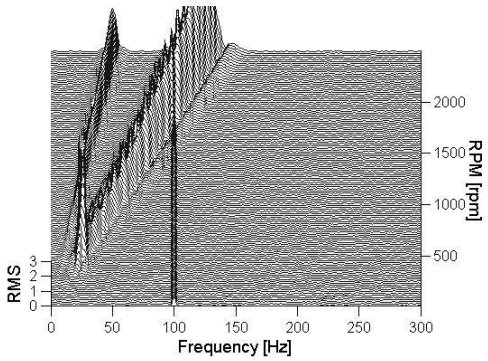

c. RPM spectrum map (based upon rotational speed ω_1)

Figure 3.7 Signal processing of raw signals

Figure 3.7(a) is the time response of the system. A clear beating effect of the signals can be seen which is due to the closely spaced sinusoidal external excitations. Figure 3.7(b) shows the signal in the frequency domain where a system resonance is present at $f_n = \frac{1}{2\pi}\sqrt{K/M} = 25.16$ Hz. The system resonance is due to the choice of the system parameters M and K. This characteristic of the system is independent of the external forces. The smeared hump with the oscillating ripples is due to the quadratically increasing rotational speed, and the two sets of external forces that cause the high oscillating ripples over a wide range. The random noise floor is also seen in the spectrum. Further, the RPM spectrum map in Figure 3.7(c) shows how the signal evolves with speed. Two sets of speed varying signals can be observed and a clear 100 Hz component appears throughout the speed range and it is not influenced by speed. The traditional signal processing methods provide a clear understanding of the signal.

b. Application of EMD

EMD may now be used to decompose the signals into IMFs, using the Hilbert Huang Transform Data Processing System (HHT-DPS1.4) obtained from NASA Goddard Space Flight Centre. The decomposition results are shown in Figure 3.8

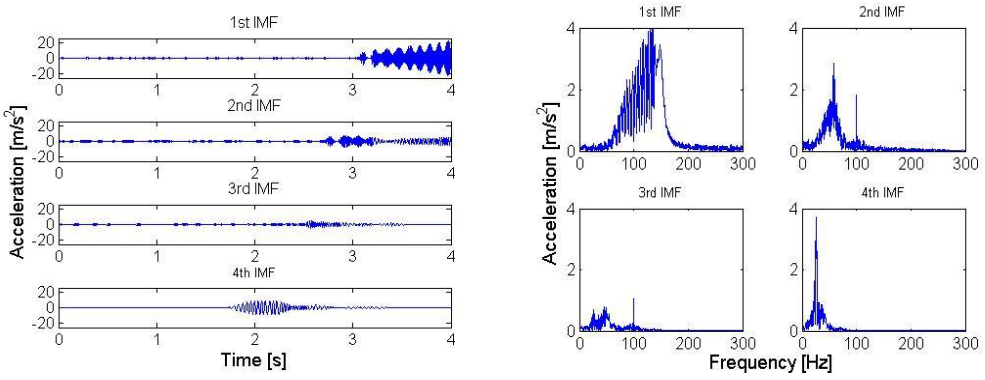

a. IMFs b. Frequency spectrum of IMFs

Figure 3.8 IMFs from EMD

Figure 3.8(a) indicates that the 1st IMF also exhibit beating effects similar to that seen in Figure 3.7(a). Figure 3.8(b) shows the frequency spectra of these IMFs. The 1st IMF spectrum shows a smeared hump with the oscillating ripples which indicate that it captures the system responses due to the closely spaced external forces. It is also clear that the system resonance is not included in the 1st IMF. The 2nd IMF also shows oscillating ripples in the spectrum in a lower frequency range, as well as a clear 100 Hz component. Clearly the oscillating ripples in Figure 3.7(b) are being separated into different IMFs and the system resonance is not evident in both 1st and 2nd IMFs. The 3rd IMF again shows part of the oscillating ripples in the spectrum and also a 100 Hz component, albeit much smaller than those in the 2nd IMF. Lastly, the 4th IMF clearly shows system resonance and it does suggest that the system resonance is being separated and specifically concentrated in the 4th IMF. From these observations of the EMD results, it is found that the system resonance components, 100 Hz component as well as the oscillating ripples are separated into different IMFs. However the physical significance of the ripples in the different IMFs is still vague.

c. Using computed order tracking to recognize order components in IMF

Therefore order tracking techniques are now used to assist in the further clarification and decomposition of the signals. Computed order tracking (COT) is applied to the IMFs referring to ω_1 in Figure 3.9. In this signal analysis, the observed signal from the speed synchronous amplitude case is also plotted for comparison. The two computed order tracking results are shown in Figure 3.9 (a) and (b). In order to compare order components in different IMFs, the highest order amplitude in the 1st IMF is used to normalize all four order spectra maps so that the amplitude relationship between IMFs can be easily seen. (This normalized process is applied to all the following order domain analyses).

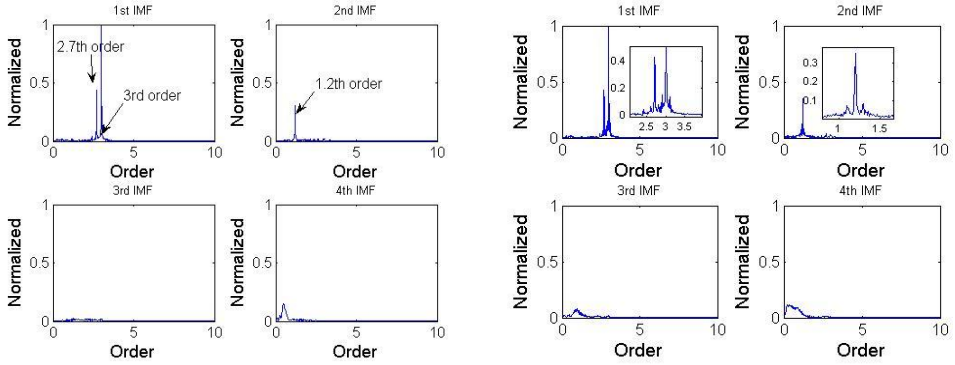

a. Speed synchronous amplitude b. Speed non-synchronous amplitude

Figure 3.9 Normalized order spectra for IMFs

Looking at Figure 3.9 (a) of the speed synchronous amplitude case, it is seen that the 1st IMF clearly consists of the 2.7th and 3rd orders. The 2.7th order is nearly half of 3rd order in amplitude, which corresponds well to the preset amplitude ratio of 0.5 in the force components. In the 2nd IMF a 1.2th order component can be seen. The 2nd IMF indeed captures another rotating speed signal, since it corresponds very well to the speed ratio of 2.5 between the two speeds. However, compared with dominant 1st IMF, this 1.2th order is much smaller. Besides, it should still be remembered that in Figure 3.8(b), both 3rd and 4th IMFs show clear spectra in the frequency domain, especially for the 4th IMF of its system resonance component. However since the re-sampling process of COT transforms equal time intervals to equal angular intervals, and then the Fourier analysis actually captures only the periodic signals with respect to angle instead of time (as is especially for the case of resonance), the system resonance and signals that non-synchronous with rotational speed, therefore, are de-emphasized once the re-sampling has been performed. This also appears in the previous VKC-OT application. As a result, the 3rd and 4th IMFs in the order spectra become much smaller than they are in frequency domain. This indicates that both 3rd and 4th IMFs are not closely related to rotational speed. Through COT analysis of IMFs

in Figure 3.9 (a), it may be concluded that the system responses due to the excitation at the two rotating speeds are well separated by EMD into the 1st and 2nd IMFs, however the close varying harmonics are not being separated in the 1st IMF.

Then, the speed non-synchronous amplitude modulation case is studied in Figure 3.9(b). Firstly, compared to Figure 3.9(a), four similar resultant order maps are rendered. Again, EMD successfully separates the system responses due to the two rotating speeds into the 1st and 2nd IMFs. At the same time it can not further separate close varying harmonics in 1st IMF. However upon closer inspection of the zoomed figures of the 1st and 2nd IMFs, sidebands appear in the order spectrum which do not occur in the speed synchronous amplitude case in Figure 3.9(a). This is due to the non-synchronous amplitude modulation of external excitation force. These signals are very important indications of system changes. However, they are quite small and easy to be neglected. In order to clearly visualize them, the zoomed figures are also plotted on top of the figures in Figure 3.9(b). Besides, with regard to these sidebands the traditional VKF-OT method can not perform the filtering properly since the sidebands are not synchronous with speed. Thus, it suggests further decomposition. The 1st IMF is chosen for illustrating this further decomposition process.

d. Application of Vold-Kalman filtering on IMF

The Vold-Kalman filter can thereafter be used for the 1st IMF in the speed non-synchronous amplitude modulation case. Firstly, the dominant 3rd order is extracted. A 20% relative filter bandwidth is used. In the top figure of Figure 3.10(a), the spectra of the 1st IMF and 3rd order are superimposed together and therefore the relationship between them can be seen. The corresponding time waveform of 3rd order is also plotted in the right hand side top figure of Figure 3.10(b). After the extraction of the 3rd order, the rest of signal is also plotted in the frequency domain in the bottom figure of Figure 3.10(a). The 2.7th order is

also extracted and its corresponding time wave is plotted in Figure 3.10(b). Clearly the majority of signals are being extracted since 1st IMF is a strongly speed related IMF.

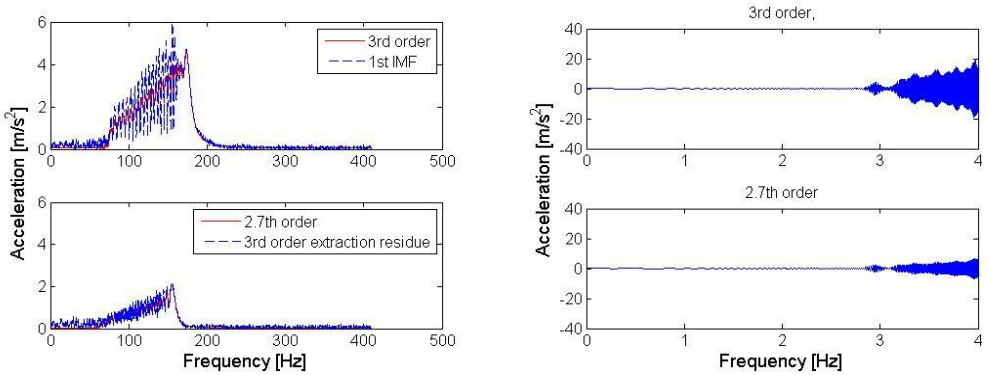

a. Spectrum maps b. Time waveform

Figure 3.10 Separation of 2.7th and 3rd orders

With the help of computed order tracking to recognize orders and Vold-Kalman filter order tracking to extract them in time waveforms, the 2.7th and 3rd order signals that are synchronous with the rotational speed are successfully decomposed from the 1st IMF. However, vibration signals that are non-synchronous with the rotational speed, especially for this case with amplitude modulation, should be further attended to. At this stage, if only VKF-OT was to be applied to the raw signals so that all the recognized orders are extracted through VKF-OT, the sidebands of the orders would be rendered and mixed together. However, instead of mixing this information, the combined IMF and VKF-OT provides the ability of focusing on the sidebands associated with the orders of interest and distinguish them for analysis. This is a unique capability of the sequential use of EMD and order tracking methods. The results are plotted in Figure 3.11.

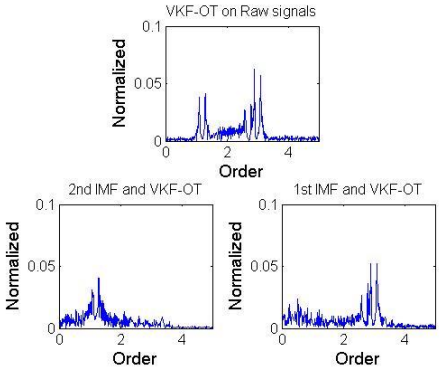

Figure 3.11 Separation of 1.2th and 3rd order sidebands

The top plot in Figure 3.11 is the order domain results of raw signals after subtracting the 1.2th, 2.7th and 3rd orders by VKF-OT. It can be seen that two sets of sidebands of 1.2th and 3rd orders remain. Since the VKF-OT can not further extract non-synchronous amplitude modulation sidebands properly, the traditional order tracking method stops here. However by using 1st and 2nd IMFs and VKF-OT, all recognized orders can be filtered out and render separated sidebands in the bottom two figures of Figure 3.11. (Note that the 100 Hz component in the 2nd IMF can also be extracted by VKF-OT through considering it as a constant rotational speed at $RPM = 100 \times 60 = 6000(rpm)$). The bottom two figures achieve further separation of sidebands with the help of different IMFs. As a result, 1.2th and 3rd order sidebands are well separated into two figures which are intractable by traditional VKF-OT as is shown in the top figure of Figure 3.11. If further comparing the results of sequence use of two methods to EMD as well as VKF-OT alone around 3rd order, it leads to Figure 3.12.

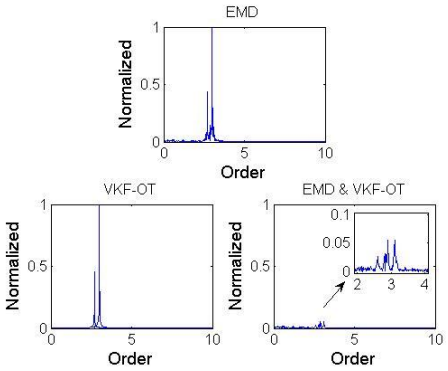

Figure 3.12 Results comparison of EMD, VKF-OT and sequence use of EMD & VKF-OT (use 1st IMF to illustrate)

For the EMD result at the top of Figure 3.12, the 1st IMF captures both 2.7th and 3rd order as well as some sidebands around dominant orders. Clearly the amplitude modulation effects on sidebands are fairly small and are emaciated by the dominant orders. EMD can not further decompose this 1st IMF. Through VKF-OT, the 2.7th and 3rd orders are properly extracted and superimposed together in the figure. However, no sideband information appears in the spectrum and therefore the ability of detecting the changes on amplitude modulation effects is lost. More importantly, since the amplitude modulation is non-synchronous with rotational speed, it is not amenable to VKF-OT. Through the sequential use of EMD and order tracking methods, the sideband information is however separated in the last figure of Figure 3.12. From Figure 3.12, it is clear that the amplitude modulation sidebands could not be extracted by using EMD or VKF-OT alone.

In the context of machine diagnostics, it should be emphasised that the un-extractable amplitude modulation effects by using either EMD or VKF-OT, are extracted through combining the two techniques in sequence. The extraction of amplitude modulation effects around the 3rd order excludes the interference from the other order, i.e. 1.2th order, so that analyst may focus on the amplitude variations of the 3rd order. This makes the condition monitoring process more flexible and selective. In short, the sequential use of EMD and order tracking

methods provides an advantage compared to EMD or VKF-OT in isolation. Information which would be un-extractable through both techniques alone can be achieved by combining them in sequence.

3.2 Simplified gear mesh model simulation analysis

3.2.1 Simplified gear mesh modelling

A simplified gear mesh model shown in Figure 3.13 is used for the simulation study. This model was also used by Stander and Heyns (2006) to investigate the advantages of instantaneous angular speed for gearbox condition monitoring. It is adopted here to obtain simulated gear mesh signals. The model comprises four degrees of freedom. A unique feature of the model is the incorporation of a translating mass M_1 to represent conventional translational vibration monitoring on the gear case. Model characteristics are given in Table 3.3.

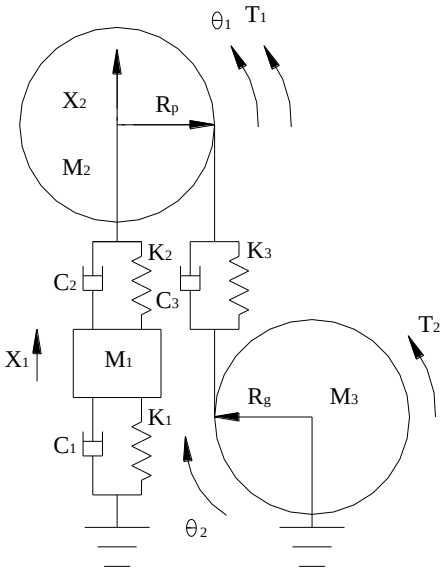

Figure 3.13 Dynamic gear mesh model

Table 3.3 Model characteristics and system load

M_1	Translating mass	0.05 kg
M_2	Pinion mass	0.05 kg
M_3	Gear wheel mass	0.05 kg
I_1	Inertia of pinion gear $I_1 = \frac{1}{2} M_2 R_p^2$	2.5×10^{-6} kg • m^2
I_2	Inertia of gear wheel $I_1 = \frac{1}{2} M_3 R_g^2$	2.5×10^{-6} kg • m^2
K_1	Structural damping	100 kN/m
K_2	Bearing stiffness	100 kN/m
K_3	Gear mesh stiffness	$100\{1 - 0.01\sin(N \times \theta_1)\}$ kN/m
C_1	Structural damping	1.2 Ns/m
C_2	Bearing damping	1.2 Ns/m
C_3	Gear mesh damping	1.2 Ns/m
R_p	Pinion base circle radius	0.01 m
R_g	Gearwheel base circle radius	0.01 m
N	Number of gear teeth	10
GR	Gear ratio	1:1
f_s	Sampling frequency	8192 Hz
I	Number of re-sampling intervals within one revolution	2000

Input torque	$T_1 = 1 + 0.1\sin\omega t$, $\omega = 2\pi \times 25$
Load	$T_2 = K_s\dot{\theta}_2^{\,2}$, $K_s = 16.2$

The gear mesh stiffness K_3 is modelled to allow a 2% sinusoidal variation of the nominal gear mesh stiffness so as to simulate the fundamental gear mesh harmonic. This is based upon the work of Howard et al. (2001). A simple viscous damping model is assumed.

A unity input torque T_1 is applied to the input pinion of the model with a 20% variation in time in order to simulate the fluctuating input and therefore causes the variations of rotational speed. The load on the system is set proportional to the square of the gearwheel speed, which enables the system to accelerate up to a nominal speed during the simulation. A proportional constant K_s is chosen to control the resultant nominal steady-state rotational speed of the system. Choosing K_s = 16.2, one obtains a nominal system rotational speed of 1500 rpm.

The equations of motion describing the model are presented in Eqs. (3.5) – (3.8)

$$M_1\ddot{X}_1 + (C_1 + C_2)\dot{X}_1 + (K_1 + K_2)X_1 - C_2\dot{X}_2 - K_2X_2 = 0 \tag{3.5}$$

$$M_2\ddot{X}_2 + (C_2 + C_3)\dot{X}_2 + (K_2 + K_3)X_2 - C_2\dot{X}_1 - K_2X_1 - C_3R_g\dot{\theta}_2 \tag{3.6}$$

$$- K_3R_g\theta_2 + C_3R_p\dot{\theta}_1 + K_3R_p\theta_1 = 0$$

$$I_1\ddot{\theta}_1 + R_p^{\,2}C_3\dot{\theta}_1 + R_p^{\,2}K_3\theta_1 - R_pR_gC_3\dot{\theta}_2 - R_pR_gK_3\theta_2 + R_pC_3\dot{X}_2 + R_pK_3X_2 = T_1 \tag{3.7}$$

$$I_2\ddot{\theta}_2 + R_g^{\,2}C_3\dot{\theta}_2 + R_g^{\,2}K_3\theta_2 - R_gR_pC_3\dot{\theta}_1 - R_gR_pK_3\theta_1 - R_gC_3\dot{X}_2 - R_gK_3X_2 = T_2 \tag{3.8}$$

The model was written into state space format and implemented in MATLAB for simulation with the ode45 differential equation solver.

3.2.2 Application of intrinsic cycle re-sampling method

In the following, signal analysis is now done to explore two questions:

a) How does the ICR result relate to order analysis in the simulation model?
b) How does ICR perform as an alternative condition monitoring tool?

a. Choosing an appropriate IMF

Before the above questions can be addressed, the first step is to choose an appropriate IMF for the analysis. To do this the relationship between the original gear casing velocity signal $\dot{X}_1$ and its IMFs is first considered. For this purpose the gear response was simulated over a 5 s period. The last 1 s of this response, after steady conditions have been reached, is now considered in the following analysis. In this steady state the variation of the rotational speed of the gear still remains due to the fluctuating load. For illustrative purposes, a section of 0.25 s of this signal is depicted in Figure 3.14(a). The low frequency fluctuation at 25 Hz, due to the variation in input torque, can easily be observed in this figure. Higher frequencies are the result of gear meshing which corresponds to 250 Hz (the 10^{th} order) at the nominal rotational speed of 1500 rpm. The response at this frequency and its harmonics is of great importance for obtaining information about the deterioration of the gear (i.e. stiffness). Basic Fourier analysis is performed in Figure 3.14(b). Except for the rotational frequency peak at 25 Hz and the gear mesh frequency of 250 Hz, it shows several sidebands around the gear mesh frequency. This is due to the fluctuation of the rotational speed caused by the fluctuating load.

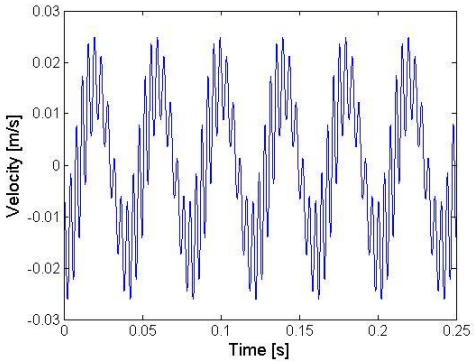

a. Velocity $\dot{X}_1$

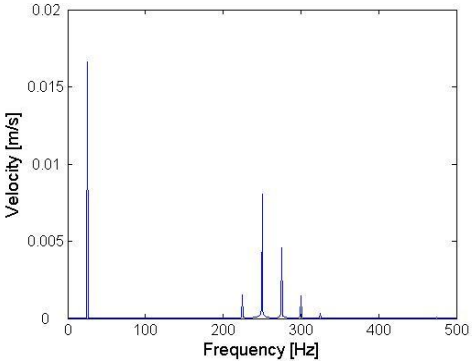

b. Fourier spectrum of velocity $\dot{X}_1$

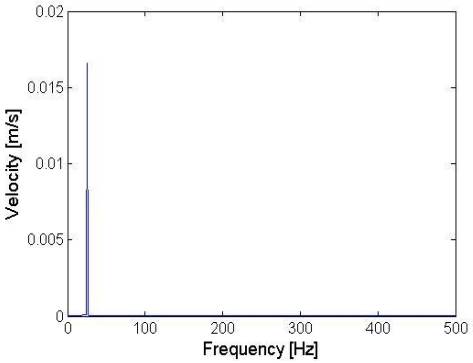

c. Fourier spectrum of 2nd IMF

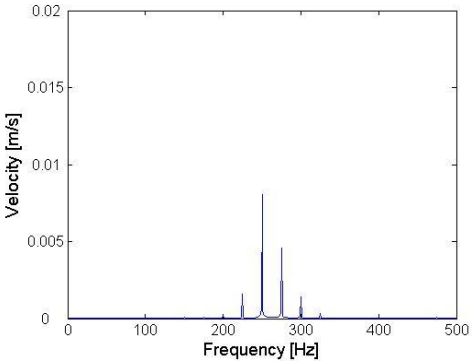

d. Fourier spectrum of 1st IMF

Figure 3.14 Velocity $\dot{X}_1$ and associated Fourier spectrum

EMD is now applied to the signal and the spectra of the 1st and 2nd IMFs are plotted in Figures 3.14(d) and (c) respectively. The 1st and 2nd IMFs successfully separate the lower and higher frequency content. This can of course also be achieved by using low and high pass filters but, in this case is accomplished empirically. The 2nd IMF captures the rotational frequency at 25 Hz while the 1st IMF extracts the gear mesh frequency content and its sidebands. Clearly, the 1st IMF which relates to the gear mesh frequency content, captures the changes of gear stiffness and is therefore the appropriate IMF for further analysis of the ICR method in condition monitoring.

b. Comparison of ICR result to order analysis in the simulation model

To investigate how the ICR results relate to order tracking analysis in this model, results from conventional order tracking analysis and ICR on the 1st IMF, are compared in Figure 3.15. Since the 1st IMF is focused on the gear mesh vibrations, the conventional order tracking analysis also focuses on gear mesh vibration for comparative purposes. The 10th order is extracted from the raw signal by Vold-Kalman filter order tracking (VKF-OT), through which the gear mesh order (10th order) is obtained. (A 20% relative filter bandwidth is used.). Then computed order tracking is applied to the extracted gear mesh order into order spectrum. For further comparison to the ICR results, the figure is normalized in terms of the highest order peak which renders Figure 3.15(a). The ICR method is applied to the 1st IMF and gives Figure 3.15(b) which is also normalized in terms of highest frequency peak.

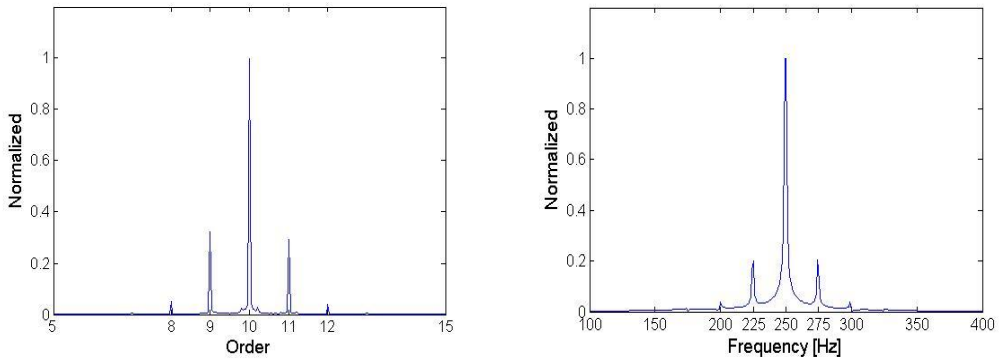

a. 10th order analysis b. ICR on 1st IMF

Figure 3.15 Comparison of COT and ICR results

Through comparison of Figures 3.15(a) and (b), it is firstly clear from the abscissa that unlike order tracking analysis in Figure 3.15(a), the ICR result remains in the frequency domain, in stead of the order domain, as is shown in Figure 3.15(b).

This is accomplished by employing the new sampling frequency of equation (2.12) in chapter 2, paragraph 2.3.2.

Secondly, from the two normalized figures it can be seen that both the order tracking and ICR spectral maps feature similar shapes with one main peak and evenly distributed sidebands. For the order map in Figure 3.15(a), the order sideband spacing is 1 with the 8th, 9th, 11th and 12th orders present. Similarly, the frequency sideband spacing in Figure 3.15(b) is 25 Hz with peaks at 200 Hz, 225 Hz, 275 Hz and 300 Hz. The 25 Hz corresponds to the nominal rotational speed. However, the ratio of the highest sideband to the main peak between two figures is slightly different. For Figure 3.15(a) this ratio is 0.3 and 0.2 for Figure 3.15(b). The difference is due to the decomposition of the 2nd IMF as is shown in Figure 3.14(c). The 25 Hz amplitude modulation is the same frequency as the nominal rotational speed, which has been partly separated into the 2nd IMF. This reflects the fact that the ICR method is influenced by the decomposition process of EMD. However, both figures share similar attributes in analyzing the order of interest.

Thirdly, the peaks on the order analysis results in Figure 3.15(a) are sharper than the ICR result in Figure 3.15(b). This also suggests a difference between the two methods. Firstly, the original sampling frequency in the simulation was set at $f_s = 8192\,Hz$ in Table 3.3. After re-sampling, the new sampling frequency for the ICR analysis changes to $f_{new} = \frac{S_{resample}}{t_{period}} = \frac{48001}{1} = 48001 Hz$ as defined in equation (2.12). (In this case, within a 1 s signal, there are 24 revolutions and 250 intrinsic cycles. The re-sampling interval in one revolution is $I = 2000$ (see Table 3.3). Thus the number of re-sampled intervals for the computed order tracking analysis is $24 \times 2000 = 48000$. To keep the same number of analysis samples for ICR, 192 intervals within one intrinsic cycle is chosen, therefore, the $f_{new} = 48001 Hz$). And the Nyquist frequency for this ICR analysis

is $f_{Nyquist} = \frac{f_{new}}{2} = 24000.5Hz$. For order analysis, the order sampling frequency is $O_{sample} = \frac{1}{2\pi/I} = \frac{1000}{\pi} = 318.3$ order and the Nyquist order is $O_{Nyquist} = \frac{O_{sample}}{2} = \frac{500}{\pi} = 159.15$ order. Considering the ratio of the dominant components in the order spectrum and the ICR results to their Nyquist values, a difference can therefore be calculated that the dominant nominal gear mesh vibrations, f_N, in the ICR spectrum occurs at $\frac{f_N}{f_{Nyquist}} = \frac{250}{24000.5}100\% = 1.04\%$ of $f_{Nyquist}$. However for order analysis, the corresponding gear mesh at the 10^{th} order, occurs at $\frac{O_{10th}}{O_{Nyquist}} = \frac{10}{159.1}100\% = 6.29\% \text{ of } O_{Nyquist}$. Clearly, the ratio of the frequency components in the ICR spectrum and the order component in order spectrum are different from their Nyquist values. As a result, the order spectrum in Figure 3.15(a) looks sharper than ICR spectrum in Figure 3.15(b). This indicates that the new sampling frequency for ICR analysis may influence the visual appearance of the of the spectrum map.

Lastly, it should always be borne in mind that ICR is strictly speaking not an order tracking analysis. It reflects changes of the signal itself. Only when the frequency variation in signals is caused by rotational speed, it may serve as an alternative order tracking approximation. Fortunately, in many practical applications for rotating machine vibrations, such an assumption is applicable. This is the case in this simulation study for a gearbox in good condition.

c. ICR as an alternative condition monitoring tool

Traditional signal processing methods

Subsequently a typical seeded fault is introduced. The gear mesh stiffness K_3 is reduced to 98% of the nominal gear mesh stiffness at an angle from $160°$ to $165°$ of the shaft rotation. Firstly, traditional signal processing methods are applied to the signals from the gearbox in good condition and with the seeded fault, so that a clear picture of how traditional signal processing methods respond to the fault can be obtained. Thus, time, frequency and order domain analyses are first compared in Figure 3.16.

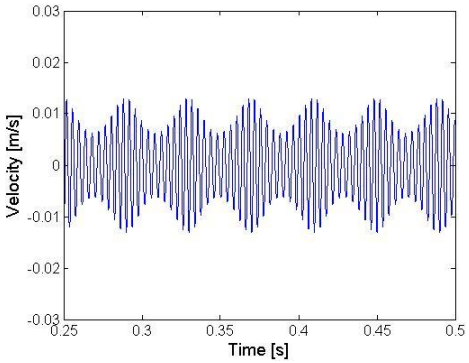

a. 1st IMF for good condition

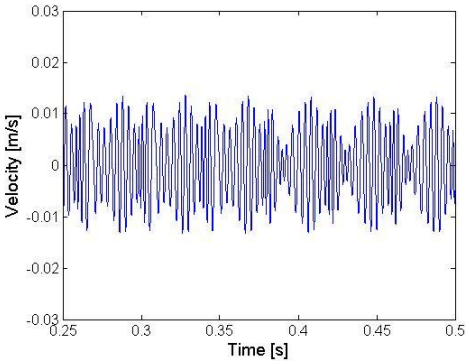

b. 1st IMF for fault condition

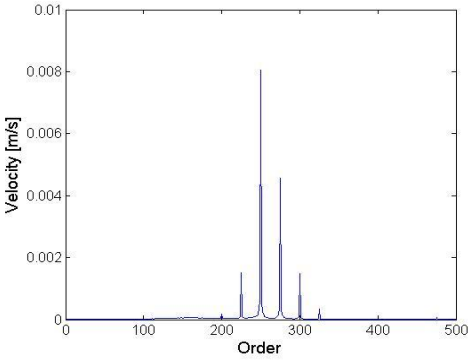

c. FFT on 1st IMF for good condition

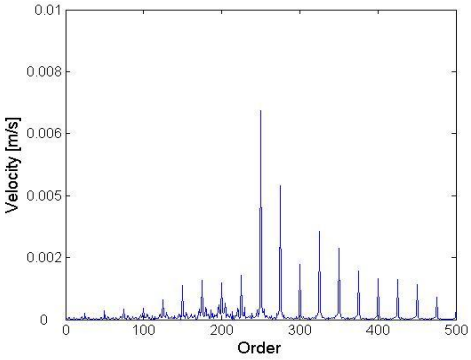

d. FFT on 1st IMF for fault condition

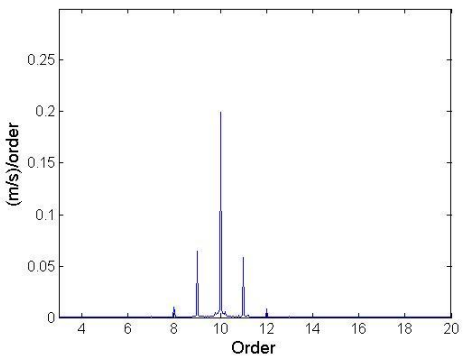

e. Order tracking for good condition

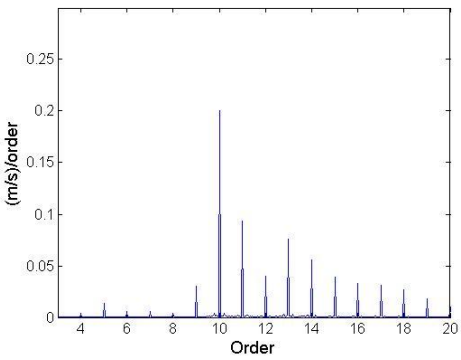

f. Order tracking for fault condition

Figure 3.16 Comparison of good and seeded fault conditions

The 1st IMF time domain velocity signals for good and fault conditions in Figures 3.16(a) and (b) show that the high frequency gear mesh signal has been extracted

from the original velocity. In Figures 3.16(a) and (b), the amplitude variations are both clearly visible. Comparing the two figures indicate that the gear mesh vibrations change due to the introduction of the fault.

In the frequency domain, Figures 3.16(c) and (d) show the frequency spectra of the 1st IMF signals. Sideband peaks are very clear in both figures. With the introduction of the fault, the corresponding spectrum in Figure 3.16(d) shows more sidebands and some of its peak amplitudes change. Figures 3.16(e) and (f) consider the order domain, to test the ability of the computed order tracking method for raw signals. Compared with Figure 3.16(d) in the frequency domain, the order domain spectrum features cleaner order components. This is due to the exclusion of speed variation effects. However by the reduction of gear mesh stiffness to 98%, more sidebands and order peak amplitude variations occur. This implies that the order tracking method also detects the changes in the system. In short, it may be noticed that traditional signal processing techniques detect the system changes in terms of amplitude changes in the time domain and peak amplitude changes in the spectrum as well as more sidebands appearance.

ICR as an alternative tool

Unlike the traditional methods discussed above, the way in which ICR responds to the fault, follows the fundamental characteristics of re-sampled IMF as is discussed in chapter 2 paragraph 2.3.2. The two aspects of the ICR results that respond to the fault are examined, namely the sidebands variation (S.V.) due to $A_{ICR}(t)$ and the value of the main frequency (M.F.) due to f_{ICR}. To trend the changes in the ICR results, a range of six fault conditions are considered. They are 100%, 99.6%, 99.2%, 99%, 98.5% and 98% of the original gear mesh stiffness. The ICR results for these cases are plotted in Figure 3.17.

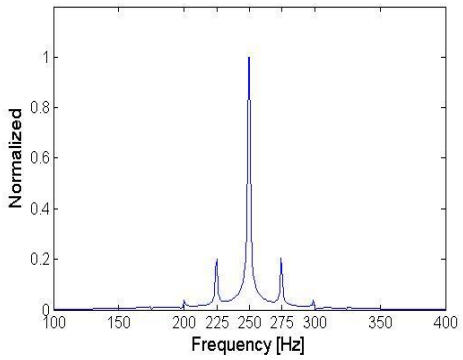

a.100% stiffness (good condition)
S.V.: two clear sidebands and peak ratio 0.2 ; M.F.: 250 Hz

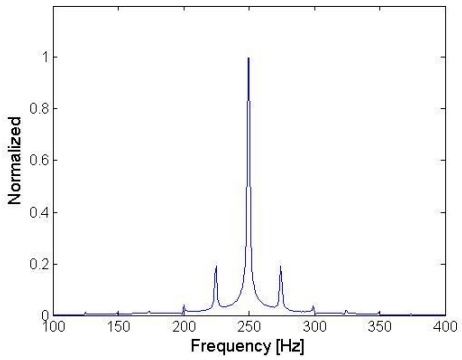

b. 99.6% stiffness
S.V.: two clear sidebands and peak ratio 0.19; M.F.: 250 Hz

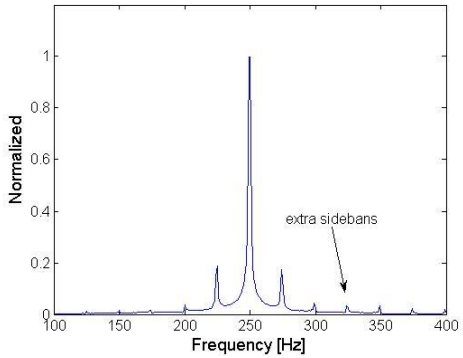

c. 99.2% stiffness;
S.V.: extra sidebands and peak ratio 0.185; M.F.:250 Hz

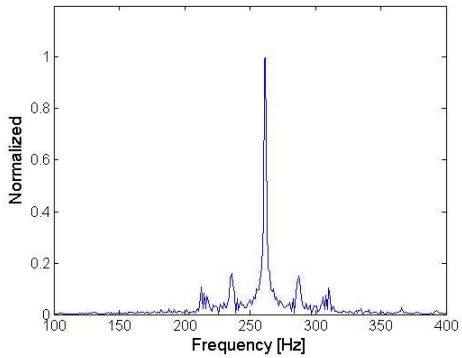

d. 99% stiffness
S.V.: 4 deformed extra sidebands M.F.:262 Hz

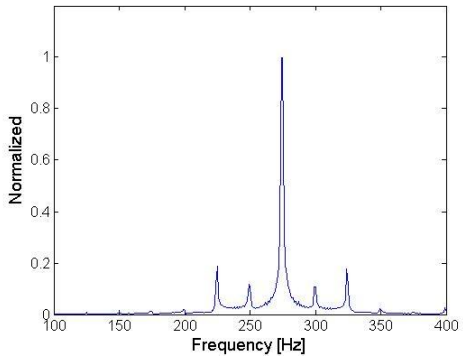

e. 98.5% stiffness
S.V.: 4 clear uneven amplitude sidebands
M.F.: 275 Hz

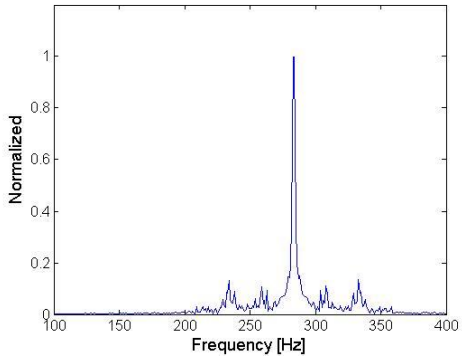

f. 98% stiffness
S.V.: more deformed sidebands
M.F.: 283 Hz

Figure 3.17 ICR results on different fault conditions

Figure 3.17 shows the variation of the ICR results with the development of the fault. Instead of many sidebands appearing as happens in the frequency and order domains, the two aspects (S.V. and M.F.) show the progress of the fault. For this simulation study, the faults can be categorized into two stages in terms of M.F: Initially (Figures 3.17(a) to (c)) the M.F. is stationary. For Figures 3.17(d) to (f) M.F. is varying. This corresponds to point (a) in the guidance provided chapter 2 in paragraph 2.3.2.

In the first stage, the peak ratio between the highest sidebands to the main frequency peak can be used as a distinct indicator of changes in the signals. The S.V. ratio decreases with the development of the fault from 0.2 to 0.19 and then change to 0.185. This indicates that a variation of $A_{ICR}(t)$ occurs, albeit very small. Considering further the S.V. effects, it can be seen that (especially in Figure 3.17(c)) extra sidebands grow with the development of the fault. This further confirms that $A_{ICR}(t)$ is varying and it requires more sidebands to represent these changes. Due to the stationarity of the M.F. as well as the above discussions on the changes in S.V., it may be concluded that during the first stage, the fault does not severely influence the 1st IMF or gear mesh vibrations, although it is developing.

In the second stage, the M.F. values may be used as a distinct indicator of the system changes. With the development of the fault, the M.F. becomes 262 Hz, 275 Hz and 283 Hz respectively. It is also found that the sidebands become uneven in amplitude in Figures 3.17(d), (e) and (f). The shapes of the sidebands become severely deformed in Figures (d) and (f). However, it should be noted that in figure (e) sidebands are smoother than the other two figures. Especially it is smoother than figure (d) where the fault on gear mesh stiffness is smaller. In

such a case, according to the discussion of chapter 2 paragraph 2.3.2, M.F. values should be first considered as the indicator of fault severity, despite with smoother sidebands, figure (e) however shows more serious fault than figure (d) due to the bigger value of M.F. Besides, the smoother sidebands of figure (e) indicate that, compared to the other two fault conditions in (d) and (f), the amplitude part of the re-sampled IMF, $A_{ICR}(t)$, can be represented by much simpler sidebands in (e). In fact, it is an intermediate period of fault development. In such a case, when M.F. is different, the S.V. is not a decisive factor to determine the severity of the fault however M.F. should be considered first. According to the theoretical studies in chapter 2 paragraph 2.3.2 guidance (c), in this second stage, the seeded faults severely influence the 1st IMF or gear mesh vibrations, the shift of M.F. with severe S.V. indicates a big variation of signals, thus apparently the severity of the damage is increasing.

Comparisons of ICR to tradition signal processing methods

In the end, one should compare the differences between the ICR with traditional condition monitoring methods. The good and fault condition (at 98% nominal gear mesh stiffness) figures are plotted for comparison. All figures are normalized in terms of highest spectrum peaks in Figure 3.18.

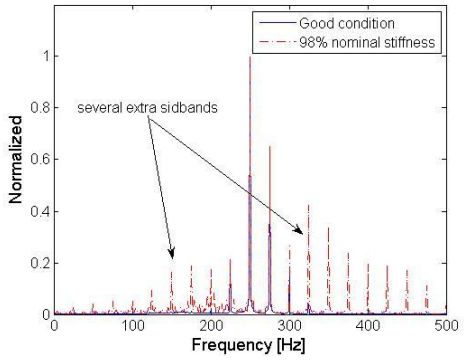

a. Frequency domain on 1st IMF

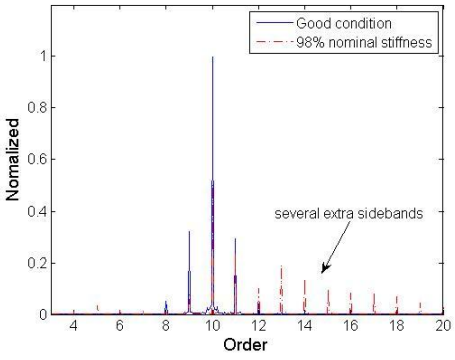

b. Order domain

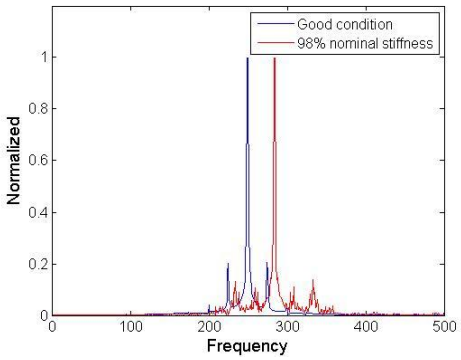

c. ICR result

Figure 3.18 Comparisons between traditional methods with ICR result

Figure 3.18 clearly shows that the traditional methods in figures (a) and (b) indicate the fault is mainly revealed in terms of several extra sidebands as are indicated in both figures. There is significant variation in the frequencies and order peaks. To trend the system changes, one needs to attend to all these peaks. However, instead of presenting several extra sidebands, the ICR technique in

figure (c) with its fundamental characteristics of re-sampled IMF, S.V. and M.F., can be used to trend the changes of system variations. It may be observed that the ICR method also present distinct changes in the results, especially for the unique shift of the M.F., where traditional methods do not have similar indicators. This suggests the ICR technique as an alternative method for machine fault diagnostic with distinct indicators for condition monitoring purposes.

3.3 Summary

In this chapter, two simulation models are used to explore the abilities of three novel improved order tracking techniques. The first simple rotor model is used to demonstrate the ability of VKC-OT and IVK-OT. Under non-stationary and noisy signal environments, the VKC-OT technique presents its unique ability to feature clear and focused order component. This overcomes the disadvantages of non-stationarity in the Vold-Kalman filter result and the inability of separating orders using computed order tracking. The VKC-OT no doubt provides a better perspective to inspect individual order components.

IVK-OT combines the empirical nature of IMF and the strict mathematical nature of VKF-OT to explore a sequential way of using two methods to separate modulated order signals which provides an edge for order tracking techniques to obtain vibrations that modulate orders, especially for those vibrations that are not synchronous with rotational speed.

Finally, the gear mesh model proves the ability of ICR technique. The re-sampling process takes advantage of an intrinsic mode function of symmetric, oscillating and zero mean nature to reconstruct an intrinsic mode function into a re-sampled intrinsic mode function which suppress frequency variations of the signal. In this way an approximation of order tracking effects is obtained without the need for rotational speed. At the same time, the method further brings

advantages for condition monitoring, in that the re-sampled intrinsic mode function offers more specific characteristics for trending machine conditions. These simulation studies lay a good foundation for the experimental analysis in the following chapter.

Chapter 4 Experimental Studies

In Chapter 2, three improved order tracking techniques are theoretically developed. The fundamental ideas and logic of implementing these techniques are also described. In chapter 3, the abilities of these techniques are demonstrated in simple rotor and gear mesh simulation models. In this chapter, the techniques are demonstrated in real rotating machinery environments. Following the logic of the simulation studies, two experimental setups in the Sasol Laboratory for Structural Mechanics at the University of Pretoria are used to acquire rotating machine vibration signals. These setups comprise an automotive alternator set-up and a transmission gearbox test rig. Vibration signals are sampled in both good and seeded fault conditions. The first two techniques, VKC-OT and IVK-OT, are applied to signals from the alternator experimental set-up, in line with simulation studies in Chapter 3. And the gear box vibrations are used to illustrate the ability of the ICR technique.

4.1 Automotive alternator set-up data analysis

4.1.1 Experimental automotive alternator set-up

Wang and Heyns (2009) established an experimental set-up in Sasol laboratory for Structural Mechanics at the University of Pretoria, to investigate the ability of VKF-OT in condition monitoring. Typical run-up data (vibration and tachometer signals) from the automotive alternator were obtained. The experimental set-up is shown in Figure 4.1(a) and the monitoring process is schematically represented in Figure 4.2. The key components of the experimental set-up are the alternator, the variable speed motor, the controller and the battery. The alternator is driven

by a variable speed induction motor via a normal V-belt. The variable speed motor is controlled by a DC controller. The alternator charges an automotive battery which in this case is used as the system load.

a. Experimental set-up b. Monitoring devices

Figure 4.1 Experimental set-up

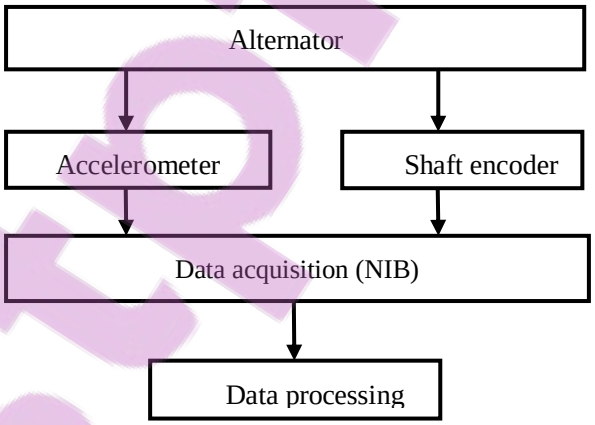

Figure 4.2 Monitoring process

The monitoring equipment for this experimental set-up, comprise an accelerometer and a shaft encoder, with a National Instruments Board (NIB) and computer. The accelerometer was mounted on the outer surface of the alternator (see Figure 4.1(b)), and the acquired signal was amplified and transferred through a PCB

amplifier and NIB to the computer. The rotational speed signal was monitored simultaneously through the shaft encoder, which was mounted on a specially made rotor shaft extender as is shown in Figure 4.3. The acquired signal first goes to the shaft encoder signal transfer box and then to the NIB before it finally also reaches the computer.

Figure 4.3 Shaft extender

4.1.2 Experimental fault description

An electrical short was artificially introduced on the stator windings. A blade was used to scratch off the resin on the outer isolation layer of windings at the location shown in Figure 4.4(b). This introduced an inter-turn short between the windings, referred to in this study as the seeded fault for the alternator experimental set-up. The original condition is shown in Figure 4.4(a). Since there are 36 winding bars, and an accelerometer which was mounted on the surface of the winding bars, this fault could be expected to influence orders which are multiples of 36. Thus for this alternator, the 36^{th} order or its multiples is of particular importance as a signature of the fault.

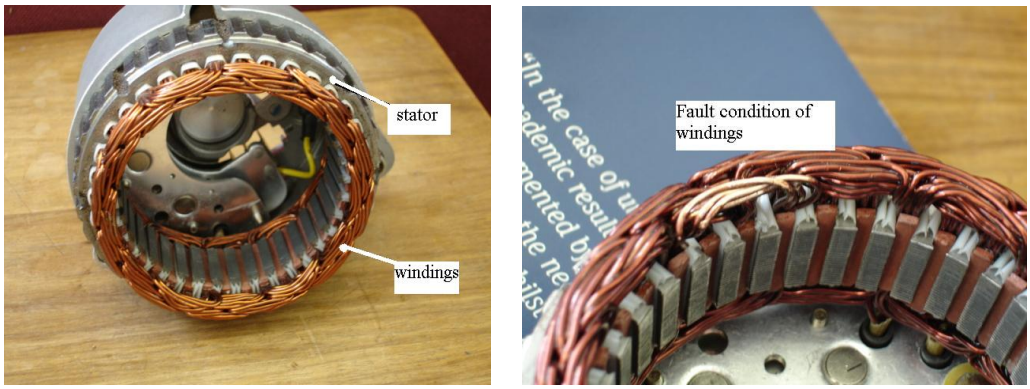

a. stator and windings b. seeded fault on windings

Figure 4.4 Seeded faults

4.1.3 Application of VKC-OT and IVK-OT techniques on the alternator experimental set-up

4.1.3.1 Application of Vold-Kalman filter and computed order tracking

This experimental set-up was first used by Wang (2008) to investigate the ability of VKF-OT in condition monitoring. Vibration signals obtained from this experimental set-up can also be used for verifying the ability of VKC-OT and IVK-OT. A typical set of measured data and the corresponding rotational speed is plotted in Figure 4.5, and shows how the vibration as well as the speed changes with time.

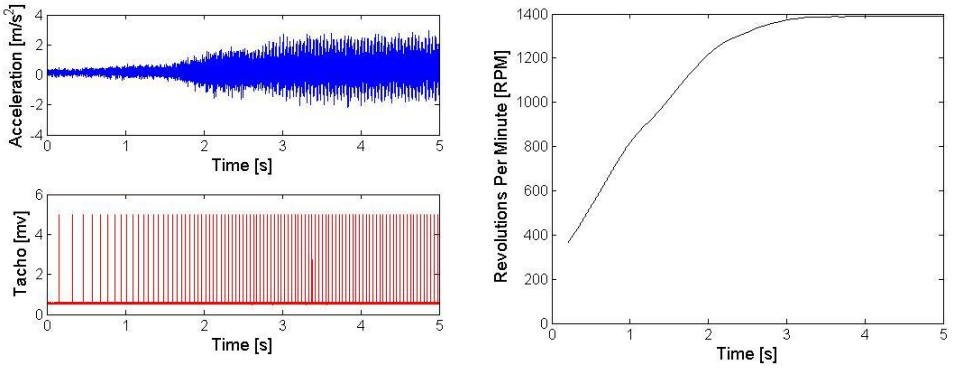

a. Measured data b. RPM

Figure 4.5 Raw data set

Clearly, this data is acquired during acceleration and the signal is quite non-stationary. Using this data, the VKC-OT technique can be applied here to extract a clear order component. Since there are 36 stator bars in the alternator, the Vold-Kalman filter is used here to extract the 36th order. Similar as to what have been done in chapter 3 of the simulation studies, some basic PSD analyses are performed. They are PSDs for the raw data, the 36th order by VKF-OT, computed order tracking and VKC-OT for the 36th order, and are plotted in Figure 4.6.

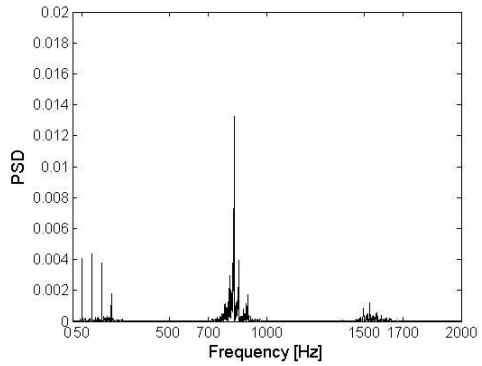

a. PSD on raw data

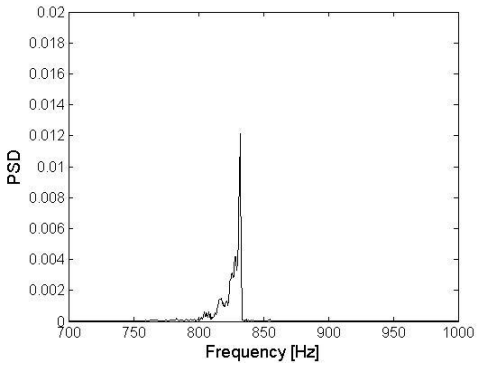

b. PSD on VKF-OT for 36th order

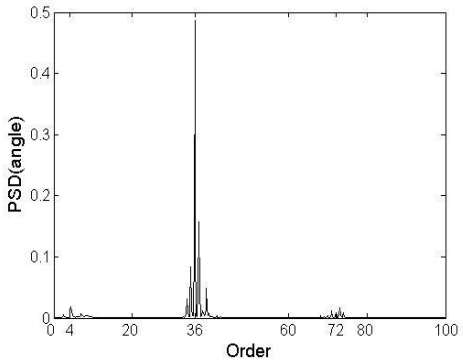

c. PSD on COT data

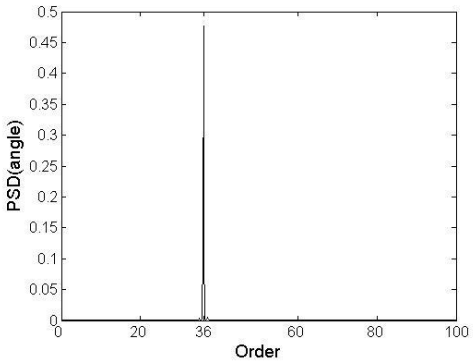

d. PSD on VKC-OT for 36th order

Figure 4.6 PSD results for alternator data

Figure 4.6(a) shows the PSD of the raw data. There are several frequency peaks around 50, 100, 150 Hz, and some higher frequency peaks around 700 – 1000 Hz and 1500 – 1700 Hz. Since the alternator output frequency is 50 Hz, it is expected to have frequencies at 50 Hz and its multiples. Besides, based upon the rotational speed measurement, full speed of the alternator can be seen to nearly approach 1400 RPM or ≈ 23.3 Hz. Since there are 36 stator bars, therefore $36 \times 23.3 = 838.8$ Hz and its multiples may appear, e.g. $72 \times 23.3 = 1677.6$ Hz. These two frequencies are clearly within these ranges of higher frequencies (700 – 1000 Hz and 1500 – 1700 Hz). It is however difficult to obtain any specific information from Figure 4.6(a).

If the Vold-Kalman filter based order tracking is performed with a relative filter bandwidth of 30%, the associated PSD spectrum is plotted in Figure 4.6(b) for the 36th order. In order to clearly see the filtered 36th order, the abscissa is zoomed over a range from 700 Hz to 1000 Hz. The 36th order is now much clearer than in Figure 4.6(a), but the smearing effect still exist and it is still not ideal for monitoring purposes. Figure 4.6(c) is the PSD (angle) of the COT result. It can be clearly seen that order 36 and its sideband orders are all included in the figure and also lower orders at around 4 as well as higher orders at around 72. It is however quite clear that it cannot focus on one order only and several order peaks are featured in the figure. The PSD (angle) does however not focus on one individual order component - in this case for example the 36th order which is of great importance for condition monitoring purposes. Finally, VKC-OT is applied to the data to extract the 36th order in Figure 4.6(d). It can be seen that a clear and clean 36th order peak exists which effectively excludes other sideband orders as well as the smearing effect. This result demonstrates the unique ability of VKC-OT technique which is intractable by using any of order tracking techniques in isolation alone. Therefore, by using VKC-OT technique, it achieves to represent a clear and individual order component in a real application.

4.1.3.2 Application of intrinsic mode function and Vold-Kalman filter order tracking

The proposed IVK-OT technique was subsequently applied to the same experimental set-up. Firstly, a data set corresponding to the alternator in good condition was considered. Again since there are 36 stator bars in the alternator, the 36th order and its multiples are key features of the signal. Therefore, EMD and VKF-OT were used to focus on the 36th order. The extracted 36th order by VKF-OT is used to compare the EMD results. In order to identify which IMF captured the 36th order, some basic frequency analysis was first performed.

Firstly, a frequency analysis of the Vold-Kalman filter result for the 36th order was done, and then a frequency analysis for each IMF was compared with the results from the Vold-Kalman filter. In this way, it was recognized that, in this case, the 6th IMF captured most of the energy associated with the 36th order. Figure 4.7 shows the results in the time domain as well as in the frequency domain.

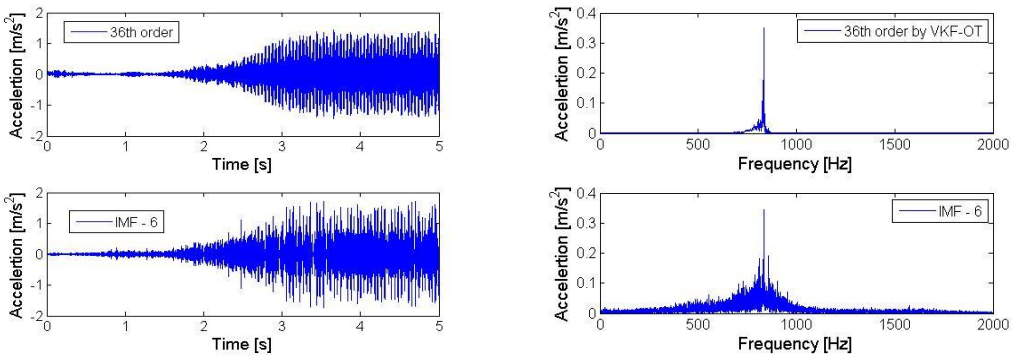

(a) Time domain waveforms (b) Frequency domain spectrum

Figure 4.7 The 36th order by VKF-OT and in IMF-6

It can be seen from Figure 4.7(a) that roughly speaking, the 36th order by VKF-OT and the 6th IMF are more or less equivalent in amplitude and shape. Strictly speaking, the result from VKF-OT is much cleaner and more uniform than its counterpart 6th IMF. This follows from the mathematical definition of equation (2.5) in which the sinusoidal nature is impressed on the filtered order of VKF-OT. Furthermore, the basic frequency analysis in Figure 4.7(b) shows that both the two time-domain waves capture the same fundamental frequency at around 838.8 Hz as has been calculated for the previous technique. However, it should be noted that the 6th IMF is obviously more complex than the 36th order by VKF-OT. This complexity is due to the resolution of the intrinsic mode function, in that all the signals that modulate the 36th order may be included, on condition that the final shape of the wave satisfies the requirements of an IMF. Clearly the 6th IMF captures the majority of the 36th order and the corresponding highest frequency

peak coincides with the Vold-Kalman filter result. The inclusion of other frequency components in one IMF is one of the shortcomings of EMD when extracting a mono-order component in real applications. However, it is also due precisely to this attribute that IMF may capture machine fault signals that modulate the order of interest. This observation from Figure 4.7 points to the possible further decomposition of the 36^{th} order related IMF and the decomposition of the signal may be useful for condition monitoring. Besides, it should also be borne in mind that the EMD process in fact separates the 36^{th} order together with vibrations that modulate it from other interference of orders, such as multiples of the 36^{th} order, like the 72^{nd} order. Therefore, all attention can now be focused on the modulated 36^{th} order.

From the experience gained in the simulation study in chapter 3, the computed order tracking results may help to recognize orders for signals. Therefore, in the following, COT is again used to transform all the analysis signals into the order domain. The 6^{th} IMF is then further decomposed. In Figure 4.8, the order domain results of the 6^{th} IMF, the Vold-Kalman filter for the 36^{th} order from 6^{th} IMF and the sequential use of the two techniques are presented.

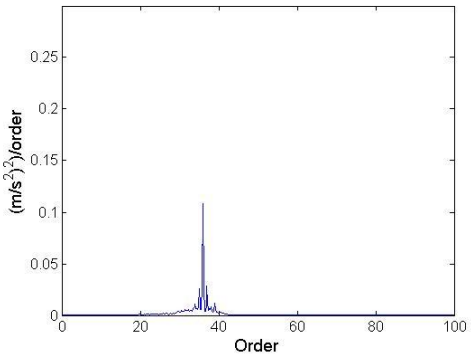

(a) 6th IMF

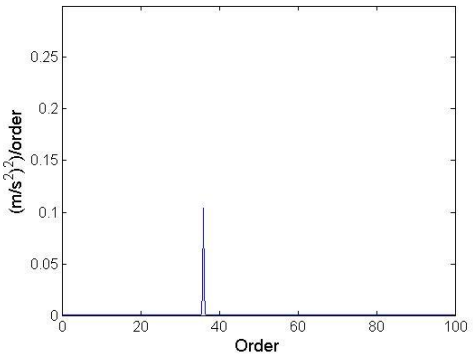

(b) Vold-Kalman filter order 36

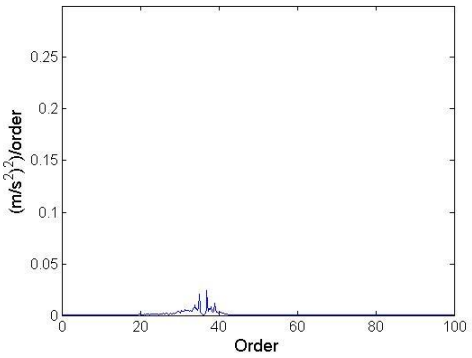

(c) Residue signal

Figure 4.8 PSD on 6th IMF, Vold-Kalman filter 36th order from 6th IMF and residue signal in order domain (good condition)

It is clear from Figure 4.8(a) that the 6th IMF includes the 36th order and some sidebands. After applying the Vold-Kalman filter, the 36th order is clearly extracted from the 6th IMF as shown in Figure 4.8(b). Figure 4.8(b) suggests that the Vold-Kalman filter succeeded in extracting the 36th order from the 6th IMF using a 20% relative filter bandwidth. Then the residue signal after sequential use of the two techniques contains the sidebands of the 36th order, as is depicted in the order domain as shown in Figure 4.8(c). Based upon the order domain analysis of the 6th IMF, it is clear that this IMF is dominated by 36th order signal. Only some sidebands are included. There are no other prominent orders appearing around the 36th order and therefore no need to further extract other

orders. Besides, as was learnt from the simulation studies, amplitude modulation may cause sidebands around dominant orders. This is a very useful indication of machine condition. Thus, the residue signals of the 6th IMF which hold sideband information will be useful for condition monitoring. This information cannot be extracted by traditional VKF-OT, but through further decomposition of 6th IMF. For illustration, the time domain residue signal is also plotted in Figure 4.9 (a) for this good condition data.

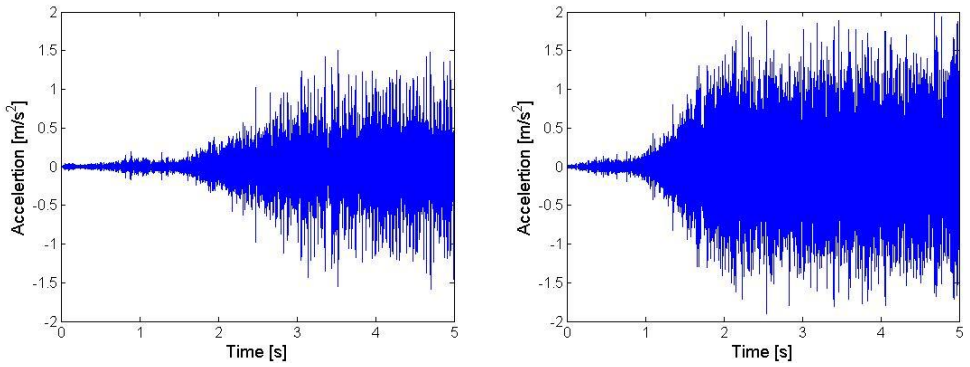

(a) Residue signal (good condition) (b) Residue signal (bad condition)

Figure 4.9 Residue signal in good and fault condition

The seeded fault signal is subsequently considered. The same COT analysis was again performed for 6th IMF, the 36th order by VKF-OT from 6th IMF and the results of combing the two techniques are shown in Figures 4.10(a), (b) and (c).

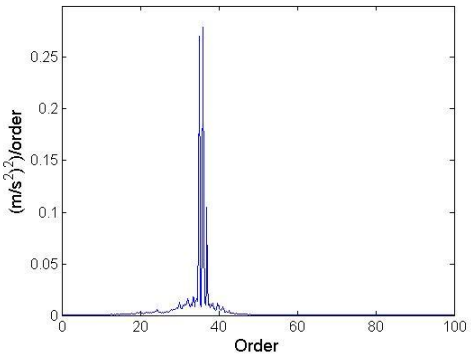

(a) 6th IMF

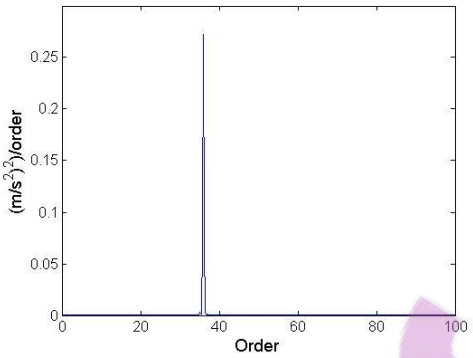

(b) Vold-Kalman filter order 36

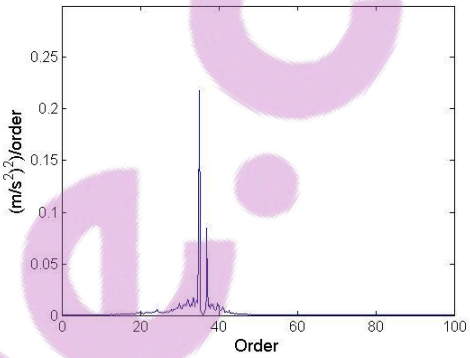

(c) Residue signal

Figure 4.10 PSD on 6th IMF, Vold-Kalman filter 36th order from 6th IMF and residue signal in order domain (seeded fault condition)

Due to the seeded fault, the amplitudes of the order component peaks in all three plots of Figure 4.10 have now clearly increased compared to the good condition shown in Figure 4.8. This is to be expected because the short circuit between the stator windings changes the electromagnetic field and causes changes in the vibration amplitude. This is especially the case for the 36th order, which corresponds to the 36 stator bars in the alternator. Clearly, Figure 4.10 again shows the successful decomposition of the 6th IMF. The corresponding time-domain residue signal is also plotted in Figure 4.9(b). When compared with its counterpart in Figure 4.9(a), the system changes can be clearly identified simply

from the amplitude of the two residue time-domain signals. Besides, the order domain peaks in Figures 4.10(b) and (c) have both substantially increased.

However, most importantly, with the help of order tracking techniques, 6th IMF has been further decomposed into 36th order and sideband residues. This kind of separated vibrations is not achievable by the EMD method or VKF-OT alone. Thus, the 36th order as well as its sideband information is available and it is worthwhile studying each part of the signal to track the system changes in this real case and see how the different parts of signals contribute to the overall changes. Therefore, one of the most frequently used time-domain techniques, namely root mean square (RMS) analysis, was used here to demonstrate the diagnostic ability of time-domain signals of different parts. Three RMS values were compared for good and seeded fault conditions, as shown in Table 4.1.

Table 4.1 RMS for different signals

Signals	RMS - good	RMS - seeded fault	$\frac{(RMS(fault) - RMS(good))}{RMS(good)}$
IMF-6	0.3244	0.5758	77.5%
36th order from IMF-6	0.1568	0.2686	71.3%
Residue	0.2770	0.4974	79.57%

It can be concluded from this table that the changes in the 6th IMF are caused by both the 36th order and its residue. Clearly the RMS values of all of these signals change substantially. This result is reasonable, since the seeded fault in the inter-turn short circuit in the stator winding would influence the vibrations of both the 36th order and its sidebands. An inter-turn short in the stator windings of an alternator would not introduce simple parameter changes in the system but

influences the electromagnetic forces between stator and rotor in that entire area so that the vibration amplitude in that area is disturbed. Consequently, it should be expected that both order signals and sideband signals would be influenced by the introduction of the seeded fault. However, the further decomposition of the 6th IMF enables detailed studies of 36th order and its sideband vibrations in the time domain. For this specific case, changes in the sidebands to the residue signal are higher than the changes in the 36th order, by 79.57% and 71.3% respectively. Both of these signals are indicators of the stator inter-turn short. However, different part of signals may indicate the changes of different scenarios of machine conditions. When both the 36th order and its sidebands increase evenly, it means the whole electromagnetic force is increased, whereas, if additional sidebands increase compared to the dominant 36th order, this means that more amplitude modulation occurs.

Thus, from these detailed studies of the signals, it may be deduced that, after introduction of the seeded fault, the amplitude modulations of the 36th order become more severe than for the good condition. This is a clear indication of a machine inter-turn short which causes the change of electromagnetic force in a certain area and result in amplitude modulation of vibrations in the 36th order. As a result, the further decomposition of 6th IMF in this experimental study provides a method to examine in detail each part of the signal so as to provide in-depth understanding of machine condition. The experimental study therefore demonstrates that IVK-OT technique may be employed to further decompose the IMFs and therefore provides additional diagnostic capabilities for distinguishing and evaluating fault severity in machine vibration signals.

4.2 Transmission gearbox set-up data analysis

4.2.1 Experimental gear box set-up

For illustration of the ICR technique in condition monitoring, the technique is now demonstrated in a real working environment on signals from an experimental gearbox. The gearbox test rig was designed to conduct accelerated gear life tests on a Flender E20A gearbox under varying load conditions at the University of Pretoria Sasol Laboratory for Structural Mechanics. The experimental set-up consisted of three Flender Himmel Motox helical gearboxes, driven by a 5 kW three phase four pole Weg squirrel cage electrical motor. A 5.5 kVA Mecc alte spa three phase alternator was used for applying the load. The direct current (DC) fields of the alternator were powered by an external DC supply in order to control the load that was applied to the gears. A sinusoidal load with minimum to maximum loads from 7.4 to 14.7 (Nm) was applied to the alternator. Two additional Flender E60A gearboxes were incorporated into the design in order to increase the torque applied to the small Flender E20A gearbox which was being monitored shown in Figure 4.11. The gear mesh frequency is 215Hz at 5 Hz shaft rotational speed. For details about the test rig the reader may also refer to the paper by Stander and Heyns (2006) and the master's dissertation of Schön (2006). In this case however the response measurements were taken with a Polytec PDV-100 laser Doppler vibrometer with a 500 mm/s measurement range (see Figure 4.11).

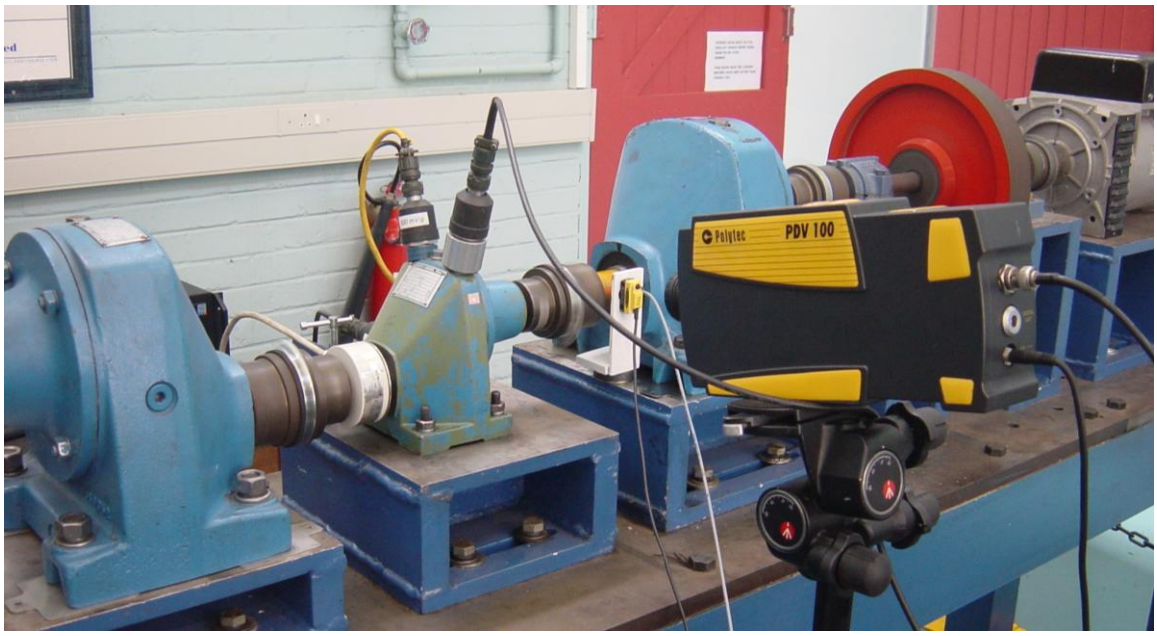

Figure 4.11 Experimental test rig

4.2.2 Experimental fault description

During the experimental process, the gear in Flender E20A gearbox at the centre of the set-up, was artificially damaged through overloading. This resulted in severe wear which eventually culminated in several broken teeth and ultimately stripped gear teeth. The original shape of the drive gear and its final state when all the teeth are removed are shown in Figure 4.12(a) and (b). However not all the obtained data is being considered in this experimental study. Only the data when the first gear tooth is removed is being used for the seeded fault studies in this experimental set-up.

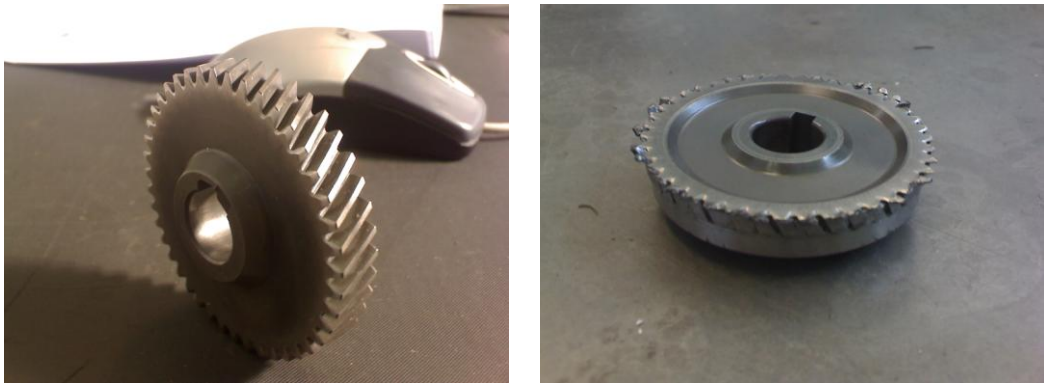

a) Original status of drive gear b) Final status of drive gear

Figure 4.12 Gear damage

4.2.3 Application of intrinsic cycle re-sampling

a. Traditional signal processing analysis on good condition

The monitored gearbox was set to run at about 300 rpm. To begin with, a 2 s signal was measured before damage was first introduced. The time domain waveform with the corresponding rotational speed, frequency spectrum of the translational velocity and computed order maps around 1× gear mesh order are shown in Figure 4.13.

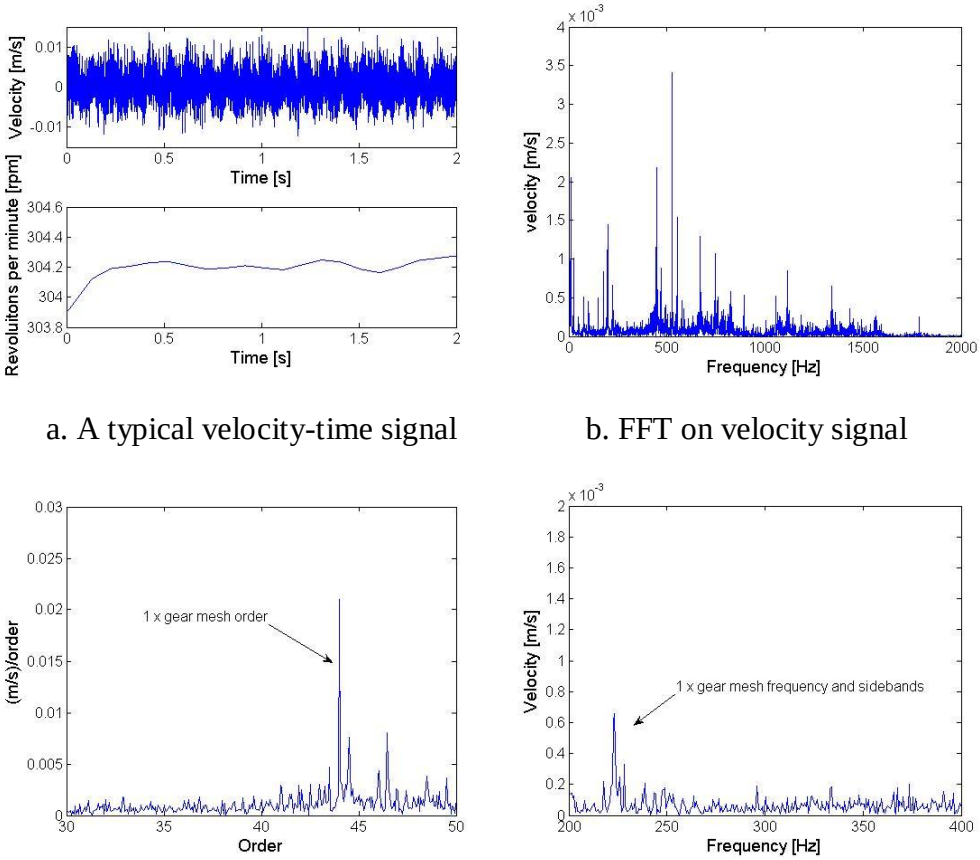

a. A typical velocity-time signal b. FFT on velocity signal

c. Computed order tracking d. Zoom in for 1× gear meshing frequency

Figure 4.13 Traditional signal processing methods

In these figures no damage has been introduced yet and no clear impacts occur in the time domain signal (Figure 4.13(a)). However amplitude modulation is visible throughout the period. Although the gearbox operates in a stable condition, the load fluctuation influences the rotational speed which leads to the frequency variation in the signal. From the Fourier analysis (Figure 4.13(b)) it is clear that the real gearbox data is much more complex than the simulated signal in chapter 3. Many frequency peaks appear throughout the spectrum. For condition monitoring purposes, we focus on the gear mesh frequency in the frequency spectrum. The spectrum after zooming in around 1× gear mesh frequency is shown in Figure 4.13(d). In figure (d), some sidebands around the

gear meshing frequency are also visible which are spaced at approximately 5 Hz. This corresponds to the rotational frequency of the gear. As expected the sidebands for the undamaged gear are few and small. The computed order tracking map in Figure 4.13(c) which zooms in around $1\times$ gear mesh order is also plotted. It should also be noted that although the order analysis excludes the speed variation effects, the spectra are still fairly complex and show several order sidebands around the gear mesh order.

b. Choosing an appropriate IMF

Once one has a basic understanding of the raw signal, EMD may be applied to the signal to extract the gear mesh information for further ICR application. The 5th to 8th IMFs are plotted in Figure 4.14 as velocity as a function of frequency.

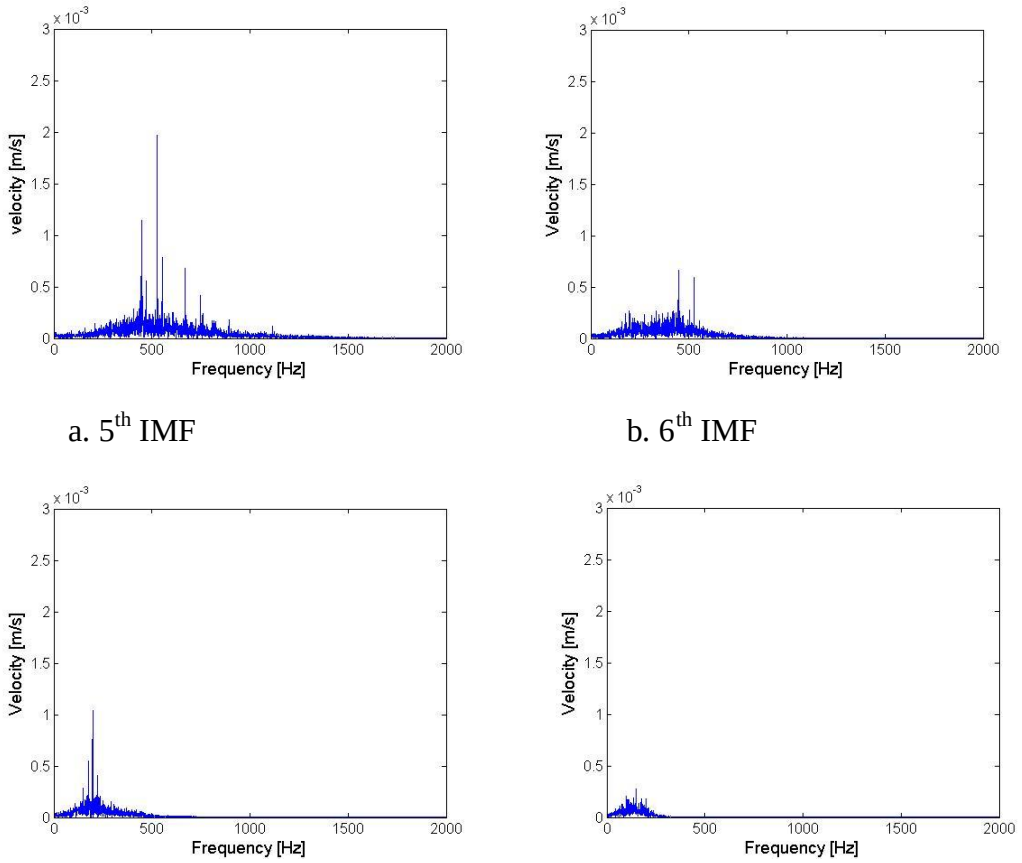

a. 5th IMF b. 6th IMF

c. 7th IMF d. 8th IMF

Figure 4.14 IMFs of system response

It can be seen from Figure 4.14 that the 7th IMF captures the signal content which is relevant to the nominal gear mesh frequency at 215 Hz. Although some energy is present in the 6th and 8th IMF, this is however fairly small. For the 5th IMF very little energy is observed in that range. As a result, the 7th IMF is of great importance for condition monitoring of gear mesh conditions. Therefore ICR is performed on the 7th IMF and result is shown in Figure 4.15. The result shows that the sidebands around the main frequency peak are oscillating and a clear two distinct sidebands appear around main frequency peak. The whole spectrum only concentrates on frequency range from 150 Hz to 250 Hz in which only those gear mesh related vibrations are being focused. Outside this frequency range, spectrum becomes negligible. This is very different from traditional methods as in Figure 4.13. In this case, the main frequency component is located at 210 Hz which is very close to the calculated nominal gear mesh frequency at 215 Hz, it is clear that the 7th IMF captures the gear mesh vibrations for this good condition case data.

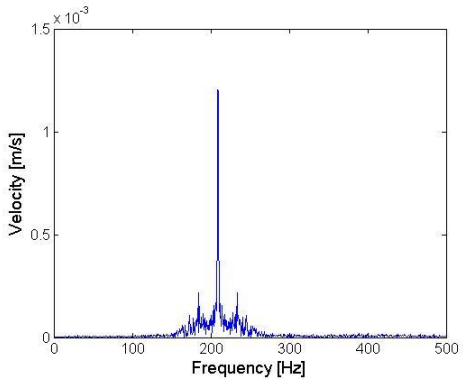

Figure 4.15 ICR on 7th IMF result

c. Traditional signal processing methods on fault detection

Once the seeded fault as described in the experimental set-up has been induced, the measured signals were considered over the same period as before. Firstly,

traditional signal processing methods are used to detect the system changes. Thus, time, frequency and order domain results are analyzed and compared in different figures as is shown in Figure 4.16. In order to clarify the differences between figures, the results for good and seeded fault conditions are superimposed on the same plot and normalized in terms of the highest frequency or order peaks that in frequency and order domain.

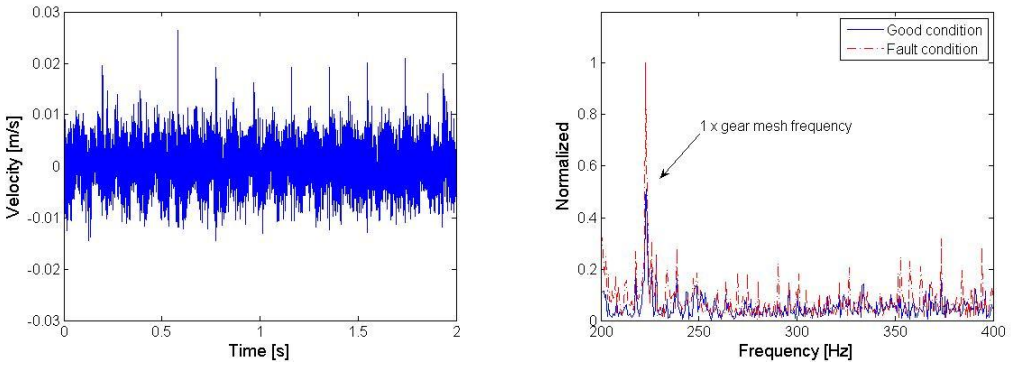

a. Time domain signals (fault) b. Zoomed in 1 × gear meshing frequency

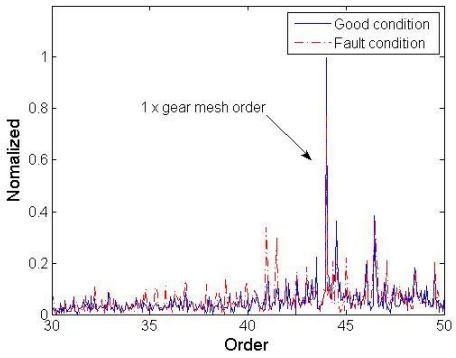

c. Zoomed in 1 × gear mesh order

Figure 4.16 Signals with broken tooth

Firstly, Figure 4.16(a) clearly shows that a periodic impact occurs in the signal, and that the period of this impact is approximately 0.2 s with a corresponding frequency of 5 Hz, which suggests that this impact occurs once per revolution. This is consistent with the induced fault scenario. Secondly, in the frequency

domain, it shows that more sharp sidebands appear in the spectrum and all the amplitudes of frequency peaks are increased, especially the 1× gear mesh frequency component. It is well known that if additional sidebands appear and existing sidebands increase around the gear mesh frequency, this indicates a broken gear tooth problem in the gearbox. Further, computed order analysis comparisons in Figure 4.16(c) again confirms that extra orders around gear mesh order increased due to the seeded fault on gear teeth, but it also shows that relative amplitude of several order sidebands compared with gear mesh order does not change as much as happened in the frequency domain. However, in this case, the additional order sidebands show the detection of the changes for gear mesh conditions. In short, experimental studies using traditional time, frequency and order domain methods achieve the detection of the seeded fault.

d. ICR result on seeded fault gearbox data

ICR is then applied to the faulted gear experimental data. In order to clearly show the difference of the spectrum before and after the seeded fault, the figure is also superimposed with the good condition result and normalized in terms of highest peak. Figure 4.17 shows the results.

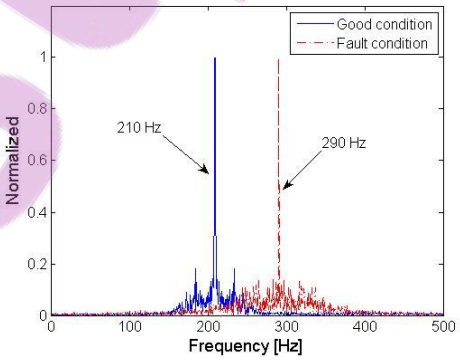

Figure 4.17 ICR result on faulted gear experimental data

As was learnt from the simulation studies in chapter 3, two aspects of the ICR results which respond to faults, are examined in Figure 4.17. These are M.F. and S.V. Clearly, for the seeded fault case, the M.F. value displays a significant shift from 210 Hz in good condition to 290 Hz. This is a clear indication of the increase of ICs, therefore a shift of f_{ICR}. From the perspective of S.V., firstly, the sidebands changed dramatically, therefore, the variation of the signal could not merely have been caused by rotational speed. This corresponds to chapter 2 paragraph 2.3.2 guideline (b). Secondly, although the highest sideband amplitudes do not change dramatically relative to the main frequency peak in the fault condition, many more sideband peaks appear in the spectrum. This is very different from the good condition where two highest sidebands appear distinctly. This indicates that the amplitude modulation part $A_{ICR}(t)$ of the seeded fault case is fundamentally changed. The above observations correspond to chapter 2 paragraph 2.3.2 guidelines (c) and (d). Clearly the fault introduced here does not represent a trivial influence to the gear mesh vibrations, which is consistent with the known broken gear tooth damage.

In short, observations from the ICR results clearly show the changes in the gear mesh vibrations. Comparing Figure 4.16(b), (c) and Figure 4.17 in frequency, order and ICR results respectively, it is not difficult to determine that the ICR technique provides simple and clear indicators for detecting the changes in terms of M.F. and S.V., especially for the distinct shift of M.F. However traditional methods will present many sidebands and amplitude variations in frequency or order domain which may complicate the process of decision making on fault diagnostic. As a result, compared with traditional methods in fault diagnostic in this experimental study, ICR provides effective and unique indicators for detecting seeded fault which make ICR technique can be a good alternative method to condition monitoring.

4.3 Summary

The two experimental setups provide opportunities to verify the three improved order tracking techniques in real rotating machinery environments. The VKC-OT technique presents its unique ability of featuring an individual clear order component under the varying rotational speed. The IVK-OT technique separates the order component and those vibrations that modulate order in an IMF which provides a deep understanding and ability to track machine conditions. The ICR technique transforms complicated gear mesh vibration related IMFs into simple signal spectrum figures which first empirically exclude frequency variation effects in the signal and then features more specific indicators, namely sidebands variations (S.V.) and main frequency component (M.F.), for condition monitoring. The experimental studies confirm the abilities of all three improved order tracking techniques.

Chapter 5 Conclusions

5.1 Contributions of the research

5.1.1 A brief review of the development of three improved order tracking approaches

As have been reviewed in chapter 1, various kinds of order tracking methods are presented in the literature. In this research, however three widely available and proven effective order tracking methods were chosen and studied to explore their characteristics in relation to each other, so that improved order tracking approaches could be developed for the purpose of condition monitoring rotating machines. The three methods that have been selected for developing the improved approaches are computed order tracking (COT), Vold-Kalman filter order tracking (VKF-OT) and the extraction of intrinsic mode functions (IMFs) through empirical mode decomposition (EMD).

Each of the techniques has their own advantages and disadvantages in different applications. Through the discussions of these pros and cons in chapter 1 paragraph 1.2, improved approaches to order tracking by combining these methods are presented in Table 1.1 and explained thereafter in chapter 1. This leads to the further development of advantages and avoidance of limitations to order tracking analysis by combing these three order tracking methods, namely (as is indicated in Table 1.1) VKF/COT, IMF/VKF and IMF/COT. Further, in the scope of work as outlined in paragraph 1.4 (Figure 1.4), the inter-relationships between the different order tracking methods are schematically depicted. Three improved order tracking approaches are formally introduced, namely Vold-Kalman filter and

computed order tracking (VKC-OT), Intrinsic mode function and Vold-Kalman filter order tracking (IVK-OT) and Intrinsic cycle re-sampling (ICR).

These three improved approaches may be summarised as follows:

VKF/COT →VKC-OT:

COT and VKF-OT are complementary to each other with respect to specific advantages and disadvantages. On the one hand, COT transforms non-stationary time domain data into the stationary order domain, while VKF-OT does nothing to transform the data to stationarity. On the other hand, COT cannot focus on each individual order as can be done by VKF-OT. Therefore, the combined application of the two methods is developed, namely VKC-OT.

IMF/VKF →IVK-OT:

VKF-OT results can constitute components of IMFs. Firstly, VKF-OT exhibits excellent filtering abilities for the extraction of order components. However precisely because of this ability to focus on orders of interest, it is incapable to capture the vibrations that modulate the orders, especially for speed non-synchronous vibrations. IMFs from EMD, however include both order vibrations and vibrations that modulate orders. Therefore, VKF-OT is used to further decompose the IMFs so that the orders as well as the vibrations that modulate them, can be separated for condition monitoring purposes. As a result, the IVK-OT method is developed.

IMF/COT→ICR:

IMF and COT in fact are not directly related. However, the advantages of the especially simple data structure of an IMF and the idea of re-sampling to transform

non-stationary data to stationary data in COT can be reconciled so that the ICR technique may be developed, and approximated order tracking effects on the IMFs can be achieved. This offers benefits for condition monitoring.

Through the development of the approaches in chapter 2 and the simulation and experimental demonstrations in chapters 3 and 4, the nature of the improved order tracking approaches become clear and are proven effective.

In the following the improvements offered by the proposed approaches are elaborated upon. These approaches are subsequently discussed in the context of condition monitoring.

5.1.2 Contributions of each improved order tracking approach

Vold-Kalman filtering and computed order tracking (VKC –OT)

This specific technique is mainly for extracting order components and excluding speed variation effects to render simple order components in the order spectrum. Advantage is taken from the definition of Vold-Kalman filter order tracking to extract and ensure the harmonic nature of an order component. In addition advantage is also taken from the re-sampling ability of computed order tracking to transform non-stationary effects due to the variation of rotational speed into stationarity. The contributions of this technique are primarily:

1. The analyst may focus on orders of interest which may be non-dominant amongst the signals and signals are strongly influenced by rotational speed.

2. Due to the use of VKF-OT, the VKC-OT technique has been imparted with the ability of extracting harmonic and smooth order signals and at the same time COT transforms non-stationary data to stationary data due to the variations of

rotational speed. Thus, the signals after application of VKF-OT and COT become more suitable for subsequent Fourier analysis and therefore render clearer order spectra for condition monitoring purposes.

In short, the VKC-OT technique capitalise on the advantages of VKF-OT and COT to present focused and clear order spectra. Again, the advantages of VKF-OT in terms of its strict mathematical filter to focus on orders of interest, and COT in its re-sampling procedure to exclude speed variation effects in signals, make the VKC-OT method more focused on orders of interest than COT and results in cleaner spectrum results than VKF-OT.

Intrinsic mode function and Vold-Kalman filter order tracking (IVK-OT)

This technique is specially developed for further decomposition of IMFs from EMD. The EMD process may decompose signals into different IMFs ranging from high to low frequency content. Applying this process to rotating machine vibration signals may separate order signals into different IMFs. These order related IMFs differ from traditional order tracking results such as VKF-OT. For one order related IMF, order signals together with vibrations that modulate orders are all possible to be included in an IMF. And these vibrations that modulate orders may consist of speed synchronous and non-synchronous vibrations. However traditional order tracking methods, e.g. VKF-OT, can only focus on vibrations that are synchronous with rotational speed. In reality, rotating machinery fault vibration signals are very likely in the form of vibrations that modulate order signals. These vibrations that modulate orders may therefore contain abundant machine condition information and not necessarily all synchronous with rotational speed. The IVK-OT technique is thus used to further decompose order related IMFs in terms of rotational speed, so that speed synchronous order vibrations and other vibrations that modulate orders in IMFs may be further distinguished. An important area - speed non-synchronous vibrations that modulate orders - that

un-extractable through EMD and traditional order tracking methods can be approached through IVK-OT technique. In summary, contributions of this technique lie in:

1. By using EMD the analysis exploits its powerful empirical nature which allows obtaining results which are intractable by most order tracking techniques. This empirical decomposition process can separate vibration orders into different IMFs. Each IMF is very similar to order tracking results, such as VKF-OT.

2. The relationship between an order and an IMF is discussed in this research and it is clear that this issue has not been properly discussed by researchers in the current literature. Thus another contribution of this work is the introduction and discussion of this issue.

3. Vibrations that modulate order components in the time domain (especially those vibrations that are non-synchronous with rotational speed) is captured. This is intractable by using other order tracking techniques and useful for rotating machinery fault diagnosis.

4. The adaptive nature of both IMF and VKF-OT allows the IVK-OT technique to follow the changes of non-stationary signals due to variations of rotational speed. Both of the techniques can also be treated as filters, therefore the IVK-OT technique is a kind of adaptive filter method to deal with non-stationary rotating machine vibrations.

In conclusion, from the theoretical point of view, the discussion on technique provides a description of the relationship between an order and an IMF which fills a gap in the literature. From the condition monitoring rotating machinery point of view, the IVK-OT technique provides an adaptive and order focused method to diagnose rotating machines and further provides the ability to separate vibrations

that modulate orders, especially those vibrations that are not synchronous with rotational speed. The vibrations that modulate orders are often useful indicators of machine faults and may not be easily extracted by EMD or traditional order tracking methods in isolation alone.

Intrinsic cycle re-sampling (ICR)

The ICR technique is based upon IMF from EMD. Taking advantage of the simple data structure of IMF, the novel concept of an intrinsic cycle (IC) is introduced. Further, considering computed order tracking technique in dealing with non-stationary rotational speed vibrations, the re-sampling idea is borrowed into an IMF through ICs so that the frequency variation effects due to rotational speed can be largely excluded between ICs in an IMF. The contributions of this technique are:

1. The result of this technique offers a simple method to approximate computed order tracking effects without the need for a rotational speed measurement, which makes this a practical albeit approximate approach for real vibration monitoring.

2. Through the exclusion of speed variation effects by empirical re-sampling ICs on an IMF, ICR provides unique frequency domain indicators for condition monitoring. The exclusion of frequency variation effects makes the interpretation of a re-sampled IMF more specific than the original IMF. It provides a simple and alternative method for the analyst to understand the condition of machines.

In short, the novel idea of using ICs in IMF and the borrowed idea of signal re-sampling from COT enables ICR to empirically exclude non-stationary rotational speed influences and approximate computed order tracking effects, so that the

re-sampled IMF becomes more specific to interpret and is therefore beneficial for condition monitoring on rotating machinery. The ICR technique as a possible alternative vibration monitoring tool and was demonstrated to render useful results.

5.1.3 Contributions of the three improved order tracking approaches as a whole in order related vibration signals

The previous discussions emphasised the usefulness of all three improved order tracking approaches in their own right. However, their contributions as a whole essentially provide a useful platform for order tracking analysis in condition monitoring. In the context of condition monitoring of rotating machines, order tracking analysis basically need to address two classes of vibration signals. Traditionally, order tracking analysis only focuses on the speed synchronous vibrations. But, vibrations that modulate order signals are also very important information for condition monitoring. Therefore, this is an indispensable part of order tracking analysis in terms of condition monitoring. The three improved order tracking approaches are in fact developed for dealing with both of these classes of vibration. Table 5.1 summarises the emphasis of the three improved order tracking approaches.

Table 5.1 Emphasis of three improved order tracking approaches

	0rder vibrations	Vibrations that modulate orders
VKC-OT	√	
IVK-OT		√
ICR	√	√

Firstly, the VKC-OT method is developed to focus on obtaining better order spectra of speed synchronous orders. Only speed synchronous order signals are

considered in this technique. Therefore, the technique is useful for order vibrations. Secondly, the IVK-OT method is developed to separate vibrations that modulate orders through which IMFs can be further decomposed in terms of rotational speed (see Table 5.1). The vibrations that modulate orders, therefore, can be achieved. Lastly, both order signals and vibrations that modulate orders are considered as a whole in the ICR technique. Signal changes in order related vibrations as well as in vibrations that modulate orders, will all be reflected in re-sampled IMF through ICR. As a result, the ICR technique addresses both order vibrations and vibrations that modulate orders, as is indicated in Table 5.1. In short, three improved order tracking approaches have been developed for contributing to order tracking analysis of rotating machinery condition monitoring. Each of these techniques is complementary in the overall perspective of order tracking analysis.

5.2 Future work

In this work, efforts have been focussed on developing improved order tracking techniques. Further applications of these techniques in real practice are needed. Systematically integrating three improved order tracking approaches into current condition monitoring software packages is also useful for enhancing abilities of order tracking analysis.

Appendix The smoothness condition for a Vold-Kalman filter

Howell (2001) defines the smoothness condition as follows:

To be smooth over an interval (α, β), a function $x(t)$ must satisfy two conditions:

- $x(t)$ must be differentiable (and hence continuous) everywhere on (α, β), and
- $x'(t)$ must also be a continuous function on (α, β)

This requires further definition of the terms continuous and differentiable (Howell, 2001):

A function $x(t)$ is continuous at a point t_0 if $x(t_0)$ and $\lim_{t \to t_0} x(t)$ both exist and $\lim_{t \to t_0} x(t) = x(t_0)$.

A function $x(t)$ is differentiable at a point t if and only if $\lim_{\Delta t \to 0} \frac{x(t+\Delta t) - x(t)}{\Delta t}$ exist. If $x(t)$ is differentiable at every point in a given interval (α, β), then $x(t)$ is said to be differentiable on the interval (α, β).

These concepts can now be applied to the structural equation for a 2-pole filter as given by Tůma at equation (2.3) in chapter 2,

$$x(n) - 2x(n+1) + x(n+2) = \varepsilon(n)$$

Illustration:

For a 2-pole Vold-Kalman filter, the sequence as filtered according to the structural equation may be written as $x(n) = 2x(n+1) - x(n+2) + \varepsilon(n)$ (equation

(2.4) in chapter 2). If adjusting it to be continuous form, it becomes $x(t)=2x(t+\Delta t)-x(t+2\Delta t)+\varepsilon(t)$. Since $\varepsilon(t)$ is the error which is minimized by global solution of the data and structural equations (Tůma, 2005), it may be neglected for the purposes of the illustration, and the equation becomes $x(t)=2x(t+\Delta t)-x(t+2\Delta t)$.

From the above, smoothness now requires that $x(t)$ must be differentiable (and hence continuous) everywhere on certain interval (α,β) and $x'(t)$ must also be a continuous function on (α,β).

Differentiability

$$\lim_{\Delta t\to 0}\frac{x(t+\Delta t)-x(t)}{\Delta t}=\lim_{\Delta t\to 0}\frac{2x(t+\Delta t+\Delta t)-x(t+\Delta t+2\Delta t)-2x(t+\Delta t)+x(t+2\Delta t)}{\Delta t}$$

$$\lim_{\Delta x\to 0}\frac{0}{0}=1$$

The limit will always exist. Thus, this function is differentiable (and hence continuous).

Continuity of $x'(t)$

Since $x(t)$ is differentiable, then $x'(t)=2x'(t+\Delta t)-x'(t+2\Delta t)$, thus

$$\lim_{t\to t_0}x'(t)=\lim_{t\to t_0}2x'(t+\Delta t)-x'(t+2\Delta t)=\lim_{t\to t_0}2x'(t+\Delta t))-\lim_{t\to t_0}x'(t+2\Delta t)$$

$$\Rightarrow$$

$$\lim_{t\to t_0}x'(t)=\lim_{t\to t_0}\left[\lim_{\Delta t\to 0}2\frac{x(t+\Delta t+\Delta t)-x(t+\Delta t)}{\Delta t}\right]-\lim_{t\to t_0}\left[\lim_{\Delta t\to 0}\frac{x(t+2\Delta t+\Delta t)-x(t+2\Delta t)}{\Delta t}\right]$$

Swap the limits and notice that $x(t)$ is differentiable and hence continuous, then $\lim_{t\to t_0}x(t)=x(t_0)$, thus,

$$\lim_{t\to t_0} x'(t) = \lim_{\Delta t\to 0}\left[\lim_{t\to t_0} 2\frac{x(t+\Delta t+\Delta t)-x(t+\Delta t)}{\Delta t}\right] - \lim_{\Delta t\to 0}\left[\lim_{t\to t_0}\frac{x(t+2\Delta t+\Delta t)-x(t+2\Delta t)}{\Delta t}\right]$$

$$\Rightarrow$$

$$\lim_{t\to t_0} x'(t) = \lim_{\Delta t\to 0} 2\frac{x(t_0+\Delta t+\Delta t)-x(t_0+\Delta t)}{\Delta t} - \lim_{\Delta t\to 0}\frac{x(t_0+2\Delta t+\Delta t)-x(t_0+2\Delta t)}{\Delta t}$$

$$\Rightarrow$$

$$\lim_{t\to t_0} x'(t) = 2x'(t_0+\Delta t) - x'(t_0+2\Delta t) = x'(t_0)$$

So $x'(t)$ is continuous.

From the above the filtered signal from 2-pole Vold-Kalman filter is continuous and smooth. Similar procedures may be applied to 1 and 3 pole filters.

References

Albright M. F. and Qian Sh. (2001), A comparison of the newly proposed Gabor order tracking technique vs. other order tracking methods. *SAE paper*, No.2001-01-1471.

Blough J. R. (2003), A survey of DSP methods for rotating machinery analysis, what is needed, what is available. *Journal of Sound and Vibration*, 262, pp707-720.

Bossley K. M., Mckendrick R. J., Harris C. J. and Mercer C. (1999), Hybrid computed order tracking, *Mechanical Systems and Signal Processing* 13(4), pp627-641.

Brandt A., Thomas L., Ahlin K. and Tůma J. (2005), Main principles and limitations of current order tracking methods. *Sound and Vibration*, March 2005.

Brüel and Kjær (2007), Product Data: Vold-Kalman order tracking filter - Type 7703 for Pulse. Available at: http://www.bksv.com/pdf/bp1760.pdf/ [Accessed: 11 Sep 2007.]

Chen H. G., Yang Y. J. and Jiang J. S. (2007), Vibration-based damage detection in composite wingbox structures by HHT, *Mechanical Systems and Signal Processing*, 21, pp307-321.

Chen J. Sh., Yu. D. J., Tang J. Sh. and Yang Y. (2009), Local rub-impact fault diagnosis of the rotor systems based on EMD, *Mechanism and Machine Theory*, 44, pp784-791.

Cohen L. (1995), *Time-frequency analysis*. Englewood Cliffs, NJ: Prentice-Hall.

Daetig M., and Schlurmann T. (2004), Performance and limitations of the Hilbert-Huang transformation (HHT) with an application to irregular water waves, *Ocean Engineering*, 31, pp1783–1834.

Eggers B. L., Heyns P. S. and Stander C. J. (2007), Using computed order tracking to detect gear condition aboard a dragline. *The Journal of Southern African Institute of Mining and Metallurgy*, 107, pp1-8.

Feldman M. (2008), Theoretical analysis and comparison of the Hilbert transform decomposition methods, *Mechanical Systems and Signal Processing*, 22, pp509-519.

Feldman M. (2009), Analytical basics of the EMD: Two harmonic decomposition, *Mechanical Systems and Signal Processing*, 23, pp2059-2071.

Feldbauer C. and Holdrich R. (2000), Realisation of a Vold-Kalman Tracking Filter – A Least Square Problem, *Proceedings of the COST G-6 Conference on Digital Audio Effects*, DAFX 1-4, Verona Italy, December 7-9.

Flandrin P., Rilling G. and Gonçalvés P. (2004), Empirical mode decomposition as a filter bank, *IEEE Signal Processing Letters*, 11(2).

Fyfe K. R. and Munck E. D. S. (1997), Analysis of computed order tracking. *Mechanical Systems and Signal Processing*, 11(2), pp187-205.

Rilling G., Flandrin P. and Goncalves P. (2003), On empirical mode decomposition and its algorithms, in: IEEE-EURASIP. *Workshop on Nonlinear Signal and Image Processing NSIP-03*, Grado (I).

Gade S., Herlufsen H., Konstantin-Hansen H. and Vold H. (1999), Characteristics of the Vold-Kalman order tracking filter, *Brüel and Kjær Technical review*.

Gao Q., Duan C., Fan H. and Meng Q. (2008), Rotating machine fault diagnosis using empirical mode decomposition, *Mechanical Systems and Signal Processing*, 22, pp1072-1081.

Guo D. and Peng Z. K. (2007), Vibration analysis of a cracked rotor using Hilbert-Huang transform, *Mechanical Systems and Signal Processing*, 21, pp3030-3041.

Guo Y., Chi Y. L. and Zheng H. W. (2008), Noise reduction in computed order tracking based on FastICA, Proceedings of the 2008 IEEE/ASME, *International Conference on Advanced Intelligent Mechatronics*, July 2-5, 2008, Xi'an, China.

Guo Y., Tan K. K., Huang S. N. and Zhang Y. (2008), Noise removal in Vold-Kalman order tracking based on independent component analysis, *Proceedings of the IEEE International Conference on Automation and Logistics* Qingdao, China September 2008.

He L., Zhang Y. and Wen B. (2007), Experiment Research on Gear wearing Using order tracking, *12th IFToMM World Congress*, Besançon (France), June 19-21, 2007.

Herlufsen H., Gade S. and Konstantin-Hansen H. (1999), Characteristics of the Vold/Kalman order tracking filter. *Proceedings of the 17th International Modal Analysis Conference*, Kissimmee, Florida.

Howard I., Jia S. X. and Wang J. D. (2001), The dynamic modelling of a spur gear in mesh including friction and a crack, *Mechanical Systems and Signal Processing*, 15(5), pp831 -853.

Howell K. B. (2001), *Principles of Fourier analysis,* Chapman & Hall/CRC.

Huang N. E., Shen Z., Long S. R., Wu M. C., Shin H. H., Zheng Q., Yen N. C., Tung Ch. Ch. and Liu H. H. (1998), The empirical mode decomposition and the Hilbert spectrum for nonlinear and non-stationary time series analysis, in: *Proceedings of the Royal Society, London*, 454, pp903-995.

Huang N. E., Wu Z. H. and Long S. R. (2006), On instantaneous frequency, in: Workshop on the recent developments of the Hilbert-Huang Transform methodology and its applications, Taipei, 15-17 March 2006.

Li H. (2007), Gear Fault Monitoring Based on Order Tracking and Bi-spectrum under Running-up Condition, Proceeding of the Fourth International Conference on Fuzzy Systems and Knowledge Discovery(FSKD 2007), 4, pp379-383.

Li H. L., Deng X. Y. and Dai H. L. (2006), Structural damage detection using the combination method of EMD and wavelet analysis, *Mechanical Systems and Signal Processing*, 21, pp298-306.

Li H. G. and Meng G. (2005), Detection of harmonic signals from chaotic interference by empirical mode decomposition, *Chaos, Solutions and Fractals,* 30, pp930-935.

Liu Y. and Jiang S. (2007), A simple method of computing signal order tracking fast in time domain, *Second International Conference on Innovative Computing, Information and Control*, 5-7 Sep. 2007, pp523-526.

Liu B., Riemenschneider S. and Xu Y. (2006), Gearbox fault diagnosis using empirical mode decomposition and Hilbert spectrum, *Mechanical Systems and Signal Processing*, 20, pp718-734.

Pan M. Ch. and Lin Y. F. (2006), Further exploration of Vold-Kalman filtering order tracking with shaft-speed information-I: Theoretical part, numerical implementation and parameter investigations. *Mechanical Systems and Signal Processing* , 20(5), pp1134-1154.

Pan M. Ch., Liao Sh. W. and Chiu Ch. Ch. (2007), Improvement on Gabor order tracking and objective comparison with Vold-Kalman filtering order tracking. *Mechanical Systems and Signal processing*, 21(2), pp653-667.

Pan M. Ch., Li P. Ch. and Cheng Y. R. (2008), Remote online machine condition monitoring system, *Measurement*, 41(8), October 2008, pp 912-921.

Pan M. Ch. and Wu Ch. X. (2007), Adaptive Vold-Kalman filtering order tracking. *Mechanical Systems and Signal Processing*, 21(8), pp2957-2969.

Potter R. (1990), A new order tracking method for rotating machinery, *Sound and Vibration*, 37(6), pp30-34.

Rai V. K. and Mohanty A. R. (2007), Bearing fault diagnosis using FFT of intrinsic mode functions in Hilbert-Huang transform, *Mechanical Systems and Signal Processing*, 21(6), pp2607-2615.

Rato R. T., Ortigueira M. D. and Batista A. G. (2008), On the HHT, its problems, and some solutions, *Mechanical Systems and Signal Processing*, 22, pp1374-1394.

Saavedra P. N., Rodriguez C. G. (2006), Accurate assessment of computed order tracking, *Journal of Shock and Vibration*, 13(1), pp13-32.

Schwartz M., Bennett W. R. and Stein S. (1966), *Communications Systems and Techniques*. New York: McGraw-Hill.

Stander C. J. and Heyns P. S. (2006), Transmission path phase compensation for gear monitoring under fluctuating load conditions. *Mechanical Systems and Signal Processing*, 20, pp1511-1522.

Schön P. P. (2006). Unconditionally convergent time domain adaptive and time-frequency techniques for epicyclic gearbox vibration. Master's thesis at University of Pretoria.
Available at: http://upetd.up.ac.za/thesis/available/etd-08282007-142010/
[Accessed: 30 August 2009]

Sharpley R. C. and Vatchev V. (2006), Analysis of the intrinsic mode functions, *Constructive Approximation*, 24 (1), pp17–47.

Tůma J. (2005), Setting the pass bandwidth in the Vold-Kalman order tracking filter. *Twelfth International Congress on Sound and Vibration*, 11-14 July 2005, Lisbon.

Tůma J. (undated study notes), *Vold-Kalman Order Tracking Filtration*. Faculty of Mechanical Engineering, Department of Control Systems and Instrumentation.

Vibratools (2005), MATLAB toolbox. Axiom EduTech, Sweden,

Vold H., Herlufson H., Mains M. and Corwin-Renner D. (1997), Multi axle order tracking with the Vold-Kalman tracking filter. *Sound and Vibration Magazine*, 13(5), pp30-34.

Vold H. and Leuridan J. (1993), High Resolution Order Tracing Using Kalman Tracking Filters – Theory and Application. SAE Paper, No. 931288.

Vold H., Mains M. and Blough J. (1997), Theoretical foundations for high performance order tracking with the Vold-Kalman tracking filter. *SAE Paper* 972007, pp1083–1088.

Wang K. S. (2008), Vibration monitoring on electrical machine using Vold-Kalman filter order tracking. Dissertation submitted for the degree of MSc at the University of Pretoria.
Available at:
http://upetd.up.ac.za/thesis/available/etd-08282008-171945/unrestricted/dissertation.pdf
[Accessed: 30 August 2009]

Wang K. S. and Heyns P. S. (2008), Inspecting FFT order components through the joint use of computed order tracking and Vold-Kalman filter order tracking. Comadem 2008, Prague, June 2008.

Wang K. S. and Heyns P. S. (2009), Vold-Kalman filter order tracking in vibration monitoring of electrical machines. *Journal of Vibration and Control*, 15(9), pp1325-1347.

Wu F. J., Qu L. S. (2009), Diagnosis of subharmonic faults of large rotating machinery based on EMD, *Mechanical Systems and Signal Processing*, 23, pp467-475.

Yang Zh. J., Yang L. H., Qing Ch. M. and Huang D. (2008), A method to eliminate riding waves appearing in the empirical AM/FM demodulation, *Digital signal processing*, 18, pp488-504.